

11

Viral Infections of the Lung

Sherif R. Zaki and Christopher D. Paddock

The most widespread and fatal of all acute diseases, pneumonia, is now Captain of the Men of Death.

—Sir William Osler, 1901¹

The lungs are among the most vulnerable to microbial assault of all organs in the body. From a contemporary vantage, lower respiratory tract infections are the greatest cause of infection-related mortality in the United States, and rank seventh among all causes of deaths in the United States.^{2,3} From a global and historic perspective, the scope and scale of lower respiratory tract infection is greater than any other infectious syndrome, and viral pneumonias have proven to be some of the most lethal and dramatic of human diseases. The 1918–1919 influenza pandemic, perhaps the most devastating infectious disease pandemic in recorded history, resulted in an estimated 40 million deaths worldwide, including 700,000 deaths in the U.S.⁴ The global outbreak of severe acute respiratory syndrome (SARS) during 2003, although considerably smaller in scale, resulted in 8098 cases and 774 deaths⁵ and is a dramatic contemporary example of the ability of viral pneumonias to rapidly disseminate and cause severe disease in human populations.

Although viruses are commonly identified causes of pneumonia of infants and young children, they are relatively infrequently recognized as agents of community-acquired pneumonia in adults.⁶ In several large series that investigated a microbiologic cause of community-acquired pneumonia, viral etiologies were identified in only 9% to 18% of cases (Table 11.1).^{7–12} However, it is likely that viral pneumonias are underrecognized and underdiagnosed for various reasons. Although some agents may cause distinct cytopathology or inclusions (e.g., adenoviruses, herpesviruses, and paramyxoviruses), many important pathogens (e.g., influenza viruses) do not, and none of these agents are resolved specifically in tissue by routine histologic stains. Viruses require live cells for cultivation, and are generally more difficult than bacteria to isolate from clinical samples. For some viral pneumonias,

the pathogen appears to initiate a cascade of destructive host responses that continue or progress even in the absence of the specific infectious agent, and in these patients the etiologic agent may be absent from host tissues at the time of autopsy.¹³ Thirty to sixty percent of community-acquired pneumonias are etiologically undetermined,¹⁴ and it is entirely possible that viruses directly cause more episodes of pneumonia than currently appreciated.

Because viral infections of the lower respiratory tract often precede bacterial pneumonias, viruses may indirectly exert considerable influence on the cumulative morbidity and mortality of infectious pneumonias.^{15,16} The mechanisms by which viruses may facilitate bacterial invasion of the respiratory tract are complex and varied. Certain viruses cause the death of ciliated respiratory epithelium and thereby disrupt normal ciliary activity. Viruses may also inhibit the phagocytic or bactericidal activities of neutrophils, T lymphocytes, and alveolar macrophages, and predispose the host to secondary infections. Certain gram-positive and gram-negative bacteria adhere to and colonize virus-infected epithelium more readily than to noninfected cells by various hypothetical mechanisms, including alteration and induction of receptors at the host–cell surface and changes in the extracellular environment.^{17–19} Finally, viral infections of the lung may exacerbate noninfectious pulmonary conditions (e.g., asthma and chronic obstructive pulmonary disease) and indirectly contribute to aggregate morbidity and mortality associated with these conditions.²⁰

Although influenza viruses remain the most frequently identified cause of viral pneumonia in adults (Table 11.1), the diversity of agents identified as causes of viral pneumonias has expanded considerably. Several newly recognized viral pneumonias have been identified since 1992 that are among the most feared and lethal of all emerging infections, including those caused by hantaviruses, Nipah virus, and SARS coronavirus (CoV).^{13,21–23} Certain causes

TABLE 11.1. Viral etiologies identified by culture isolation or serologic assays in adult patients with community-acquired pneumonias

Reference	Study interval	No. of patients studied (% with viral etiology)	Influenza A or B	No. of viral etiologies identified					
				RSV	HPIV	Adeno	CMV	Varicella	Other ^a
Fekety et al. ¹¹	1965–66	100 (17)	10	0	3	1	0	0	3
Sullivan et al. ⁹	1967–68	292 (12)	27	1	4	3	0	0	0
Macfarlane et al. ⁸	1980–81	127 (9)	7	2	0	1	0	1	0
Woodhead et al. ¹⁰	1984–85	236 (13)	19	5	1	5	0	0	1
Ortvist et al. ⁷	1987	277 (16)	7	8	13	15	0	0	0
de Roux et al. ¹²	1996–2001	338 (18)	37	5	11	5	0	0	3
Total (% of viral etiologies identified)		107 (54)		21 (11)	32 (16)	30 (15)	1 (0.5)	1 (0.5)	6 (3)

^aRubella (2), rhinovirus (1), mixed viral infections (3).

Source: Adapted from Greenberg.⁶

of viral pneumonia, particularly those that occur in vulnerable patient cohorts, have diminished during this same interval. By example, the U.S. incidence of varicella pneumonia has dropped by two thirds since universal childhood vaccination for varicella was implemented in 1995,^{24,25} and advances in the clinical management of transplant recipients have reduced the incidence of cytomegalovirus (CMV) pneumonia.²⁶ Also occurring during the last decade has been the development and use of powerful molecular techniques that have unveiled the identity of historic pathogens (e.g., the H1N1 “Spanish” influenza A virus),^{27,28} and have facilitated the rapid characterization of emerging agents (e.g., SARS-CoV).¹³

It should be noted that the disease manifestations of several of these agents (e.g., human parainfluenza virus [HPIV], respiratory syncytial virus [RSV], and influenza) are often confined to the upper airway and are not invari-

ably associated with pneumonia. With some of these pathogens (e.g., influenza viruses, RSV, hantaviruses, and HPIV viruses) respiratory disease is the primary manifestation. For other agents, such as measles, Nipah virus, and herpesviruses, typically the lungs are involved as part of a multisystem syndrome.

The diagnosis of viral pneumonia, suspected by patient history and clinical manifestations, also can be supported histopathologically, and the general pattern of histopathologic lesions may suggest a specific diagnosis. Many viruses can be identified in lung by examining the tissue response and cytopathic changes. Some of these viruses cause recognizable tissue reaction patterns including necrotizing tracheobronchitis, bronchiolitis, and interstitial pneumonia. A summary of the key diagnostic histopathologic and ultrastructural features for the most common viral pathogens that cause a majority of pulmonary infections is provided in Tables 11.2 and 11.3.

TABLE 11.2. Diagnostic histopathologic features of viral pneumonias

Family	Virus	Inclusions (location)	Pulmonary tissue reaction
Adenoviridae	Adenovirus	Yes (nuclear)	Necrotizing bronchiolitis; smudge cells; DAD
Bunyaviridae	Hantavirus	No	Severe edema, early DAD
Coronaviridae	SARS Coronavirus	No	Interstitial pneumonia; DAD; occasional multinucleation
Herpesviridae	Cytomegalovirus	Yes (nuclear and cytoplasmic)	Interstitial pneumonia; DAD; cytomegaly
	Herpes simplex	Yes (nuclear)	DAD; necrosis and rare multinucleation
	Varicella-zoster	Yes (nuclear)	DAD; necrosis and rare multinucleation
Orthomyxoviridae	Influenza	No	DAD; necrotizing bronchiolitis
Paramyxoviridae	Measles	Yes (nuclear and cytoplasmic)	Interstitial pneumonia with multinucleation DAD
	Parainfluenza	Yes (cytoplasmic; ill-defined)	DAD; interstitial pneumonia with occasional multinucleation
	Respiratory syncytial virus	Yes (cytoplasmic; ill-defined)	Necrotizing bronchiolitis, interstitial pneumonia with occasional multinucleation
	Human metapneumovirus	Yes (cytoplasmic; ill-defined)	Recently recognized; human pathology not well described
	Nipah	Yes (nuclear and cytoplasmic)	Interstitial pneumonia with multinucleation; DAD

DAD, diffuse alveolar damage.

TABLE 11.3. Diagnostic ultrastructural features of viral pneumonias

Family	Diagnostic ultrastructural features
Adenoviridae	70–90 nm nucleocapsids (NCs) with a dense core are found in cell nuclei, sometimes in paracrystalline arrays
Bunyaviridae	Virions difficult to detect; characteristic NC granulofilamentous inclusions in endothelial cells are seen occasionally in human tissues
Coronaviridae	Spherical, enveloped virions, approx. 75 but up to 160 nm in diameter, accumulate in cytoplasmic vesicles and are often found adherent to the plasma membrane
Herpesviridae	100 nm viral NCs are found in cell nuclei; in cytoplasm, tegument surrounds the NCs; enveloped virions, 120–200 nm, are found in Golgi cisternae and extracellularly
Orthomyxoviridae	Pleomorphic and filamentous virions, 80–100 nm in diameter, are composed of enveloped, filamentous NCs found budding at the plasma membrane of infectious cells; cytoplasmic and nuclear inclusions are sometimes seen
Paramyxoviridae	<i>Paramyxovirinae</i> (measles, Nipah, HPIV) are enveloped, pleomorphic virions, 125–250 nm in diameter, consisting of an enveloped aggregation of filamentous NCs; the 18-nm-wide NCs align under plasma membranes as virions bud into extracellular space; <i>Pneumovirinae</i> (RSV, HMPV) are smaller than <i>Paramyxovirinae</i> ; the roughly spherical, enveloped particles average 90–130 nm, and contain 14 nm wide NCs

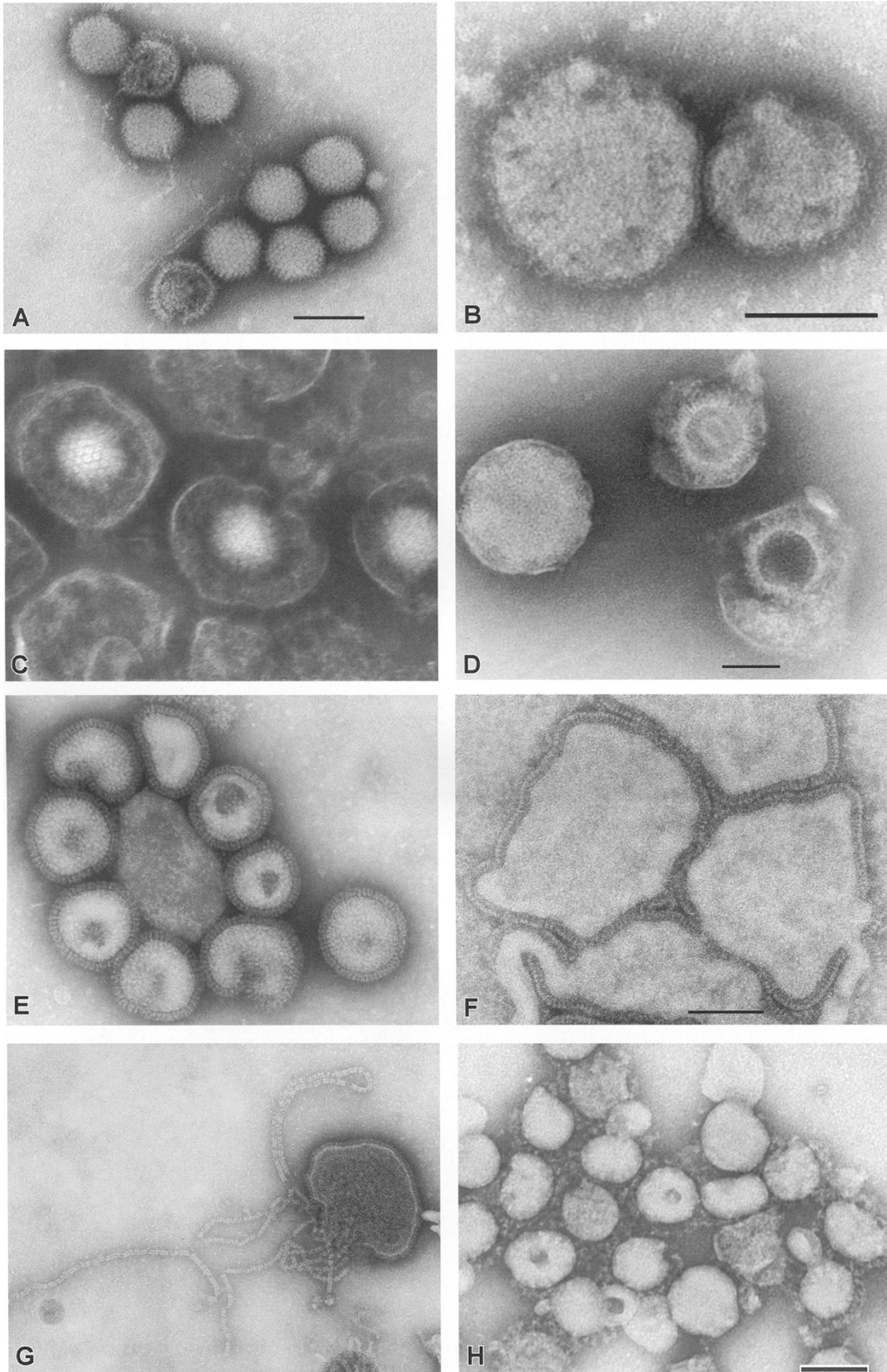
Only certain viruses can cause cytopathic changes that are sufficiently distinct to enable the pathologist to recognize a specific diagnosis on routine histologic examination of lung specimens. With the availability of special

diagnostic techniques, such as immunohistochemistry (IHC) and in-situ hybridization (ISH), many viruses can be detected in formalin-fixed, paraffin-embedded tissue samples even if specific viral inclusions cannot be found in histologic examination of tissue sections. Among the techniques, IHC utilizing specific antibodies can be routinely performed on formalin-fixed tissue and can enhance the pathologist's accuracy in identifying organisms in tissue specimens.

In addition to histologic pattern recognition, IHC, and ISH in tissue, several other diagnostic tests are available to aid the pathologist. Cell culture techniques, serology, polymerase chain reaction (PCR), and electron microscopy (EM) all play vital roles in the diagnosis of these infections. While histologic techniques can be an excellent means of demonstrating organisms, tissue culture isolation remains essential for definitive identification of the virus. When a viral pneumonia is suspected, samples of lung tissues should be evaluated by cell culture, which has the advantage of being a nonbiased method for screening purposes that does not rely on the availability of specific antibodies or probes. Electron microscopy offers the same utility as a broad scope diagnostic tool and has been especially critical in outbreaks of unknown etiology. It played a critical role during the Hendra and Nipah virus outbreaks in 1994 and 1999, respectively, and more recently, in the early recognition of a novel coronavirus associated with SARS in 2003 and in the diagnosis of emerging transplant-associated infections.^{13,22,29–33} The advantage of this approach is that viral particles may be demonstrated by negative stain or thin section EM, either directly in clinical material or after amplification in cell culture. Like culture, EM is not limited by narrow specificity of reagents or by prior clinical bias (Fig. 11.1).

FIGURE 11.1. Negative stain electron microscopic images of different viruses that can cause pulmonary infections. **A.** Adenovirus. Adenoviruses are protein-shelled icosahedral-shaped nonenveloped viruses that measure approximately 70 to 90 nm in diameter. Two of the viruses are stain penetrated revealing the DNA-containing nucleoprotein. **B.** Sin Nombre virus. Sin Nombre virus, the causative agent of hantavirus pulmonary syndrome, belongs to the genus hantavirus in the family *Bunyaviridae*. The envelopes of hantaviruses are checkerboard in appearance, and particles measure 90 to 150 nm in diameter. **C.** Herpes simplex virus. The stain has penetrated the envelope of several of these herpesvirus particles, delineating the icosahedral-shaped nucleocapsids, which measure 90 to 100 nm in diameter. **D.** Cytomegalovirus. Another herpesvirus; one virus particle (left) is intact while two nearby particles are stain-penetrated and show the viral nucleocapsids. The nucleocapsid of the upper right particle shows a central core that harbors the DNA of the virus. **E.** Influenza virus. Influenzaviruses belong to the family *Orthomyxoviridae*; viral particles are pleomorphic

and can be filamentous or spherical in shape. The evenly spaced spikes cover the entire virus surface and contain both the hemagglutinin and neuraminidase surface glycoproteins. **F.** Human metapneumovirus. These paramyxoviruses are heterogeneous in size and shape, and range in size from 150 nm to 1 μm in diameter. **G.** Parainfluenza virus. Another paramyxovirus, the viral nucleocapsid, with its typical herringbone appearance, can be seen both within the stain-penetrated particle as well as partially extruded from the virion. An important feature that can help distinguish between *Paramyxovirinae* (parainfluenza and measles viruses) and *Pneumovirinae* (human metapneumovirus and respiratory syncytial virus) is the diameter of the nucleocapsids, which measure 18 nm and 14 nm, respectively. **H.** Severe acute respiratory syndrome (SARS) coronavirus. These 80- to 100-nm particles are named for the characteristic crown-like fringe on the surface. Scale bars, 100 nm. (**A,B,D,F,H:** courtesy of C. Humphrey; **C,G:** courtesy of E. Palmer; **E:** courtesy of F.A. Murphy, all at Centers for Disease Control and Prevention, Atlanta, GA.)



Adenoviruses

Adenoviruses were first cultured and identified during the early 1950s by investigators searching for etiologic agents of acute respiratory infections. The initial adenovirus isolate was made serendipitously from adenoid tissues obtained from children during efforts to establish a primary human adenoid cell line.³⁴ A related virus was identified the following year by investigators studying respiratory disease in military recruits.³⁵ These agents were subsequently named *adenoviruses* after the original source of tissue from which the prototype strain was identified.³⁶ Adenoviruses are nonenveloped viruses with a single, linear, double-stranded DNA genome that is contained within an icosahedral capsid that measures 70 to 90nm in diameter (Fig. 11.1A). The capsid is comprised of seven known polypeptides, including the hexon capsomere, which contains group-specific antigenic determinants.³⁷

Adenoviruses are a ubiquitous and diverse group of viruses found naturally in the upper respiratory tracts and gastrointestinal systems of humans, other mammals, and birds. Most adenoviruses infect mucosal epithelium, although some pathogens of animals are trophic for endothelial cells, and endothelial infection has been identified in some immunocompromised humans.³⁸ Adenoviruses are represented by at least 51 serotypes on the basis of resistance to neutralization by antisera to other known adenovirus serotypes, and comprise six subgroups or subgenera (A through F) that are distinguished by differential hemagglutination with erythrocytes from various animal species.^{37,39,40} More than 50% of the known adenovirus serotypes are associated with human diseases of the upper and lower respiratory tract, conjunctiva, urinary tract, intestine, and occasionally heart, liver, and central nervous system. The others are rarely encountered and may or may not act as pathogens in recognizable disease.³⁷

It is estimated that approximately 5% to 10% of all pneumonias in infants and young children are caused by adenoviruses.^{41,42} Most pediatric cases of adenovirus pneumonia occur between 6 months and 5 years of age, and serotypes 3, 7, and 21 (all members of the B subgenus), are the most common causes of pneumonia in this patient cohort.⁴³⁻⁴⁵ Serotypes 3 and 7 are particularly pathogenic adenoviruses that can cause disseminated and often fatal disease in previously healthy children.⁴⁶ In adults, pneumonia is generally associated with serotypes 3, 4, and 7.⁴⁷ Periodic epidemics of adenovirus pneumonia in young adults have been identified, particularly among military recruits.^{48,49}

In a manner similar to other pathogens, adenoviruses take advantage of impaired or destroyed immune systems to establish persistent and disseminated infections in immunocompromised hosts. In this patient cohort, the

case fatality rate of adenoviral pneumonia approaches 60%, compared with an approximately 15% mortality in immunocompetent patients.³⁷ Immunocompromised patients are also susceptible to a broader range of different adenovirus serotypes. By example, the commonly recognized serotypes in normal children account for only about 50% of the adenovirus serotypes reported for children with congenital immune deficiencies.^{37,46} Because some adenoviruses establish latency in lymphoid tissues and the kidneys of their host, it is believed that many, possibly most, cases of clinical disease caused by adenoviruses in immunocompromised patients are reactivated infections.³⁷

The lungs of patients with adenovirus pneumonia are typically heavy and edematous, and the bronchi are generally filled with mucoid, fibrinous, or purulent exudates. The histopathologic findings (Fig. 11.2) include necrotizing bronchitis and bronchiolitis with extensive denudation of the surface epithelium, particularly in medium-sized (1 to 2mm in diameter) intrapulmonary bronchi (Fig. 11.2A). Affected airways may be occluded by homogeneous eosinophilic material, mixed inflammatory cells, detached epithelium, and cellular debris. The lamina propria of bronchi and bronchioles is typically congested and infiltrated by predominantly mononuclear inflammatory cell infiltrates. Bronchial serous and mucous glands are also often involved and show necrosis and mixed infiltrates.⁵⁰ As the infection progresses, there is involvement of the pulmonary parenchyma, forming bronchocentric necrosis with hemorrhage, neutrophilic and mononuclear cell infiltrates, and karyorrhexis. These findings generally occur against a background of exudative diffuse alveolar damage, with filling of the air space by macrophages, fibrin, and detached pneumocytes, and hyaline membrane formation.⁵¹ Patients with fatal pneumonia may develop disseminated intravascular coagulopathy and demonstrate fibrin thrombi in vessels of the lungs, kidney, heart, adrenals, and central nervous system (see Fig. 4.20 in Chapter 4).⁴⁸

Adenoviruses form intranuclear inclusions in respiratory epithelial cells of the trachea, bronchi, and bronchioles, in the acinar cells of bronchial glands, and in alveolar pneumocytes, and are generally most abundant at the viable edges of necrotic foci. By using the hematoxylin and eosin (H&E) stain, early inclusions appear as small, dense, amphophilic structures surrounded by a cleared zone and peripherally margined chromatin, similar to herpetic inclusions. As the cellular infection progresses, the inclusion becomes larger (as large as 14 μ m in some cells) and more basophilic, and the margins of the nuclear membrane become blurred to form the characteristic "smudge cell" (Fig. 11.2B,C).^{50,51} Tracheal aspirates of patients with adenovirus pneumonia may show distinctive features on cytologic preparations that include cells with fine strands of chromatin that radiate from a central

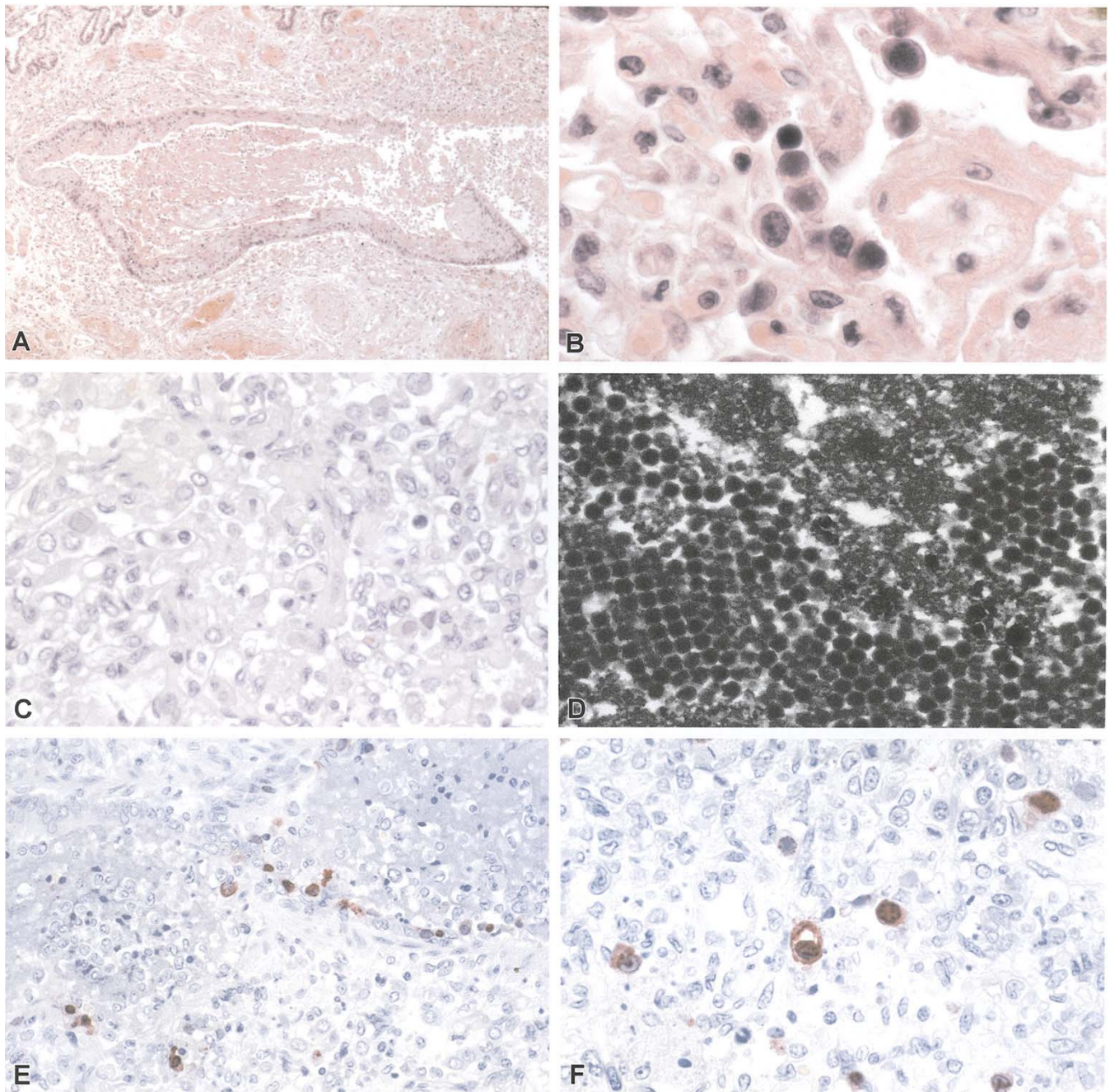


FIGURE 11.2. Adenovirus pneumonia. **A.** Bronchiole containing necrotic debris composed of surface epithelium, fibrin, and mixed inflammatory cells. **B,C.** Large, basophilic, intranuclear inclusions in alveolar pneumocytes, forming characteristic “smudge cells” that can be observed in advanced adenovirus infections. **D.** Paracrystalline arrays of 70 to 90 nm of adenovirus particles in the nucleus of an infected pneumocyte. (Courtesy

of C. Goldsmith, Centers for Disease Control and Prevention, Atlanta, GA.) **E,F.** Immunohistochemical localization of adenovirus-infected cells in the pulmonary parenchyma of patient with fatal adenovirus pneumonia. Scale bar, 100 nm. **A–C,** hematoxylin and eosin (H&E); **E,F,** immunoalkaline phosphatase staining, naphthol fast-red, and hematoxylin counterstain; **D,** uranyl acetate and lead citrate stain.

inclusion to the marginated chromatin at the nuclear membrane (“rosette cells”), and cells with foamy, “honeycomb” nuclei, as well as typical smudge cells (see Fig. 7.45 in Chapter 7).⁵²

Various methods can be used to diagnose adenovirus infections that include antigen detection, cell culture, electron microscopy, molecular assays, and serology. Direct detection techniques that identify the common group-reactive hexon antigen in tissues or body fluids include fluorescence antibody assays and enzyme immunoassays.⁵³ Immunohistochemistry staining methods have been used successfully to detect adenovirus-infected cells in formalin-fixed, paraffin-embedded tissues using various commercially available, adenovirus group-specific antibodies (Fig. 11.2E,F).^{38,51} Electron microscopy of adenovirus-infected tissues reveals a paracrystalline array of virions (Fig. 11.2D).^{54,55}

Most adenoviruses can be isolated in cell culture from bronchial washings, tracheal aspirates, or lung biopsy specimens during the early stage of the illness and grow well in various cell lines, including human embryonic kidney, HeLa, and HEp-2 cells.⁴⁷ Cell cultures infected with adenoviruses exhibit a relatively characteristic cytopathologic effect, described as a “cluster of grapes,” within 3 to 5 days after inoculation. Serotyping of the isolate is accomplished by using hemagglutination inhibition and neutralization tests with hyperimmune type-specific animal antisera.⁵⁶ Molecular assays, particularly gene amplification using PCR, and ISH methods, have been developed to detect adenovirus nucleic acid in respiratory secretions and in formalin-fixed, paraffin-embedded tissues.^{51,57,58} Broad-range, sensitive assays that can detect any adenovirus amplify common genomic sequences (e.g., the hexon gene region). Other more specific assays detect specific adenovirus types with unique genomic sequences.⁵⁹ Serologic assays include tests for group-specific antibodies (e.g., complement fixation and enzyme immunoassays), or type-specific antibodies (e.g., neutralization and hemagglutination-inhibition assays). Pitfalls associated with serologic testing for adenoviruses include occasional rises in heterotypic antibodies when type-specific assays are used, and relatively low sensitivity demonstrated by complement fixation assays.⁵⁹

Hantaviruses

Human hantaviral diseases are caused by a group of closely related, trisegmented, negative-sense RNA viruses of the genus *Hantavirus*, of the family Bunyaviridae.^{60–62} Members of the genus *Hantavirus* have similar morphologic features.^{63,64} Virus particles are 70 to 130 nm in diameter and generally appear spherical to ovoid, although pleomorphic forms may be seen. A lipid envelope containing glycoprotein spikes surrounds a core consisting of the genome and its associated proteins (nucleocapsids)

arranged in delicate tangles of filaments showing occasional granulation. The presence of characteristic inclusion bodies in thin section electron microscopy and a unique grid-like pattern on negative-stain electron microscopy differentiate these viruses from other members of the family Bunyaviridae (Fig. 11.1B).^{65,66}

The severity and disease type largely depends on the viral serotype. Two categories of hantavirus-associated illnesses are described: hemorrhagic fever with renal syndrome (HFRS) for disease in which the kidneys are primarily involved, and hantavirus pulmonary syndrome (HPS) for disease in which the lungs are primarily involved.^{67–69} The isolation of the first recognized hantavirus (Hantaan virus, named for the river in South Korea), and its subsequent identification as the causative agent of HFRS was reported in 1978.⁷⁰ In 1993, the deaths of several previously healthy individuals due to a rapidly progressive respiratory disease in the southwestern United States were etiologically linked to a previously unrecognized hantavirus. Clinically, the disease differs from HFRS in its pronounced pulmonary involvement and higher mortality rates and is known as HPS.^{23,69,71,72}

Hantavirus-associated diseases primarily affect blood vessels and result in different degrees of generalized capillary dilatation and edema.⁷³ In contrast to severe HFRS where abundant protein-rich, gelatinous retroperitoneal edema fluid is found, all HPS patients have large bilateral pleural effusions and heavy edematous lungs.^{74–77} In fatal Far Eastern HFRS, a distinctive triad of hemorrhagic necrosis can be seen in the renal medullary junctional zone, cardiac right atrium, and anterior pituitary.^{75,78} However, in patients with HPS, hemorrhages are rare, and ischemic necrotic lesions, except those attributed to shock, are not seen.^{72,74}

Histologically, morphologic changes of the endothelium are uncommon but, when seen, consist of prominent and swollen endothelial cells. Vascular thrombi and endothelial cell necrosis are rare. In HFRS, the most severe and characteristic microscopic lesions involve the kidney; however, an interstitial pneumonitis can also be seen in some fatal cases. In contrast, the microscopic changes of North and South American HPS are principally seen in the lung and spleen.^{72,74} The lungs show a mild to moderate interstitial pneumonitis characterized by variable degrees of edema and an interstitial mononuclear cell infiltrate comprised of a mixture of small and enlarged mononuclear cells with the appearance of immunoblasts (Fig. 11.3A). Focal hyaline membranes composed of condensed proteinaceous intraalveolar edema fluid, fibrin, and variable numbers of inflammatory cells are observed (Fig. 11.3B). Typically, neutrophils are scanty and the alveolar pneumocytes are intact with no evidence of cellular debris, nuclear fragmentation, or hyperplasia. In fatal cases, with a prolonged survival interval, tissues show features more characteristic of the exudative and

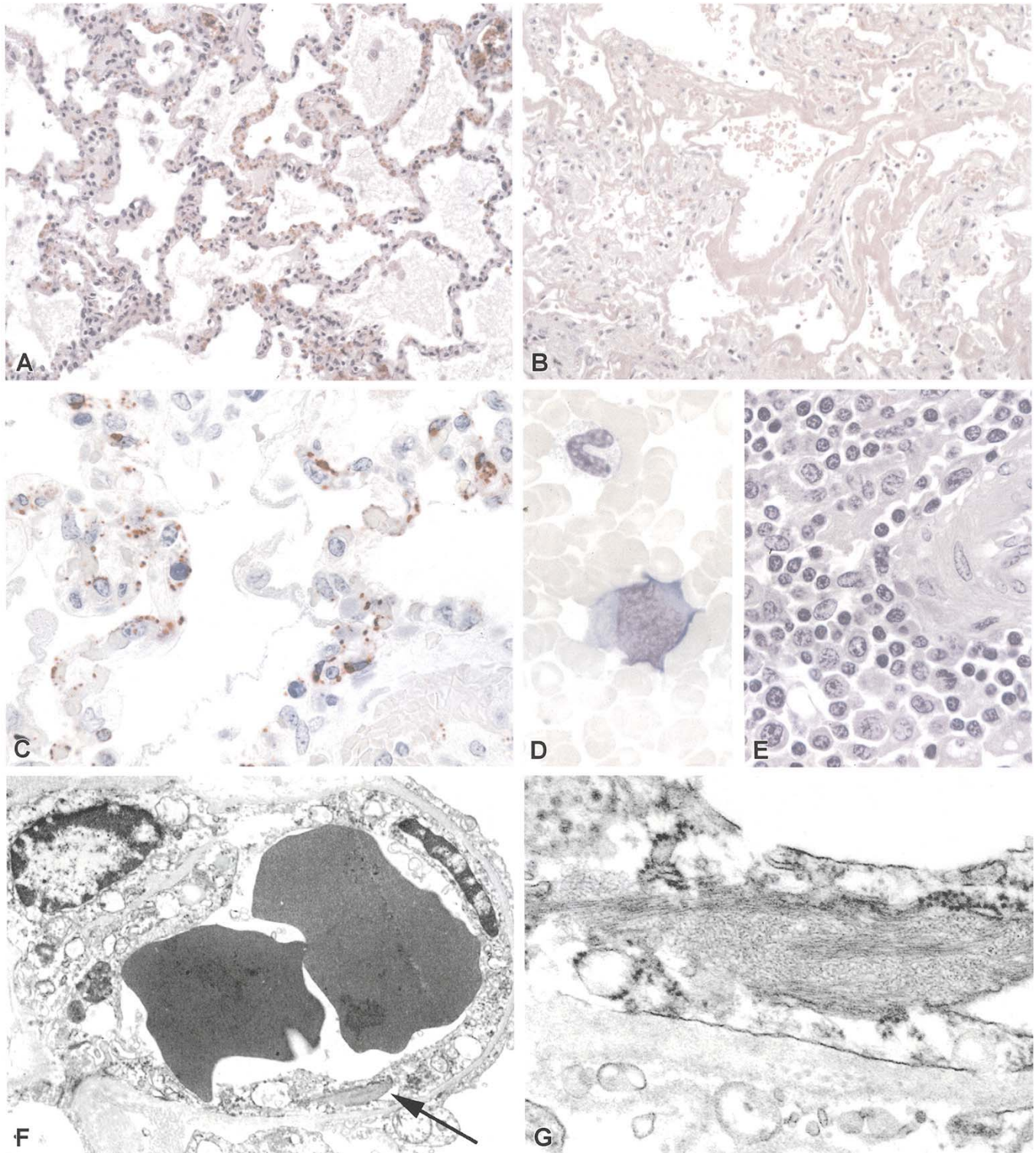


FIGURE 11.3. Hantavirus pulmonary syndrome (HPS). **A.** Lung showing a mononuclear interstitial pneumonitis and intraalveolar edema in a typical case of HPS. **B.** Patchy areas of alveolar septal thickening and prominent hyaline membranes in an HPS patient who died on the 19th day of illness. **C.** Widespread immunostaining of hantaviral antigens in pulmonary microvasculature of an HPS patient. **D.** Peripheral blood smear showing a circulating immunoblast with deeply basophilic cytoplasm, high nuclear-to-cytoplasmic ratio, and prominent nucleolus.

E. Spleen from a fatal case in which immunoblasts are seen in the periarteriolar sheath. Note prominent nucleoli and high nuclear-to-cytoplasmic ratio. **F.** Ultrastructural appearance of typical hantavirus inclusion within a pulmonary capillary (arrow). **G.** High magnification of inclusion in **F** showing a granulo-filamentous viral inclusion within capillary endothelium. **A,B,D,E,** H&E; **C,** immunoalkaline phosphatase staining with naphthol fast-red and hematoxylin counterstain; **F,G,** uranyl acetate and lead citrate stain.

proliferative stages of diffuse alveolar damage. Lung biopsies taken from patients who survive their illness appear similar with proliferated reparative type II pneumocytes, severe edematous and fibroblastic thickening of the alveolar septa, and severe air-space disorganization with distorted lung architecture (see Chapter 4). Other characteristic microscopic findings in HPS cases include variable numbers of immunoblasts within the splenic red pulp and periarteriolar white pulp, lymph nodal paracortical zones, hepatic portal triads, and peripheral blood (Fig. 11.3D,E). Similarly, in severe HFRS cases, large mononuclear cells can be present in the spleen, lymph nodes, blood, and hepatic portal triads.^{75,76}

Electron microscopic studies of HPS lung tissue demonstrate infection of endothelial cells and macrophages.^{69,72} The virus or virus-like particles observed are infrequent and extremely difficult to identify in autopsy tissues because of the considerable degree of viral pleomorphism and the postmortem deterioration of tissues. However, typical hantaviral inclusions are seen more frequently and their identity can be confirmed by immunolabeling (Fig. 11.3F,G). Similar inclusions are observed in epithelial cells in HFRS and are considered to be ultrastructural markers of hantavirus-infected cells.^{63,79,80}

Using immunohistochemistry, viral antigens are found primarily within capillary endothelium throughout various tissues in both HPS and HFRS. In HPS, marked accumulations of hantaviral antigens are in the pulmonary microvasculature and in splenic and lymph nodal follicular dendritic cells (Fig. 11.3C).⁷² Despite the extensive endothelial cell accumulations of hantaviral antigens, there is little ultrastructural evidence of cytopathic effect.

Hantavirus pulmonary syndrome should be suspected in cases of adult respiratory distress syndrome (ARDS) without a known precipitating cause among previously healthy individuals. The level of suspicion should be particularly high when patients have a known exposure to rodents in areas where *Peromyscus maniculatus* or other reservoirs of hantavirus are found. Physicians need to differentiate HPS from other common acute respiratory diseases, such as pneumococcal pneumonia, influenza virus, and unexplained ARDS. The diagnosis of HPS, suspected by patient history and clinical manifestations, can also be supported histopathologically. Although there is no single pathognomonic lesion that would permit certain histopathologic diagnosis of HPS, the overall constellation of histopathologic hematologic findings suggests the diagnosis.^{72,74} Diseases that need to be distinguished pathologically from HPS include a relatively large number of different viral, rickettsial, and bacterial infections, as well as various noninfectious disease processes.

Virus-specific diagnosis and confirmation can be achieved through serology, PCR for hantavirus RNA, or IHC for hantaviral antigens.^{21,72} Serologic testing can detect hantavirus-specific immunoglobulin M or rising

titers of immunoglobulin G in patient sera and is considered the method of choice for laboratory confirmation of HPS. Immunofluorescent assays and enzyme-linked immunosorbent assays (ELISAs), which demonstrate the presence of specific antihantaviral antibodies, are currently used as rapid diagnostic tests and provide results within a few hours. Recently, synthetic hantaviral nucleocapsid proteins have been used to improve the sensitivity and specificity of serologic assays. These proteins are more available than inactivated hantaviral antigens.^{81,82} Polymerase chain reaction detects viral RNA in blood and tissues and is extremely useful for diagnostic and epidemiologic purposes. Hantaviral RNA can also be detected in formalin-fixed, paraffin-embedded archival tissue by reverse-transcriptase (RT)-PCR.⁸³ Immunohistochemistry testing of formalin-fixed tissues can be used to detect hantavirus antigens, and is a sensitive method to confirm hantaviral infections.⁷² It has a unique role in the diagnosis of fatal HPS cases when serum samples and frozen tissues are unavailable but formalin-fixed autopsy tissues are obtainable.^{84,85}

Severe Acute Respiratory Syndrome

The causative agent of SARS is an enveloped, positive-stranded RNA virus that is a member of the genus *Coronavirus*, of the family *Coronaviridae*. Coronaviruses have the largest genomes of all RNA viruses and replicate by a unique mechanism that results in a high frequency of recombination. Maturation of SARS coronavirus (SARS-CoV) is similar to features previously described for other coronaviruses.⁸⁶⁻⁹⁰ Virions form by alignment of the helical nucleocapsids along the membranes of the endoplasmic reticulum or Golgi complex and acquire an envelope by budding into the cisternae. The cellular vesicles become filled with virions and progress to the cell surface for release of the virus particles; large numbers of particles remain adherent to the plasma membrane at the cell surface.

Severe acute respiratory syndrome was recognized during a global outbreak of severe pneumonia that began in late 2002 in Guangdong Province, China, and gained prominence in early 2003 as cases were identified in more than two dozen countries in Asia, Europe, North America, and South America. The disease causes an influenza-like illness with fever, cough, dyspnea, and headache, and in severe cases it can cause death in humans. Person-to-person transmission, combined with international travel of infected persons, accelerated the worldwide spread of the illness.^{5,13,91}

Several reports have described diffuse alveolar damage with various levels of progression and severity as the main histopathologic findings in SARS patients (Fig. 11.4A,B).^{13,92-98} Lungs typically show changes

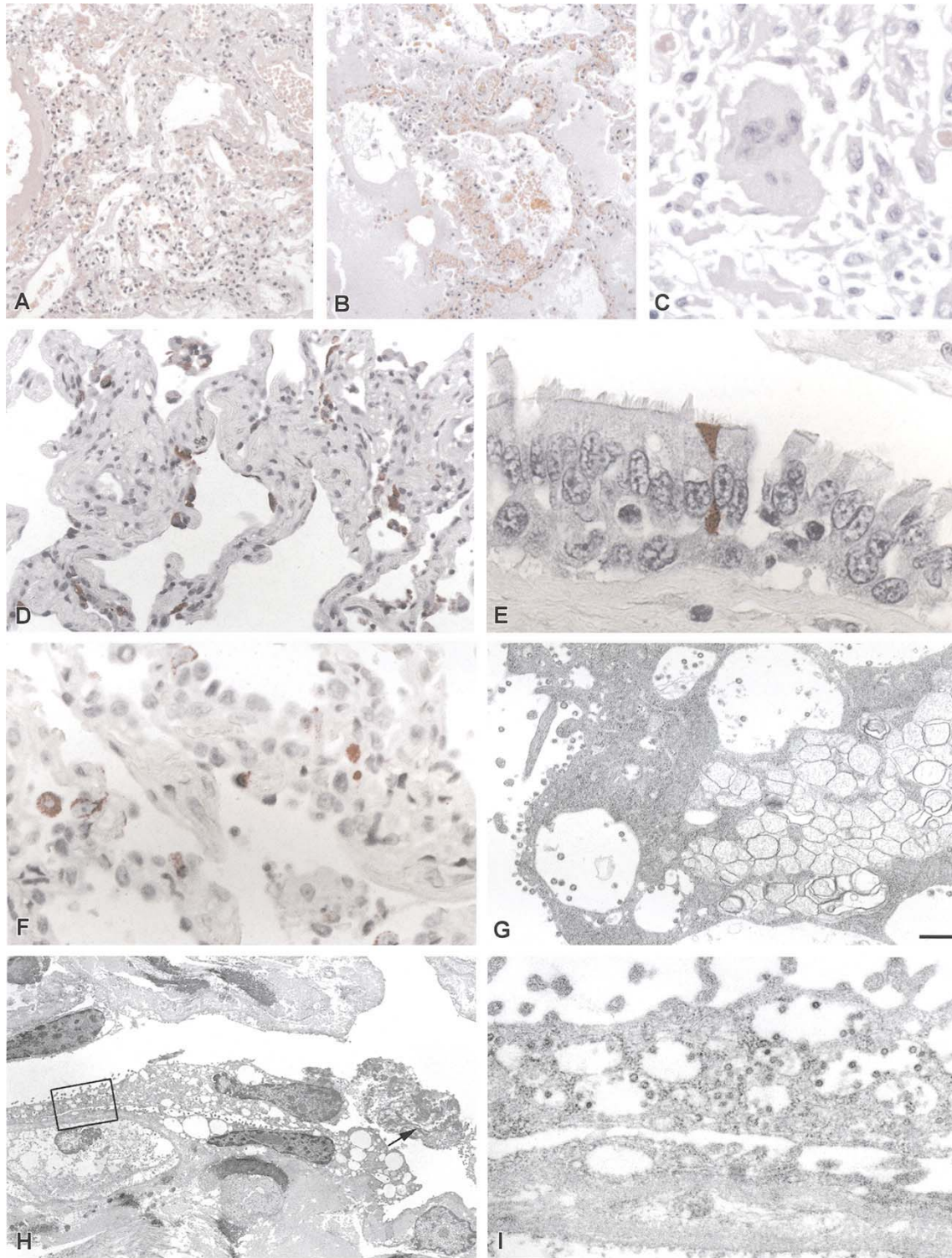


FIGURE 11.4. Severe acute respiratory distress syndrome (SARS). **A,B.** Lung showing interstitial pneumonia, patchy hyaline membranes and prominent intraalveolar edema. **C.** Multinucleated syncytial giant cells can be seen in some cases of fatal SARS. Note absence of discernible viral inclusions. **D.** Abundant immunostaining of coronavirus antigens in alveolar-lining pneumocytes. **E.** Ciliated epithelial cell in upper airway epithelium containing viral antigens. **F.** In-situ hybridization (ISH) showing abundant infected pneumocytes and intraalveolar macrophages containing viral nucleic acids. **G.** Cytoplasmic and extracellular virions are apparent in this electron micrograph of a sloughed pneumocyte from a bron-

chioalveolar lavage obtained from a patient with SARS. Note the region of double-membrane vesicles, a common feature of coronavirus-infected cells. **H.** Electron micrograph showing an infected pneumocyte, attached at one edge to the basement membrane. **I.** Higher magnification of boxed area in **H**, showing numerous coronavirus particles within the cytoplasmic vesicles of this pneumocyte. **A–C, H&E; D,E,** immunoalkaline phosphatase staining, naphthol fast-red, and hematoxylin counterstain; **F,** digoxigenin-labeled probe followed by immunoalkaline phosphatase staining, naphthol fast-red, and hematoxylin counterstain; **G–I,** uranyl acetate and lead citrate stain.

described for the proliferative phase of diffuse alveolar damage, with hyaline-membrane formation, desquamation of epithelial cells, fibrin deposit in the alveolar space, and hyperplasia of type 2 pneumocytes. Increased mononuclear infiltrate in the interstitium can be seen in some cases. Other findings identified in some patients included focal intraalveolar hemorrhage, necrotic inflammatory debris in small airways, and organizing pneumonia. In addition, multinucleated syncytial cells may be seen in the intraalveolar spaces of some patients who died 14 days or more after onset of illness (Fig. 11.4C). Infection with some coronaviruses, including SARS-CoV, is known to induce cell fusion in culture producing syncytial cells similar to those sometimes observed in lungs of patients who die from SARS. These cells contain abundant vacuolated cytoplasm with cleaved and convoluted nuclei, but without obvious intranuclear or intracytoplasmic viral inclusions. The ISH and IHC studies of tissues from SARS patients have identified coronavirus infection of upper airway bronchiolar epithelium (Fig. 11.4D–F).^{92,99–}

¹⁰¹ Infected ciliated columnar epithelial cells can be seen focally in lining epithelium of trachea and larger bronchi (Fig. 11.4E). Many of these infected cells slough from the epithelium and can be observed by using ISH within the bronchial lumen. Abundant viral antigens can also be found distributed focally in parenchyma of lungs of some patients and are seen predominantly in the cytoplasm of pneumocytes, in occasional macrophages, and in association with intraalveolar necrotic debris and fibrin (Fig. 11.4D). Double-stain studies indicate that most SARS-CoV–infected cells are type 2 pneumocytes. Double-stain studies also detected viral nucleic acids with a distribution similar to that seen in IHC studies, mainly in pneumocytes and in some macrophages.¹⁰⁰ Electron microscopic examination of lung tissues selected from areas with abundant IHC staining shows numerous coronavirus particles and nucleocapsid inclusions. Virions are seen in cytoplasmic vesicles and along the cell membranes of pneumocytes, in phagosomes of macrophages, and associated with fibrin in alveolar spaces (Fig. 11.4G–I). Because coronavirus particles may be confused morphologically with other nonviral cellular components, definitive ultrastructural identification can be achieved by using immunogold labeling electron microscopy.

The primary histopathologic lesions seen in the lungs of patients who die from SARS are somewhat nonspecific and can also be seen in acute lung injury cases caused by infectious agents, trauma, drugs, or toxic chemicals.¹⁰² Multinucleated syncytial cells similar to those seen in some SARS patients can also be found in a number of virus infections, including measles, parainfluenza viruses, RSV, and Nipah virus infections.^{102–104} In an early study of four human SARS patients,¹³ viral antigens were not detected in the lung by IHC. The most likely explanation is that all patients in the study had a clinical course aver-

aging more than 2 weeks. For many virus infections, viral antigens and nucleic acids are cleared within 2 weeks of disease onset by the host immune response. It is also possible that the pulmonary damage associated with SARS is not caused directly by the virus, but represents a secondary effect of cytokines or other factors induced by the virus infection. Similarly, in influenza virus infections, viral antigens are seen predominantly in respiratory epithelial cells of large airways and are only rarely identified in pulmonary parenchyma despite concomitant and occasionally severe interstitial pneumonitis.¹⁰⁵ In recent reports by Shieh et al.¹⁰⁰ and Chong et al.,⁹² the temporal relationship between the duration of illness and clearance of SARS-CoV in human lung tissue was examined. Viral antigens and nucleic acids were detected only in pulmonary tissues of patients who died early in the disease.

The development of specific IHC, ISH, and immunoelectron microscopy (IEM) assays to identify SARS-CoV in formalin-fixed, paraffin-embedded samples has facilitated the assessment of the cellular tropism of SARS-CoV infection in human lung tissues. Localization of SARS-CoV in the lung occurs mainly in the cytoplasm of pneumocytes, primarily type 2, and occasionally in alveolar macrophages (Fig. 11.4F). Type 2 pneumocytes are known to secrete pulmonary surfactant, resulting in reduced surface tension and preservation of the integrity of the alveolar space. These cells also play an important role in tissue restitution following lung damage. Moreover, there is mounting evidence to support their contribution to the development of acute inflammatory lung injury following exposure to biological or chemical agents. Additional studies are needed to further define the role of type 2 pneumocytes and alveolar macrophages in SARS-CoV infection.

Cynomolgus macaques inoculated with SARS-CoV develop pathologic findings of pneumonia and have been proposed as an animal model.¹⁰⁶ Haagmans et al.¹⁰⁷ showed extensive SARS-CoV antigen expression in experimentally infected macaques 4 days after infection. The antigens were mainly in alveolar lining epithelial cells with morphologic characteristics of type 1 pneumocytes, indicating type 1 pneumocytes are the primary target for SARS-CoV infection early in the disease. Type 1 pneumocytes normally represent 90% of the alveolar epithelial cell volume and are easily damaged during pulmonary infections or other types of injury. In a more recent study on nonhuman primates,¹⁰⁸ evidence of infection of type 1 pneumocytes in addition to some type 2 pneumocytes and macrophages was found.

Small animal models, such as rodents, would be very useful for evaluating vaccines, immunotherapies, and antiviral drugs, and we have recently identified the mouse as an animal model for this purpose.¹⁰⁹ In those studies, microscopic examination of trachea, bronchus, lung,

thymus, and heart on day 2 after infection revealed mild and focal peribronchiolar mononuclear inflammatory infiltrates with no significant histopathologic change in other organs. Viral antigens and nucleic acids were focally distributed in bronchiolar epithelial cells, and virions were found in these same areas by ultrastructural analysis. Data suggest that SARS-CoV replicates in mice to a titer sufficient to evaluate vaccines and antiviral agents. The mouse and other small animal models¹¹⁰ might also be used to test the ability of the virus to replicate and cause disease and facilitate identification of host-immune mechanisms that contribute to the resolution of SARS-CoV infection.

Cytomegalovirus

Cytomegaloviruses (CMV) comprise a distinct and ancient group of herpesviruses that are widely distributed in nature, share similar growth characteristics in cell culture, and cause cellular enlargement and form distinctive inclusions in infected cells. These cytopathic changes, identified by early pathologists in the salivary glands of children dying from various unrelated diseases,¹¹¹⁻¹¹³ led to the early designation of cytomegalic inclusion disease many years before the causative agent was isolated in the mid-1950s. The name *cytomegalovirus* was proposed in 1960 to reflect the cytopathic changes caused by these viruses.¹¹⁴

Cytomegaloviruses are highly host-specific, and various mammalian hosts, including nonhuman primates, rodents, and domesticated animals, are infected with their own distinct CMV. In this context, human CMV is stringently species-specific and, with rare exception, only infects cells of human origin.¹¹⁵ Several cell types are permissive for CMV replication, including alveolar pneumocytes, vascular endothelium, fibroblasts, monocytes, dendritic cells, and exocrine and endocrine glandular epithelial cells.¹¹⁶ Cytomegalovirus is a β -herpesvirus with the largest genome (230 kilobase pair [kbp]) of all the herpesviruses known to infect humans. The double-stranded linear DNA genome is contained within a 90 to 100nm icosahedral capsid and is surrounded by an amorphous material known as the tegument. These components are enclosed in a lipid bilayer envelope that is derived from the host cell nuclear or Golgi membranes and contains several virally encoded glycoproteins necessary for infection of other cells. Mature enveloped virions range from 150 to 200nm, making CMV one of the largest viruses that infect humans (Fig. 11.1D).¹¹⁷ The structure of CMV is typical of other human herpesviruses, but demonstrates some subtle ultrastructural differences from other viruses in this group including greater pleomorphism of the lipid envelope and dense body inclusions in the cytoplasm of infected cells.¹¹⁸

Cytomegalovirus is a ubiquitous human pathogen, and in North America infects approximately 50% to 90% of the population.¹¹⁷ Most of these infections are inapparent, although some cases of primary infection in otherwise healthy individuals result in a self-limited mononucleosis syndrome similar to that caused by Epstein-Barr virus; it is estimated that 20% to 50% of cases of heterophile-negative mononucleosis, and 8% of all cases of mononucleosis, are caused by CMV.¹¹⁹ Pulmonary involvement in CMV mononucleosis is infrequent and occurs in approximately 6% of these cases.¹²⁰ Congenitally acquired CMV infection has various deleterious effects on the fetus, including mental retardation, neurologic abnormalities, sensorineural hearing loss, and retinitis, and in one series pulmonary involvement occurred in 64% of symptomatic infants.¹²¹

Like all herpesviruses, CMV remains with its host for life after primary infection and establishes latency in various cell types, including vascular endothelial cells, monocytes and macrophages, neutrophils, and renal and pulmonary epithelial cells.¹²² Activation of viral replication occurs in persons with severely compromised immunity. Patients with advanced HIV disease and recipients of hematopoietic stem cell or lung transplants are particularly at risk of developing CMV pneumonia. Before the use of CMV screening and effective antiviral prophylaxis regimens, 10% to 30% of all patients undergoing allogeneic bone marrow transplantation for leukemia, and 15% to 55% of solid organ transplants, developed CMV pneumonia with case fatality rates of greater than 80% in some series.^{26,123,124} The relatively high frequency of CMV pneumonia in lung transplant recipients may be a correlate of animal model data that indicate the lungs are a major site of latent CMV infection.¹²⁵ Before the use of ganciclovir as therapy for CMV disease in AIDS patients, the case fatality rate for CMV pneumonia in this patient cohort was 75% when CMV was the only pathogen identified. Mixed infections with CMV and another pathogen had an even worse prognosis, and the case fatality rate for patients with pulmonary disease caused by CMV and *Pneumocystis jiroveci* (formerly *carinii*) was 92%.¹²⁶

Cytomegalovirus pneumonia can show various histopathologic patterns (Fig. 11.5). Extensive intraalveolar hemorrhage with scattered cytomegalic cells and relatively few inflammatory cell infiltrates may occur (Fig. 11.5A).¹²⁷ In a similar manner, extensive involvement of the alveolar epithelium with minimal inflammation or overt evidence of parenchymal injury has also been described.¹²⁸ Other patterns include multifocal lesions with mixed inflammatory cell infiltrates, hemorrhage, necrosis, and cytomegalic cells, or a diffuse, predominantly mononuclear cell infiltrate, interstitial pneumonitis with intraalveolar edema and fibrin deposition, and diffusely distributed cytomegalic cells (Fig. 11.5E).¹²⁹⁻¹³¹

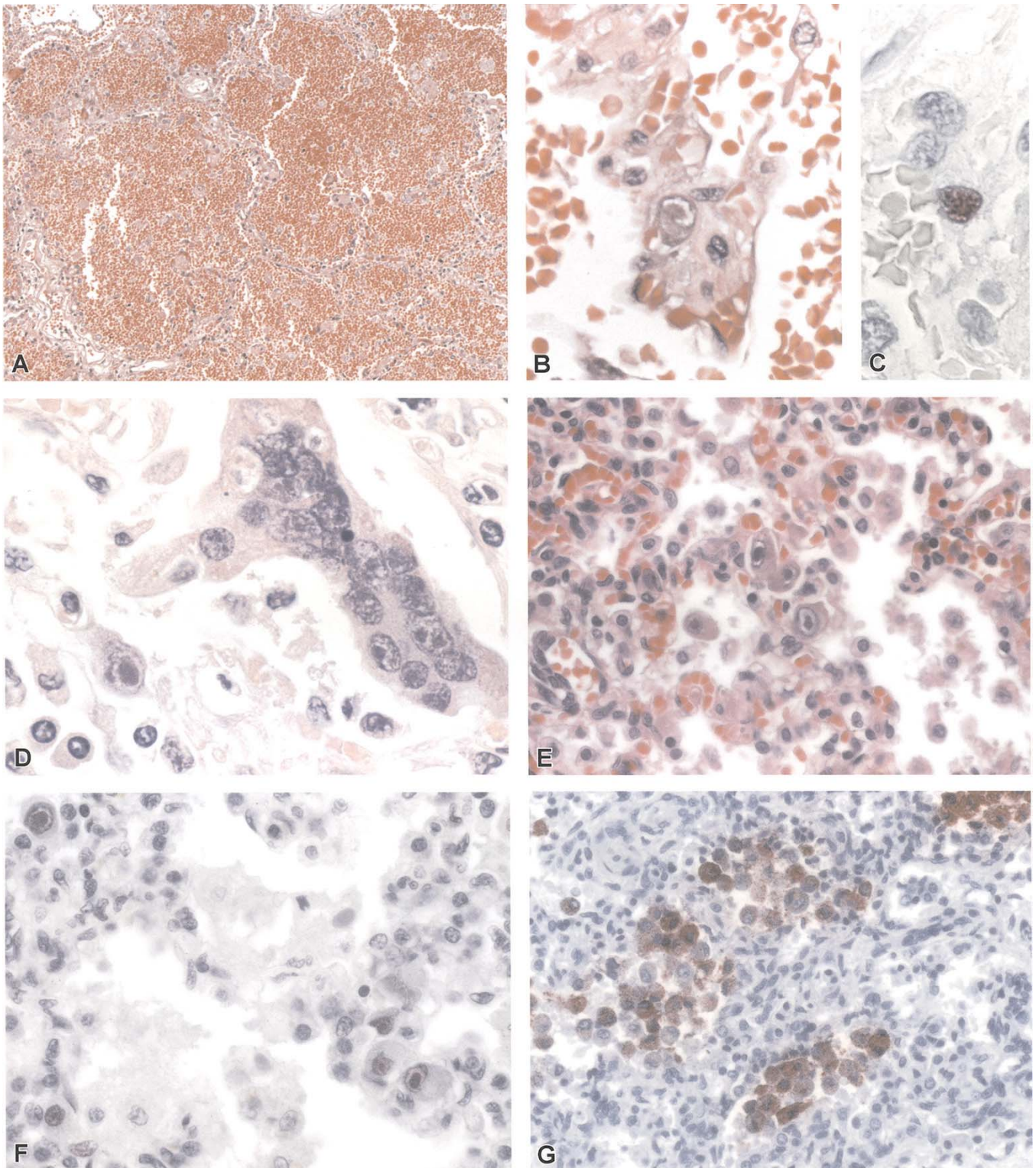


FIGURE 11.5. Cytomegalovirus (CMV) pneumonia. **A,E.** Diffuse intraalveolar hemorrhage with relatively little inflammation; interstitial pneumonitis, with diffusely distributed CMV-infected cells. **B.** CMV-infected cell showing large, amphophilic, owl's-eye intranuclear inclusion and smaller cytoplasmic inclusions. **C,F.** Immunohistochemical localization of CMV-infected cells

in the pulmonary parenchyma. **D,G.** CMV as a pulmonary coinfection in patients with fatal measles pneumonia (**D**), and in a patient with fatal pertussis (**G**). **A–D,** H&E; **C,F,G,** immunohistochemical localization of CMV-infected cells using alkaline phosphatase staining, naphthol fast-red, and hematoxylin counterstain.

The cytomegalic changes of CMV-infected cells are evident by standard H&E staining and are virtually pathognomonic of active CMV infection. The cells are enlarged (25 to 40 μm) and contain amphophilic to deeply basophilic intranuclear and intracytoplasmic inclusions (Fig. 11.5B,E). The single intranuclear inclusion is composed of viral nucleoprotein and assembled capsids, and is a large (up to 20 μm), round to ovoid body with a smoothly contoured border that is generally surrounded by a clear halo that gives the inclusion a distinctive owl's-eye appearance. The host cell nucleolus is often retained in the inclusion.¹³¹ Cytoplasmic inclusions are small (1 to 3 μm), granular bodies that appear after the intranuclear inclusion is well developed and are not uniformly present in all CMV-infected cells (Fig. 11.5B). These inclusions represent a mixture of virions and various cellular organelles, and increase in size and number as the infection progresses.¹³² Unlike the intranuclear inclusion, the cytoplasmic inclusions stain with periodic acid-Schiff stain and are deeply argyrophilic with Gomori's methenamine silver stain.¹³³

Cytomegalovirus pneumonia is defined by the presence of signs or symptoms of pulmonary disease combined with the detection of CMV in bronchoalveolar lavage (BAL) fluid or lung tissue samples. In this context, detection methods that support this definition include virus isolation, histopathologic observation of cytomegalic cells, ISH, or IHC stains (Fig. 11.5F). Detection by PCR alone is considered too sensitive for the diagnosis of CMV pneumonia and is insufficient for this purpose.¹³⁴ Cytomegalovirus is most often cultured in human diploid fibroblasts such as human embryonic lung and human foreskin fibroblasts. It grows slowly in conventional cell culture, and the cytopathic effect is generally not detected until the second week or longer after inoculation. For this reason, a shell vial method using centrifugation to enhance infectivity has become the standard isolation technique and can usually yield diagnostic results within 48 hours.¹³⁵

Herpes Simplex Viruses

For centuries, the term *herpes*, derived from the Greek *erpein* (to crawl), was used in medicine to describe any spreading cutaneous lesion. By the end of the 19th century, investigators surmised that the herpetic lesions of the lips and genitalia were manifestations of a single infectious agent, and recognized that it was a disease distinct from herpes zoster.^{136,137} As with all human herpesviruses, HSV is a large, enveloped, double-stranded DNA-containing virion with an icosahedral nucleocapsid approximately 100 to 110 nm in diameter, composed of 162 capsomers. The

nucleocapsid is surrounded by an amorphous, sometimes asymmetric material (the tegument) that is surrounded by a thin, trilaminar envelope that contains numerous glycoprotein spikes (Fig. 11.1C). The assembly of HSV begins in the nucleus of its host cell and the virus acquires its envelope as the capsid buds through the inner lamella of the nuclear membrane.^{120,138} Two serologic types are recognized and each is most frequently associated with particular disease syndromes; however, either serotype may cause any of the aggregate clinical syndromes. Herpes simplex virus-1 causes gingivostomatitis, pharyngitis, esophagitis, keratoconjunctivitis, and encephalitis, and is the serotype most commonly associated with adult HSV pneumonia. Herpes simplex virus-2 typically infects genital sites such as the penis, urethra, vulva, vagina, and cervix, and is the serotype associated with approximately 80% of disseminated disease and pulmonary infections in newborn infants.¹³⁶

All herpesviruses have the ability to persist in an inactive state for varying periods of time and then recur spontaneously following undefined stimuli associated with physical or emotional stress, trauma to nerve roots or ganglia, fever, immunosuppression, or exposure to ultraviolet radiation.¹³⁸ During the primary infection, HSV replicates at the portal of entry (typically oral or genital mucosae), and infects sensory nerve endings. The virus is transported centripetally along peripheral sensory nerves to central axons and finally to nerve cell bodies in the trigeminal, sacral, and vagal ganglia, where it replicates briefly before becoming latent.¹³⁹⁻¹⁴¹ Antiviral drugs have no effect on latent infection with HSV. Following cues that initiate viral reactivation, HSV replicates in sensory ganglia and is transported centrifugally along sensory nerves to epithelial cells on mucosal surfaces.¹³⁸ Reactivation of HSV from the trigeminal ganglion is associated with asymptomatic excretion of virus in saliva, and with the development of herpetic ulcers on the vermilion border of the lip, oral mucosa, or external facial skin.¹⁴²

Newborn infants, severely immunosuppressed or burned patients, and patients with severe trauma are at greatest risk of developing HSV pneumonia.¹⁴³⁻¹⁴⁶ Lower respiratory tract disease in neonates is most commonly associated with disseminated herpetic infections. Disseminated HSV infection in the newborn was first described in 1935 as "hepatoadrenal necrosis"¹⁴⁷ because of the prominent and frequent necroses that occur in the livers and adrenal glands of affected neonates.¹⁴⁸ Most cases of neonatal disease represent primary HSV infections and are acquired during parturition from HSV-infected mothers. The incidence of neonatal HSV infection is approximately 1 in 3200 deliveries, and disseminated disease develops in approximately 25% of infected neonates.¹⁴⁹ In disseminated infections, signs and symptoms

appear a mean of 5 days after birth (range, 0 to 12 days), and approximately 40% to 50% of these patients develop pneumonia. In the preantiviral era, 85% of neonates with disseminated disease died from the infection. With early diagnosis and high-dose acyclovir therapy, mortality has been reduced to approximately 30%.^{136,138,149} The disease can be exceedingly difficult to diagnose in a timely manner as only 10% of mothers of affected infants have clinically apparent HSV infection at the time of delivery.¹⁵⁰ Neonates that survive severe disseminated disease may develop hepatic and adrenal calcifications evident on abdominal radiographs.¹⁵¹

In adults, infection of the respiratory tract with HSV may be associated with disseminated herpetic infection, but is more commonly identified as an isolated disease manifestation resulting from reactivation of latent herpetic infections in the oropharynx. Herpetic tracheobronchitis is an ulcerative process characterized by large areas of denuded mucosal epithelium and fibrinopurulent exudate containing necrotic cells with densely eosinophilic cytoplasm. Despite extensive tissue damage, cells with intranuclear inclusions may be sparse, and, when identified, are found most often at the margins of the ulcerated epithelium or occasionally in the mucous glands subjacent to ulcerated surfaces.¹⁵² Aspiration of virus-containing secretions into the lower respiratory tract is believed to be the most frequent cause of pulmonary infection with HSV; however, oral lesions may be absent in patients with herpetic laryngotracheobronchitis and bronchopneumonia.¹⁵³ Disease can be also associated with airway trauma caused by tracheal intubation or from hematogenous dissemination of HSV.^{144,152,154} Chest radiographs of HSV pneumonia generally show ill-defined nodular or reticular densities of various sizes scattered in both lung fields. During the early stages of disease, these nodules measure 2 to 5 mm and are best seen in the periphery of the lungs. As the disease progresses, these lesions coalesce and enlarge to form more extensive infiltrates.¹³⁷

Herpetic infections of the airways and lung are characteristically difficult to diagnose clinically and HSV pneumonia was not described as a distinct clinical entity until 1949.¹⁵⁵ Several studies attest to the relative infrequency with which this diagnosis is considered in patients with respiratory disease. For example, none of the 15 cases of HSV disease of the middle and lower respiratory tract identified in a review of autopsies at Brooke Army Medical Center during 1965 to 1968 were suspected prior to autopsy.¹⁴³ In a 1982 review of 20 culture-confirmed cases of HSV pneumonia, none of the patients had been diagnosed prior to death and all 16 had oral herpetic lesions at the time of death.¹⁴⁴ Recent investigations also suggest that lower respiratory tract disease caused by HSV may be more common than currently appreciated. In a study from Sweden, HSV was cultured from pro-

ected brush and BAL specimens of 34 (26%) of 132 consecutive patients who required assisted ventilation for a suspected acute lower respiratory infection.¹⁵⁶ A similar study from Australia identified an herpetic infection of the lower respiratory tract cytologically in tracheobronchial secretions of 14 (30%) of 46 consecutive patients with ARDS.¹⁵⁷ Concomitant bacterial or fungal pulmonary infections are identified in approximately 20% to 30% of patients with HSV pneumonia.^{144,156}

A diagnosis of tracheobronchitis and pneumonia is best established histologically (Fig. 11.6). Because lower respiratory tract HSV infections are often focused in the tracheobronchial tree, open lung biopsy may be less sensitive than bronchoscopy.¹⁵⁴ Herpetic lesions show extensive necrosis and karyorrhectic debris and are associated with hemorrhage and a sparse-to-moderate neutrophilic infiltrate (Fig. 11.6A,B). Intranuclear inclusions are best appreciated in cells at the leading edge of necrotic foci (Fig. 11.6B,C). Inclusions appear either as homogeneous, amphophilic, and glassy (Cowdry type B inclusions), or as eosinophilic with a halo separating the inclusion from the nuclear membrane (i.e., Cowdry type A inclusions).¹⁵⁸ Cowdry type B inclusions contain actively replicating virus. Type A inclusions, considered noninfectious and devoid of viral nucleic acid or protein, represent the nuclear "scar" of HSV infection.^{136,141} Other changes associated with HSV, including multinucleation and nuclear molding, and ballooning degeneration of the cytoplasm, are more frequently associated with squamous epithelium and are seldom encountered in the lung. Because of the high frequency of hepatic and adrenal involvement with disseminated HSV infection in young children (Fig. 11.6F,G), liver biopsy has been suggested as a diagnostic technique in this patient cohort.¹⁴⁸ Commercially available antibodies exist for IHC detection of HSV in tissues (Fig. 11.6D).¹⁵⁹

Virus isolation remains an important diagnostic method; however, because HSV can be isolated from oropharyngeal secretions and occasionally from the lower respiratory tract of patients who lack overt pulmonary disease, virologic cultures must be interpreted in the context of complementary clinical, radiographic, and histopathologic findings as much as possible. Cell culture systems susceptible to HSV include Vero cells and foreskin fibroblasts. Cytopathic effects generally develop within 24 to 48 hours after cultures are inoculated with infectious specimens. Suitable specimens include scrapings made from mucocutaneous lesions, tracheobronchial aspirates, or BAL specimens. In infants with evidence of hepatitis, it may also be useful to obtain duodenal aspirates for HSV isolation.¹³⁸ Polymerase chain reaction methods that amplify HSV DNA from clinical specimens, including tissue and blood, can be particularly useful by specifically distinguishing between HSV-1 or HSV-2 infections.^{138,149}

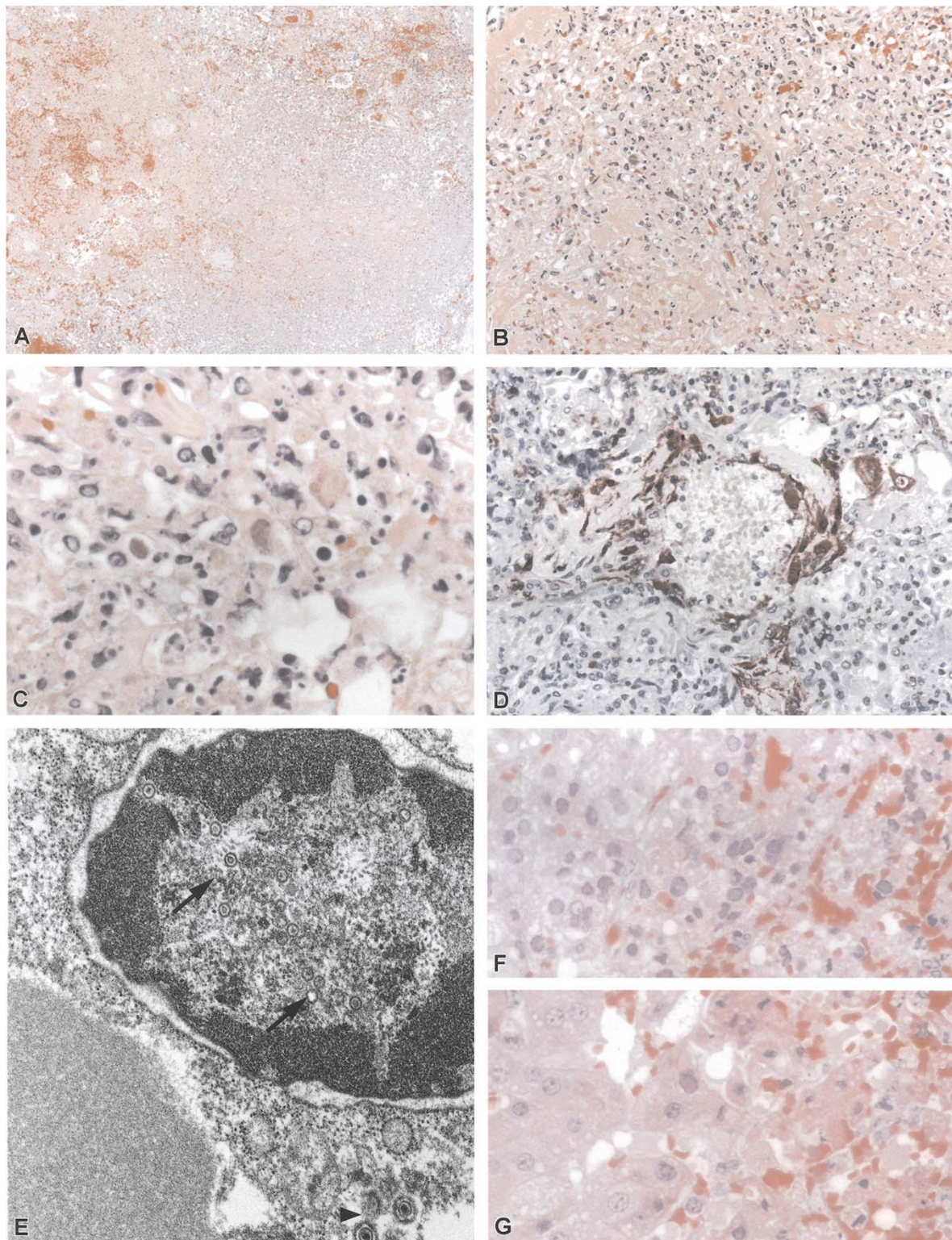


FIGURE 11.6. Herpes simplex virus (HSV) pneumonia. **A,B.** Extensive necrosis and hemorrhage and mild to moderate neutrophilic infiltrate associated with herpes simplex pneumonia. **C.** Glassy, amphophilic, intranuclear inclusions in HSV-infected cells at the margin of a necrotic focus in the lung. **D.** Immunohistochemical localization of HSV in multiple cell types in the lung of a patient with fatal HSV pneumonia. **E.** HSV-infected cell showing viral nucleocapsids (arrows)

within the nucleus and complete, enveloped virions (arrowhead) in the cytoplasm. (Courtesy of C. Goldsmith.) **F,G.** Herpetic inclusions in cells of the adrenal cortex (**F**) and in hepatocytes (**G**) of an infant with fatal disseminated HSV-2 infection. Scale bar, 100nm. **A–C,F,G,** H&E; **D,** immunoalkaline phosphatase staining, naphthol fast-red, and hematoxylin counterstain; **E,** uranyl acetate and lead citrate stain).

Varicella-Zoster Virus

Varicella-zoster virus (VZV), also known as human herpesvirus 3 (HHV-3), is a human α -herpesvirus most closely related to HSV. It has a linear, double-stranded DNA genome with approximately 125 kbp that encodes more than 70 proteins. The icosahedral nucleocapsid is indistinguishable in appearance from other herpesviruses. The nucleocapsid and the tegument are surrounded by a lipoprotein envelope derived from the host cytoplasmic membranes. The enveloped viral particle is pleomorphic to spherical in shape and 180 to 200 nm in diameter.¹⁶⁰ The primary infection is initiated by inoculation of respiratory mucosa by the virus through infectious aerosols or by direct contact of skin lesions of patients with varicella or herpes zoster. After a primary viremia in the reticuloendothelial system, and secondary viremia in circulating mononuclear cells, the virus is disseminated to the skin, where it initiates a vesicular rash, and back to mucosal sites in the lungs. The release of infectious virus into respiratory droplets is a pathogenic characteristic that distinguishes VZV from other human herpesviruses. The attack rate for previously uninfected household contacts exposed to varicella is approximately 90%. For less sustained exposure, it is estimated to be approximately 10% to 30%.¹⁶⁰

During primary infection with VZV, viral replication in keratinocytes (Fig. 11.7A) and vascular and lymphatic endothelial cells of the superficial dermis produces the generalized, pruritic, vesicular rash of varicella commonly known as chickenpox. Varicella-zoster virus also establishes latent infection within satellite cells and neurons of the trigeminal and dorsal root ganglia and can reactivate under various conditions to cause herpes zoster, a painful vesicular rash commonly referred to as shingles.¹⁶¹ The origin of the term *chickenpox* is speculative, but believed to derive from *gican*, an Old English term for itching. The term *shingles* originates from the medieval Latin *cinguls*, or girdle, and alludes to the partial encircling of the trunk by the rash of herpes zoster.^{137,160}

Varicella-zoster virus is ubiquitous in human populations around the world, and humans are the only known host. During the prevaccine era in the U.S., approximately 4 million cases, 4000 to 9000 hospitalizations, and 50 to 140 deaths were reported annually.^{25,162} The risk of severe illness during primary or recurrent VZV infection appears to depend more on host factors rather than a particular viral strain. Chickenpox is considered a relatively benign infection in children, but adult patients are approximately 25 times more likely than children to develop pneumonia. The greatest risk of severe disease and pneumonia occurs in those patients with chronic lung disease, immunosuppressing conditions, neonates, and pregnant women.¹⁶³ Varicella-zoster virus-related deaths have declined sharply in the U.S. since universal childhood vaccination was implemented in 1995.^{24,25}

Varicella pneumonia was first described in the medical literature in 1942¹⁶⁴ and is the most frequently reported complication of chickenpox in adult patients.^{24,165} Pneumonia occurs in approximately 10% to 15% of adults infected with VZV.^{166,167} The occurrence of pneumonia during herpes zoster is rare, and limited primarily to profoundly immunosuppressed patients, particularly bone marrow transplant recipients.¹³⁷ Varicella-zoster virus pneumonia generally develops within 2 to 7 days following the onset of rash and may be characterized by fever, cough, tachypnea, chest pain, and hemoptysis.^{26,168} Hypoxemia is common and may be severe. Radiographically, the lungs show multiple, scattered, defined, nodular densities. Untreated adult varicella pneumonia is fatal in approximately 10% of cases, but mortality is as high as 25% to 40% in certain high-risk cohorts, including pregnant women, transplant recipients, and neonates.^{137,169-171} Massive pulmonary hemorrhage is a frequent terminal event.

Gross examination reveals lungs that are generally two to three times heavier than normal, firm, and plum-colored. There are often multiple necrotic and hemorrhagic lesions on the visceral pleura that resemble the pox lesions of skin.^{169,172,173} Pox may also be seen on the parietal pleura, although pleural effusions are uncommon and rarely prominent.^{163,173} The trachea and bronchi are generally edematous and erythematous with occasional vesicles on the mucosal surfaces, and there may be lobular consolidation of the lungs. Microscopically, pulmonary involvement consists primarily of interstitial pneumonitis and diffuse miliary foci of necrosis and hemorrhage in the pulmonary parenchyma that involve alveolar walls, blood vessels, and bronchioles (Fig. 11.7B,D).¹⁷² Other findings may include intraalveolar collections of edema, fibrin, or hemorrhage, diffuse alveolar damage, and septal edema.^{164,168,173} Virally infected cells with intranuclear inclusions may be identified in respiratory epithelial cells, pneumocytes, interstitial fibroblasts, or capillary endothelium (Fig. 11.7E,F).¹⁶⁷ Eosinophilic intranuclear inclusions and multinucleated syncytial cells may be difficult to locate but are best identified at the edges of necrotic foci (Fig. 11.7C). In cases of disseminated disease, similar necrotizing hemorrhagic lesions and occasional viral cytopathic changes in epithelial cells or fibroblasts may be observed in other tissues and organs, including esophagus, pancreas, liver, renal pelves, ureters, urinary bladder, spleen, bone marrow, thymus, lymph nodes, adrenal glands, and brain.^{172,174} In those patients who recover from severe VZV pneumonia, some necrotic parenchymal foci may mineralize, and can be identified by chest radiograph years later as miliary, 1 to 5 mm, nodular opacities. Microscopically, the lesions are characterized as discrete collections of dense fibrous connective tissue that surround multiple, small, calcified bodies. The periphery may include a cellular zone of fibroblasts and occasional giant

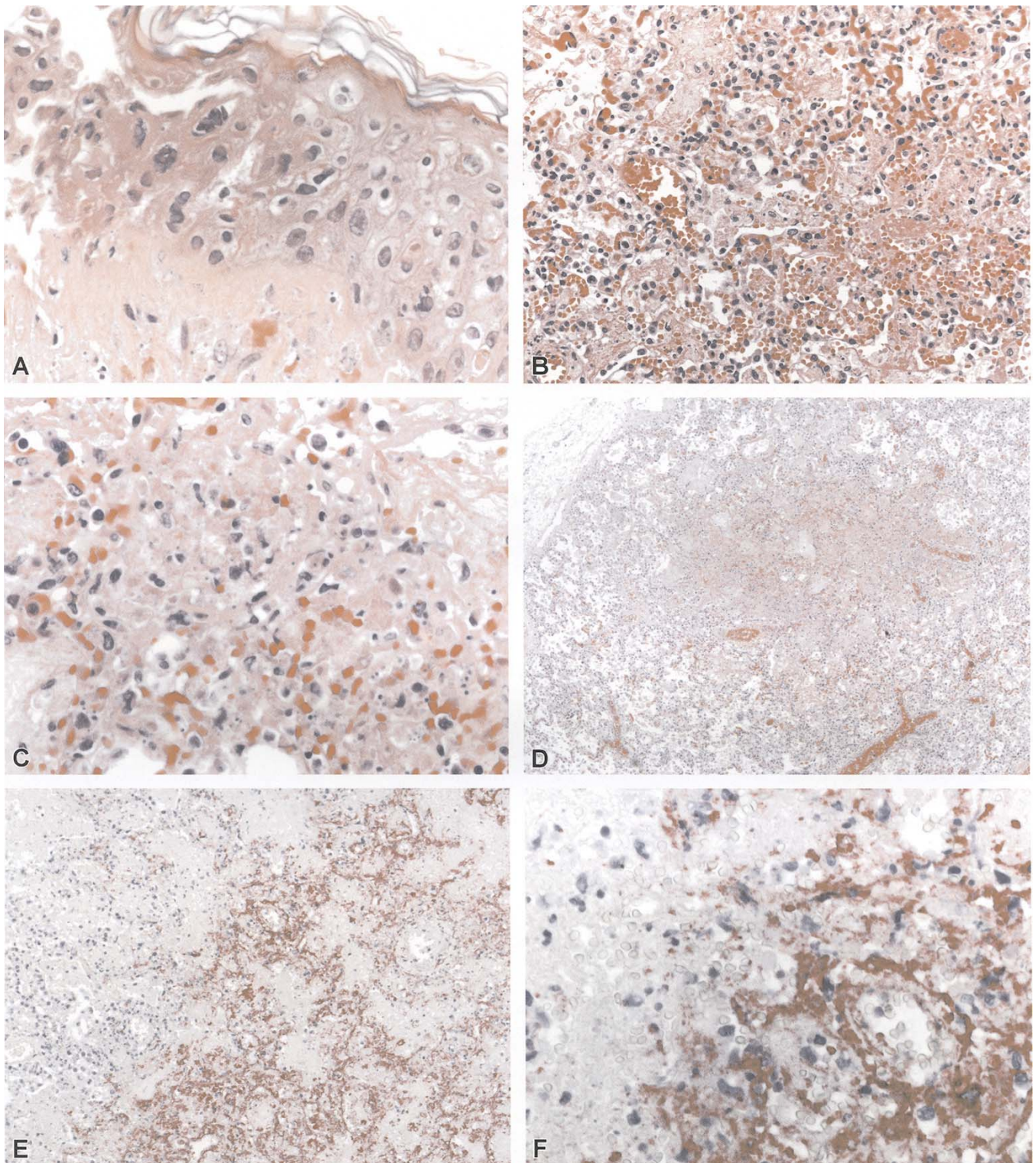


FIGURE 11.7. Varicella zoster virus (VZV) pneumonia. **A.** Viral cytopathic changes involving the keratinocytes in a cutaneous lesion of a patient infected with VZV. The histopathology includes multinucleate cells with nuclear molding and epidermal necrosis. **B.** Interstitial pneumonitis and intraalveolar collections of fibrin and hemorrhage in a patient with fatal VZV pneumonia. **C.** Eosinophilic intranuclear inclusions in VZV-infected cells at the edge of a necrotic pulmonary focus. **D.** A

miliary focus of necrosis and hemorrhage involving air spaces that is characteristic of VZV pneumonia. **E,F.** Immunohistochemical staining of VZV antigens in the pulmonary parenchyma of patient with fatal varicella pneumonia. In the lungs, VZV infects various cell types, including respiratory epithelium, pneumocytes, endothelial cells, and fibroblasts. **A–D,** H&E; **E,F,** immunoalkaline phosphatase staining, naphthol fast-red, and hematoxylin counterstain.

cells.¹⁷⁵ A radiographic survey of 16,894 persons identified pulmonary calcifications in eight (1.7%) of 463 patients who had chickenpox during adulthood compared with only eight (0.05%) of the remaining 16,431 who did not report having varicella as an adult.¹⁷⁶

A positive history of varicella predicts immunity in >95% of persons.¹⁶⁰ Because pulmonary symptoms most often occur several days following the onset of the characteristic rash of varicella, a pathologic diagnosis is seldom required for a real-time diagnosis of VZV pneumonia. However, hematopoietic cell transplant recipients may present with signs of visceral dissemination and pneumonia 1 to 4 days before the localized cutaneous eruption of herpes zoster appears, and lower respiratory tract disease has been described in the absence of skin lesions, particularly in neonates and bone marrow transplant recipients.^{26,137,177} Commercially available antigen detection kits can be used for rapid diagnosis of cutaneous VZV infection. Epithelial cells are scraped from the base of a newly formed vesicle, applied to a slide, and stained by using fluorescein-conjugated VZV monoclonal antibodies to detect specific viral proteins in the specimen. In a similar manner, the Tzanck test uses Wright-Giemsa stain to demonstrate multinucleated giant cells in these specimens; however, this test does not differentiate between HSV and VZV, and false-negative results are common. Commercially available antibodies are also available for IHC detection of VZV in tissue specimens (Fig. 11.7E,F); however, relatively few laboratories are able to provide well-validated assays. Some commercial laboratories offer PCR amplification to detect viral nucleic acid in clinical specimens.

Isolation of the virus in cell culture remains the reference standard for the diagnosis of VZV. In human melanoma cells, an excellent substrate for VZV isolation, the average time for visible cytopathic effect from the virus is 3 to 5 days.¹⁷⁸ Infectious VZV is usually recoverable from the clear fluid of cutaneous vesicles of varicella for approximately 3 days after the appearance of these lesions and for approximately 1 week from herpes zoster lesions. The lungs are the most common organ from which VZV is isolated at autopsy, but isolates have also been obtained from heart, liver, pancreas, gastrointestinal tract, brain, and eyes.¹⁶⁰

Influenza Viruses

Influenza is derived from the term *influentia*, meaning epidemic in the Italian form of Latin, originally used because epidemics were thought to result from astrologic or other occult influences. Influenza is a highly contagious, acute respiratory illness with a spectrum of clinical illness ranging from asymptomatic or mild disease with rhinitis or pharyngitis to primary viral pneumonia with

fatal outcome. Influenza may also be associated with a broad range of other disorders affecting the heart, brain, kidneys, and muscle.

Influenzaviruses belong to the Orthomyxoviridae family, which consists of four genera that include the two important influenza viruses types A and B associated with significant human disease.^{179,180} Influenza A viruses are further classified into subtypes based on the antigenicity of their hemagglutinin (HA) and neuraminidase (NA) surface glycoproteins. Only one type of HA and one type of NA are recognized for influenza B. Influenza A occurs in both pandemic and interpandemic forms. Fortunately, pandemics, defined as worldwide outbreaks of severe disease, occur infrequently. Interpandemic influenza, although less extensive in its impact, occurs virtually every year. The epidemiologic pattern of influenza in humans is related to two types of antigenic variation of its envelope glycoproteins, namely antigenic drift and antigenic shift. During antigenic drift, new strains related to those circulating in previous epidemics evolve by accumulation of point mutations in the surface glycoproteins. This enables the virus to evade the immune system leading to repeated outbreaks during interpandemic years. Antigenic shift occurs with the emergence of a “new” potentially pandemic, influenza A virus that possesses a novel HA alone or in combination with a novel NA.

There are 16 recognized HA subtypes and nine NA subtypes of influenza A virus. Viruses from all HA and NA subtypes have been recovered from aquatic birds, but only three HA subtypes (H1, H2, and H3) and two NA subtypes (N1 and N2) have established stable lineages in the human population since 1918. Since 1997, widespread avian infection with influenza A (H5N1) and associated clusters of human disease have aroused concern about the threat of a pandemic, and attention has been appropriately focused on control measures to deal with such an event.

All Influenzaviruses have a segmented, negative-sense RNA core surrounded by a lipid envelope. Influenzavirus particles are pleomorphic. Among isolates that have undergone a limited number of passages in cell culture or eggs, more filamentous than spherical particles are seen. Spherical morphology becomes dominant when the virus is extensively passaged in the laboratory. A 10- to 12-nm layer of HA (rod-shaped) and NA (mushroom-shaped) spikes project radially on the surface of the influenza A and B viruses. Hemagglutinin facilitates entry of virus into host cells through its attachment to sialic-acid receptors. Because neutralizing antibodies are directed against this antigen, it is a critical component of current influenza vaccines. Neuraminidase, the second major antigenic determinant, catalyzes the cleavage of glycosidic linkages to sialic acid and the release of progeny virions from infected cells. Accordingly, it has become an important target for drug inhibitors such as oseltamivir

and zanamivir. The M2 surface component and channel of influenza A (not present in influenza B virus) regulates the internal pH of the virus and is blocked by the antiviral drug amantadine.

Influenzaviruses are spread person-to-person primarily through the coughing and sneezing of infected persons. The typical incubation period for influenza is 1 to 4 days, with an average of 2 days. Adults can be infectious from the day before symptoms begin through approximately 5 days after illness onset. Children can be infectious for ≥ 10 days, and young children can shed virus for several days before their illness onset. Severely immunocompromised persons can shed virus for weeks or months.

Uncomplicated influenza illness is characterized by the abrupt onset of constitutional and respiratory signs and symptoms (e.g., fever, myalgia, headache, malaise, non-productive cough, sore throat, and rhinitis). Among children, otitis media, nausea, and vomiting are also commonly reported with influenza illness. Respiratory illness caused by influenza is difficult to distinguish from illnesses caused by other respiratory pathogens on the basis of symptoms alone. Influenza typically resolves after 3 to 7 days in most patients, although cough and malaise can persist for >2 weeks. Among certain persons, influenza can exacerbate underlying medical conditions (e.g., pulmonary or cardiac disease), lead to secondary bacterial pneumonia or primary influenza viral pneumonia, or occur as part of a co-infection with other viral or bacterial pathogens. Young children with influenza infection can have initial symptoms that mimic bacterial sepsis. More than 20% of children hospitalized with influenza can have febrile seizures. Influenza has also been associated with encephalopathy, transverse myelitis, Reye syndrome, myositis, myocarditis, and pericarditis. The risks for complications, hospitalizations, and deaths from influenza are higher among persons aged ≥ 65 years, young children, and persons of any age with certain underlying health conditions than among healthy older children and younger adults. Influenza-related deaths can result from pneumonia or from exacerbations of cardiopulmonary conditions and other chronic diseases.

The histopathologic features of nonfatal and fatal influenza have been well described and include necrotizing bronchitis, thrombosis, interstitial inflammation, hemorrhage, hyaline membrane formation, and intraalveolar edema (Figs. 11.8A,B, 11.9A,C, and 11.10A).^{105,181-191} The pathology is more prominent in larger bronchi, and inflammation may vary in intensity in individual patients. Viral inclusions cannot be identified by light microscopy (Fig. 11.8D). Secondary bacterial infections with organisms such as *Streptococcus pneumoniae* (group A streptococcus [GAS]), *Staphylococcus aureus*, and *Haemophilus influenzae* may occur as a complication in about 50% to 75% of fatal cases and make it difficult to recognize the pathologic changes associated with the primary viral infec-

tion.^{190,192,193} The histopathologic features in other organs may include myocarditis, cerebral edema, rhabdomyolysis, and hemophagocytosis (Figs. 11.8H and 11.9E,F). Immunohistochemistry and ISH assays demonstrate that viral antigens and nucleic acids are usually sparse and are primarily seen in the bronchioepithelial cells of larger bronchioles (Figs. 11.8C,E,F and 11.9D).^{105,189,190} Antigens are more readily identified in patients who die within 3 to 4 days of onset of illness. Recent studies suggest that unlike human influenza viruses, avian virus H5N1 preferentially infects cells in the lower respiratory tract of humans, resulting in extensive damage of the lungs with minimal pathology in the upper respiratory tract (Fig. 11.10A,C). This may help explain why the H5N1 avian influenza virus is so lethal to humans but so difficult to spread from person to person. These studies show that the avian virus preferentially binds to the α -2,3-galactose receptors, which are found only in and around the alveoli. This is in contrast to the human Influenzaviruses that preferentially bind to the α -2,6-receptors, which are found throughout the respiratory tract from the nose to the lungs.^{194,195} In birds and other animals, viral antigens can be detected in the lung as well as a variety of extrapulmonary tissues (Fig. 11.10B).

The diagnosis of influenza, suspected by history and clinical manifestations, can also be supported histopathologically. However, because of the absence of any characteristic viral inclusions and because the overall pathologic features of influenza may resemble other viral, rickettsial, and certain bacterial infections, an unequivocal diagnosis can be made only by laboratory tests such as viral culture, direct fluorescent antibody and rapid antigen assays, serology, and IHC.^{190,196,197}

Measles

Measles (rubeola) is an infectious, acute febrile viral illness characterized by upper respiratory tract symptoms, fever, and a maculopapular rash. The causative agent, a member of the genus *Morbillivirus*, of the family Paramyxoviridae,^{198,199} is an enveloped virus that contains a negative sense, single-stranded RNA genome of 16,000 nucleotides. Other human pathogens in this family include parainfluenza, mumps, and respiratory syncytial viruses. Measles virions are pleomorphic, generally spherical, enveloped particles from 120 to 250 nm in diameter. The virus is morphologically indistinguishable from other members of the Paramyxoviridae family when viewed by negative contrast electron microscopy. A lipid envelope surrounds a helical nucleocapsid composed of RNA and protein. Two transmembrane glycoproteins, hemagglutinin (H) and fusion (F), are present in the envelope and appear as surface projections. These proteins mediate viral attachment and

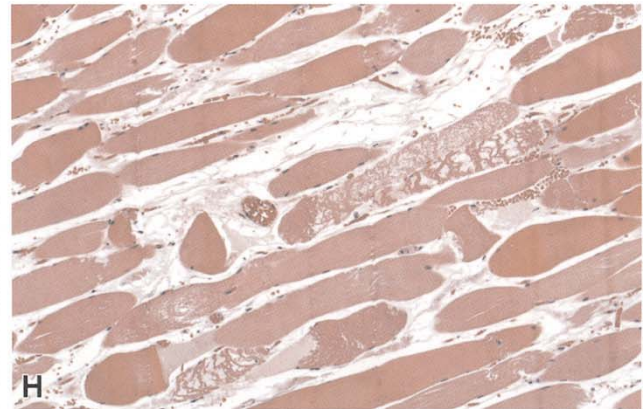
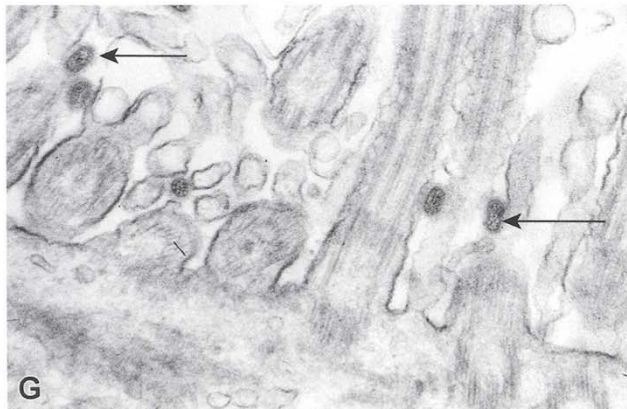
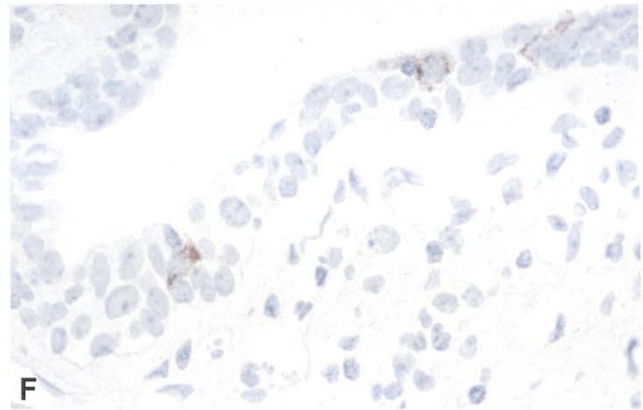
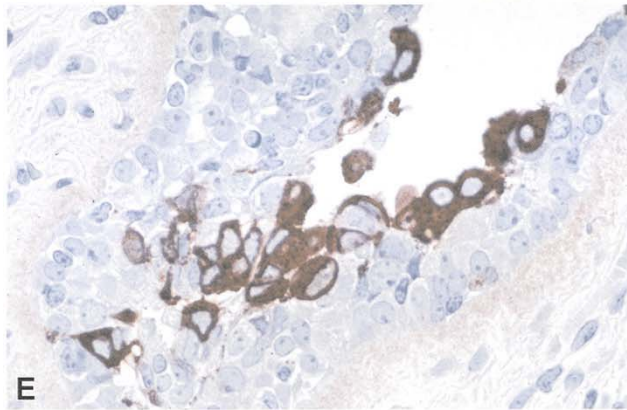
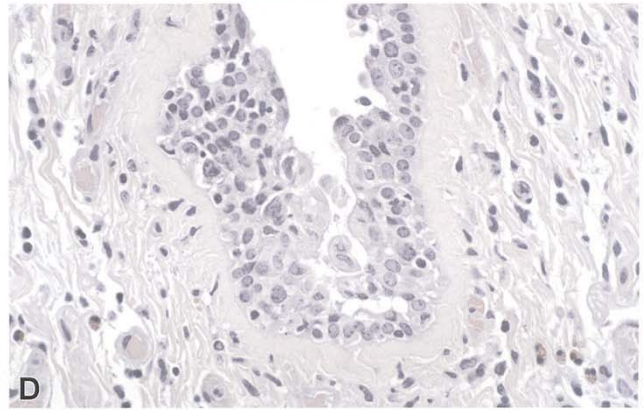
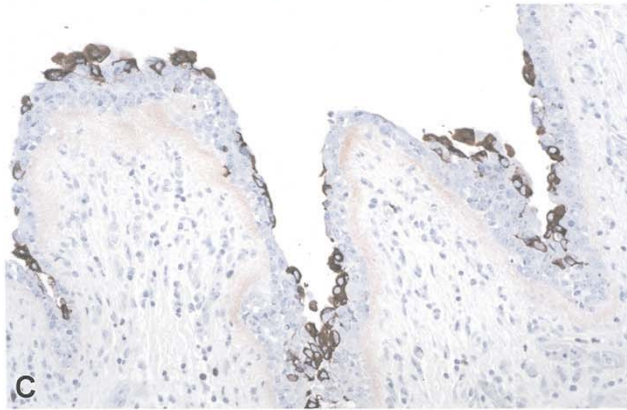
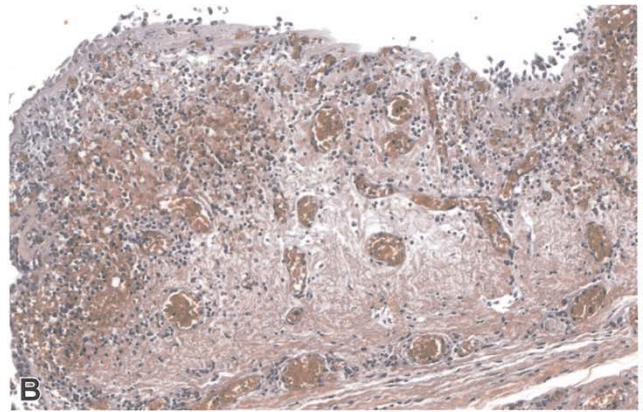
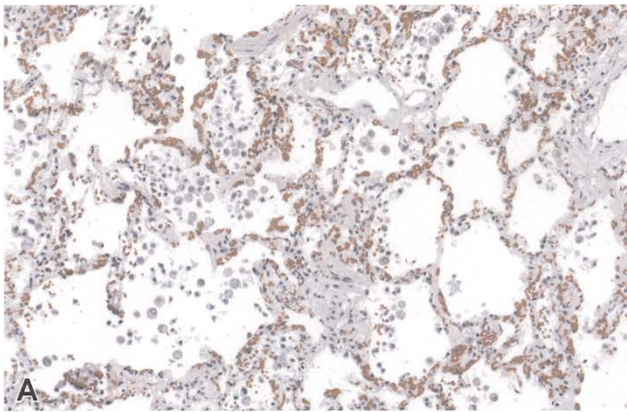


FIGURE 11.8. Influenza A. **A.** Alveolar damage in a patient with fatal influenza A showing prominent congestion with intraalveolar macrophages and fibrin deposits. **B.** Extensive ulceration of respiratory epithelium in a large airway of a patient with fatal influenza A. The lamina propria shows florid vascular congestion and focal hemorrhage, and predominantly mononuclear inflammatory cell infiltrates. **C–E.** Immunohistochemical staining (**C,E**) of influenza virus A hemagglutinin antigens in the cytoplasm of residual respiratory epithelial cells of a large airway. This same focus of extensively infected respiratory epithelium (**D**) demonstrates that, unlike many other viral respiratory pathogens, influenza viruses do not elicit specific cytopathic effects in infected cells. **F.** In-situ hybridization assay demon-

strating active replication of influenza A in respiratory epithelium in a large airway. **G.** Electron micrograph of influenza A particles (arrows) attached to the cilia of a rodent tracheal epithelial cell. Viral ribonucleoproteins are evident in the central aspect of the particles. The hemagglutinin and neuraminidase surface glycoproteins make up the peripheral spike layer. (Courtesy of F.A. Murphy.) **H.** Rhabdomyolysis in a patient with fatal influenza A. Bar, 100nm. **A,B,D,H,** H&E; **C,E,** immunoalkaline phosphatase stain, naphthol fast-red, and hematoxylin counterstain; **F,** digoxigenin-labeled probe followed by immunoalkaline phosphatase staining, naphthol fast-red, and hematoxylin counterstain; **G,** uranyl acetate, lead citrate stain.

fusion with respiratory epithelium. They are also believed to play a role in virus maturation through their interaction with the matrix (M) protein, which, in turn, is thought to interact with the nucleocapsid structure.²⁰⁰

Measles is a highly communicable disease of worldwide distribution. Before the introduction of measles vaccines, epidemics occurred about every 2 to 5 years when the percentage of nonimmune members of a population reached critical levels. Recently, epidemics have occurred in cycles of about 10 years. In small and isolated communities, measles circulation may cease altogether unless it is reintroduced. If introduced in nonimmune populations, the disease tends to be more severe and may involve more than 90% of the population because of the highly infectious nature of the virus.

Although still a significant problem in underdeveloped countries, measles infection became uncommon in the U.S. after the development and widespread use of an effective measles vaccine. However, a recrudescence of measles infection occurred in several large U.S. urban centers in recent years, associated with reduced use of the vaccine among children and young adults. During the peak of this activity (i.e., between 1989 and 1991), greater than 50,000 measles cases and approximately 150 measles-associated deaths were reported.²⁰¹

Measles virus is highly contagious, spread by aerosols and droplets from respiratory secretions of acute cases.^{202–204} Less frequently, contaminated fomites are involved in transmission. A person with acute measles is infective from just before onset of symptoms to defervescence of fever. In developed countries, likely settings for exposure to measles virus are infectious disease clinics, pediatric emergency rooms, and physicians' offices.²⁰⁵ Children are usually infected by 6 years of age, resulting in lifelong immunity, and almost all adults are immune. Clinical infection in children younger than 9 months of age is generally uncommon because of passive protection afforded the infant by the transfer of maternal antibodies. However, with the resurgence of measles in the U.S. came the realization that most women of childbearing age

acquired immunity to measles through vaccination and not through natural infection. Lower levels of maternal antibodies were found to be transferred from an immunized mother to her infant; thus, a substantial number of measles cases occurred in children younger than 1 year of age in the U.S. in recent years.

After an incubation period of about 1 to 2 weeks, the prodromal phase of measles begins with fever, rhinorrhea, cough, and conjunctivitis. Koplik's spots, which are small, irregular red spots with a bluish-white speck in the center, appear on the buccal mucosa in 50% to 90% of cases shortly before rash onset. An erythematous maculopapular rash begins on the face 3 to 4 days after prodromal symptoms and usually spreads to the trunk and extremities. The symptoms gradually resolve, with the rash lasting for approximately 6 days, fading in the same order as it appeared.

Although recovery is rapid and complete in most cases, complications can arise as a result of continued and progressive virus replication, bacterial or viral superinfections, or abnormal host immune response.^{204,206,207} The most common complications are secondary bacterial pneumonia and otitis media.²⁰⁶ Other complications include febrile convulsions, encephalitis, liver function abnormalities, chronic diarrhea, and sinusitis. Several pulmonary and central nervous system (CNS) syndromes that are often fatal have been described. Death occurs in about 1 of every 1000 measles cases; however, the risk of death and other complications is substantially increased in infants, adults, malnourished and immunocompromised individuals, persons with underlying illnesses, and nonimmunized populations in underdeveloped countries.^{208–212}

The first step in measles infection is attachment of the virus to CD46 cell surface receptors on the respiratory epithelium.²¹³ Adhesion and fusion of the virus to the respiratory epithelium is mediated by both the H and F viral glycoproteins.²¹⁴ This stage is followed by local replication in respiratory mucosa and draining lymph nodes. A primary viremia follows, with dissemination

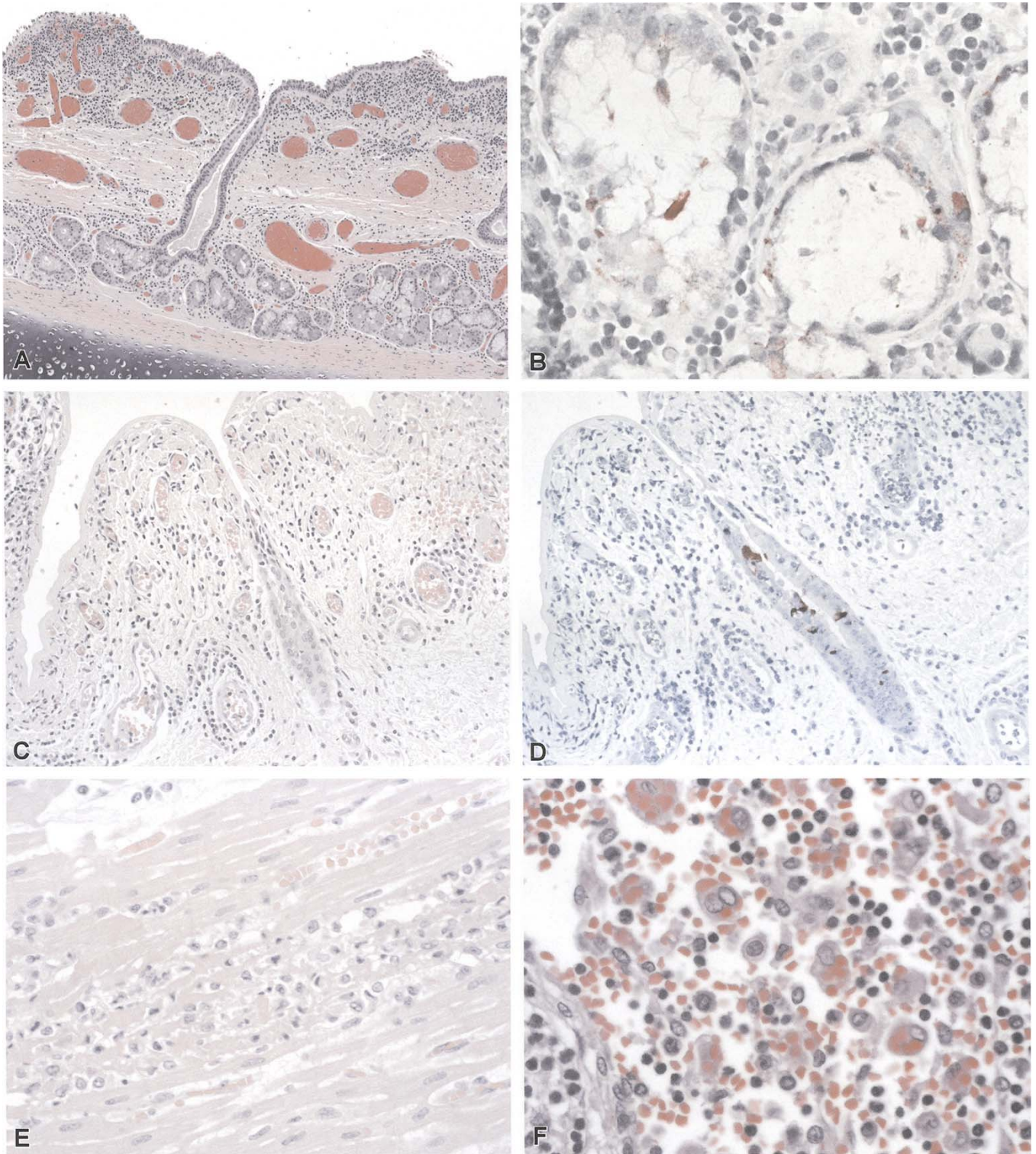


FIGURE 11.9. Influenza B. **A.** A cross-section of trachea from a child with fatal influenza B showing extensive vascular congestion and predominantly mononuclear inflammatory cell infiltrates in the lamina propria and submucosa. **B.** Immunohistochemical staining of influenza B antigens in epithelium of the tubuloalveolar submucosal glands. **C.** A bronchus of a child with fatal influenza B showing extensive denudation of the respiratory epithelium. **D.** Immunohistochemical staining of

influenza B antigens in epithelial cells lining a bronchial gland duct (same field as in **C**). **E.** Focus of myocyte necrosis accompanied by a mixed inflammatory cell infiltrate in the heart of a patient with fatal influenza B. **F.** Extensive hemophagocytosis in a parabranchial lymph node in a patient with fatal influenza B. **A,C,E,F,** H&E; **B,D,** immunoalkaline phosphatase staining, naphthol fast-red, and hematoxylin counterstain.

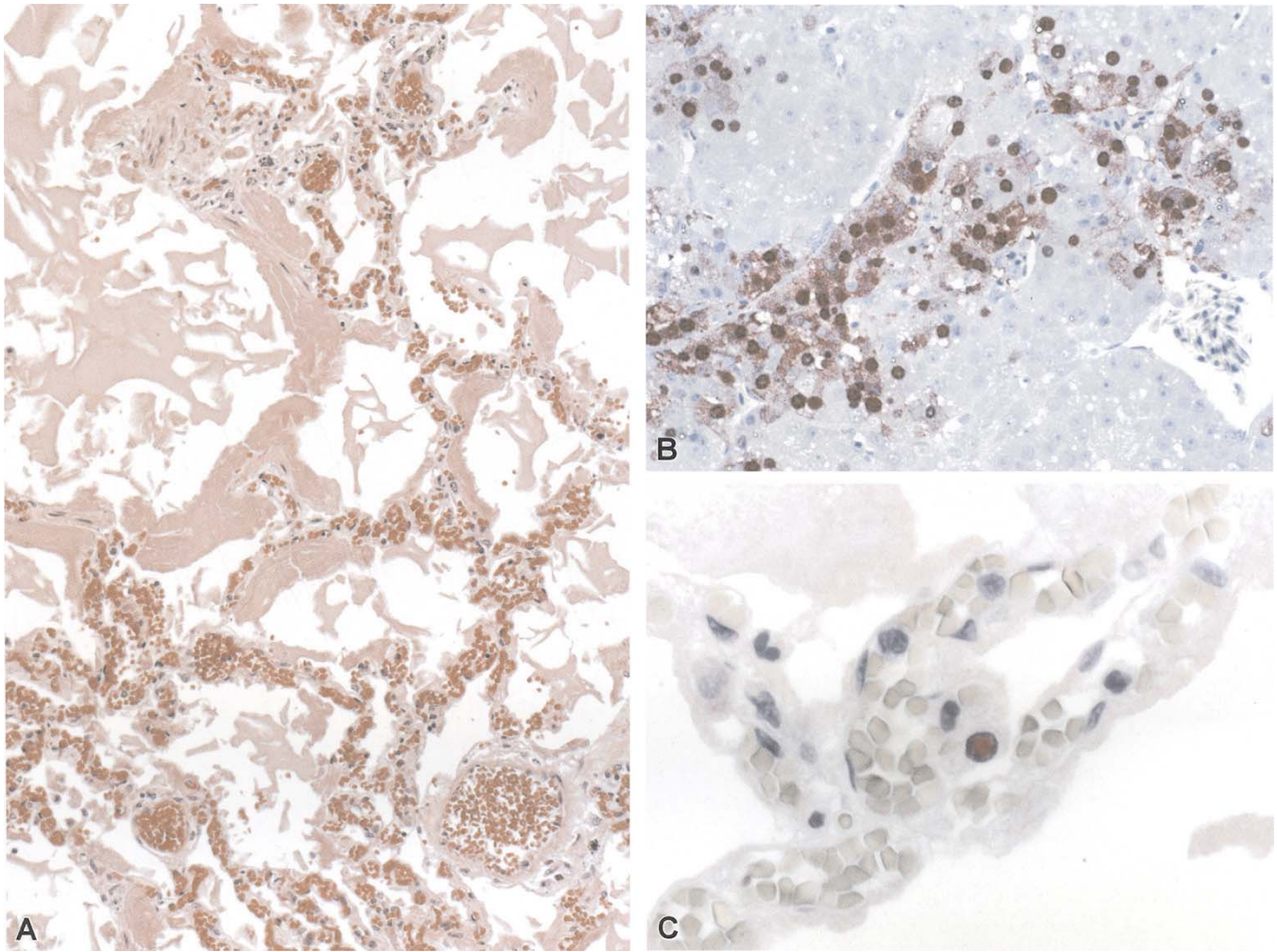


FIGURE 11.10. Avian influenza. **A.** Diffuse alveolar damage in a patient with fatal avian influenza (H5N1) showing extensive hyaline membrane formation and congestion. **B.** Influenza virus A (H5N1) antigens in the nuclei of avian hepatocytes. Influenza A is a zoonosis and aquatic birds represent the largest natural reservoir of the virus. **C.** Influenza virus A (H5N1) antigens in

the nucleus of a pneumocyte in the lung of a patient with fatal avian influenza. Unlike other influenza viruses that cause disease in humans, H5N1 preferentially infects alveolar epithelial cells, and causes relatively minimal pathology in the upper airway. **A,** H&E; **B,C,** immunoalkaline phosphatase stain, naphthol fast-red, and hematoxylin counterstain.

throughout the reticuloendothelial system. Replication of virus at the secondarily infected sites leads to lymphoid hyperplasia and the formation of characteristic reticuloendothelial multinucleated giant cells. A stage of secondary viremia soon develops, with widespread dissemination of virus to different tissues by infected lymphocytes and monocytes. At this point in the infection, prodromal symptoms, such as cough, coryza, and conjunctivitis, become more severe, and virus replication in the respiratory tract predisposes the infected individual to complications such as pneumonia and otitis media.

Two types of multinucleated giant cells have been described in patient tissues during measles infection.^{215,216} The reticuloendothelial giant cell (Warthin-Finkeldey) appears first during the incubation period and is seen in

different lymphoid tissues throughout the body. The second type is the epithelial giant cell, which has been observed in the epithelium of essentially every major organ.

The onset of the rash temporally coincides with the appearance of detectable serum antibody to measles virus. Interestingly, virus replication and giant cell formation cease with the appearance of rash. T-cell immunity is essential in the process of viral clearance from lymphoid tissue and respiratory tract. While children with congenital agammaglobulinemia respond normally to measles virus infection, patients with cell-mediated immunodeficiency develop severe disease that presents as giant-cell pneumonia or encephalopathy in the absence of an exanthem.^{208–211,217,218}

Immunity to the F surface glycoprotein is necessary to prevent the spread of measles infection.²¹⁹ An atypical measles syndrome characterized by pulmonary consolidation with pleural effusions and hilar adenopathy has been reported in children exposed to wild-type measles virus who had previously received the killed-measles virus vaccine.²²⁰⁻²²² Recipients of the formalin-inactivated vaccine have a good antibody response to the H protein, but antibodies to the functional region of the F protein and to the nucleoprotein are weak or absent. It has been suggested that the lack of a functional F antibody response may play a role in virus spread.²²³

The pathologic features of measles have been well described and several references containing detailed morphologic descriptions are recommended.^{131,209,224-230} The typical morbilliform skin lesions, Koplik's spots, and measles lymphadenitis are seldom seen by the surgical pathologist since the clinical diagnosis is usually apparent. Histopathologic changes in the skin include mild congestion, edema, and a predominantly mononuclear infiltrate surrounding small vessels of the dermis, as well as other nonspecific features. Occasional diagnostic multinucleated epithelial giant cells with eosinophilic cytoplasmic and nuclear inclusions are observed.^{228,231} Pathognomonic reticuloendothelial multinucleated giant cells can be observed in appendix specimens from patients mistakenly operated on for acute appendicitis before the emergence of diagnostic Koplik's spots and rash. These cells, which have been reported in various lymphoreticular tissues throughout the body, are typically large and contain from a few to occasionally up to 100 nuclei. These cells do not usually contain viral inclusions. The lymphoid tissues are typically hyperplastic, and the architecture is partially or totally obliterated by diffuse proliferation of immunoblasts.²³²⁻²³⁴

A focal or generalized interstitial pneumonitis, similar to that seen in many other viral infections, is seen in the lungs of measles patients. Histopathologic features seen

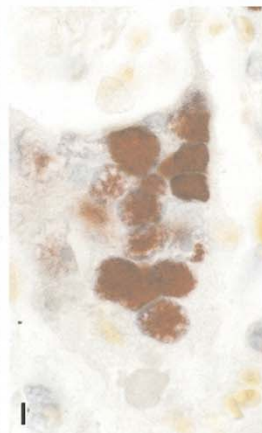
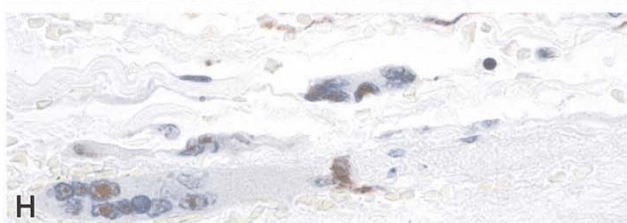
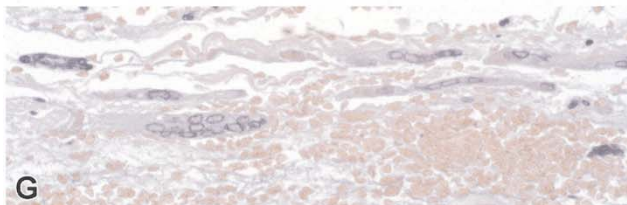
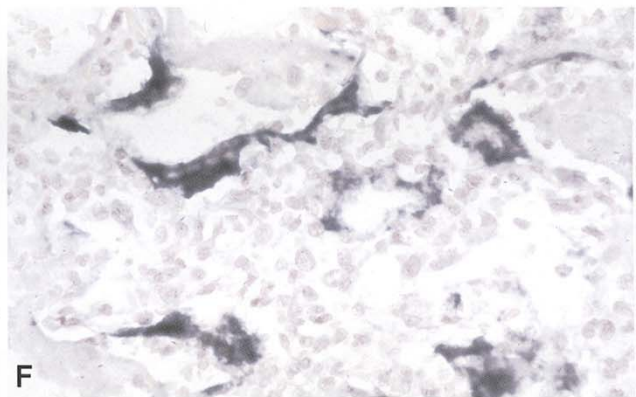
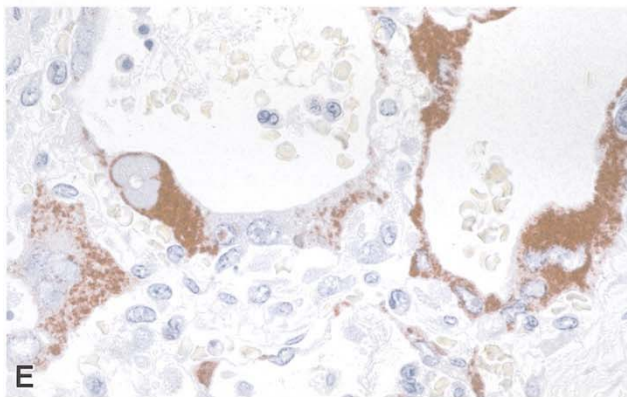
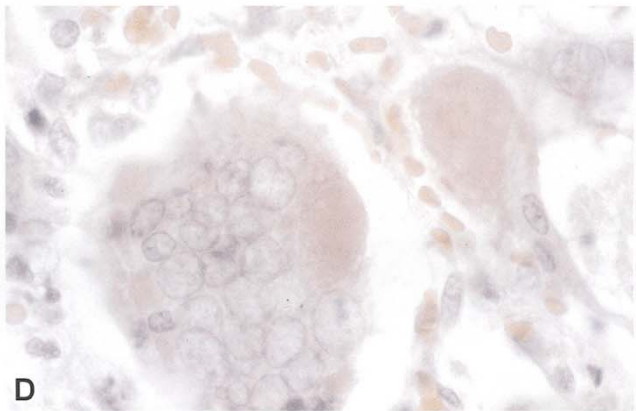
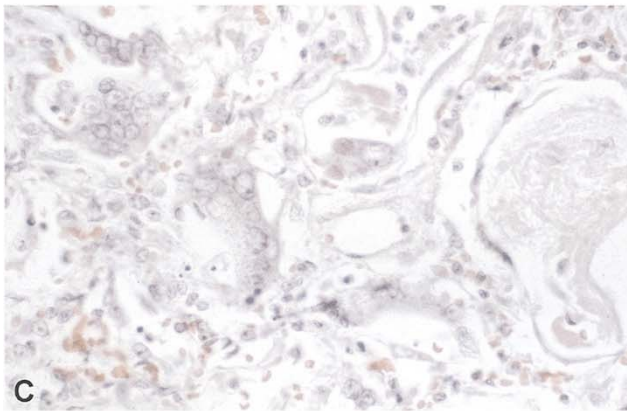
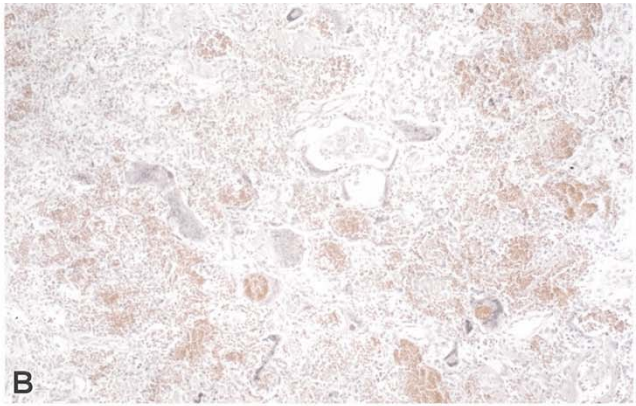
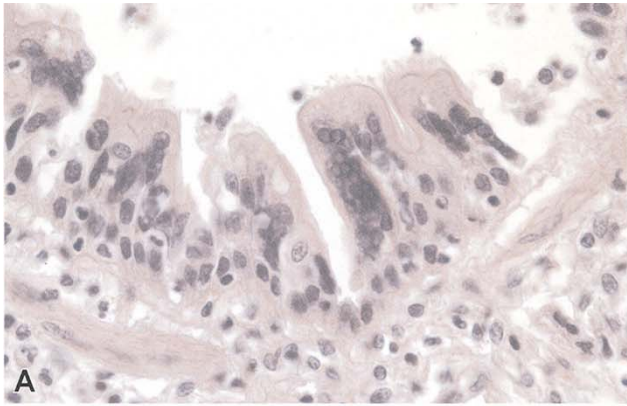
include various degrees of peribronchial and interstitial mononuclear cell infiltrates, squamous metaplasia of bronchial endothelium, proliferation of type II pneumocyte alveolar lining cells, and intraalveolar edema with or without mononuclear cell exudates and hyaline membranes. Secondary changes, such as bacterial or viral superinfection, or organizational changes may alter the original pathology.

The hallmark of the disease is the formation of multinucleated epithelial giant cells (Fig. 11.11A,B). These cells, which are often numerous, are formed by fusion of bronchiolar or alveolar lining epithelial cells (Fig. 11.11A). In contrast to the reticuloendothelial giant cells, these cells generally contain characteristic nuclear and cytoplasmic inclusions. The intranuclear inclusions are homogeneous, eosinophilic, and surrounded by a slight indistinct halo (Fig. 11.11C,D). The cytoplasmic inclusions are deeply eosinophilic, vary in size, and some form large masses with a "melted tallow" appearance (Fig. 11.11D). These giant cells may undergo degenerative changes with progressive loss of cytoplasm, increasing basophilia, and shrinkage of nuclei. The presence of measles virus in these giant cells may be demonstrated by immunofluorescent,^{235,236} IHC,^{210,237} and ISH techniques (Fig. 11.11E,F). These giant cells can also be seen in extrapulmonary tissues (Fig. 11.11G,H).

The diagnosis of typical cases of measles can usually be made on the basis of clinical signs and symptoms. Other causes of a similar rash, but without other features of measles, include rubella, dengue virus, enteroviruses, and drug reactions, especially to ampicillin. The typical case of measles giant-cell pneumonia generally presents little diagnostic difficulty for the surgical pathologist. The presence of giant cells with both intranuclear and intracytoplasmic inclusions in a setting of interstitial pneumonitis is highly specific for measles infection. However, multinucleated giant cells are not seen in all cases of measles pneumonia and their absence should not exclude the

FIGURE 11.11. Measles pneumonia. **A.** Several multinucleated giant cells are seen in the epithelial cells lining a bronchiole. **B.** Low-power photomicrograph showing interstitial pneumonitis, hemorrhage, and abundant giant cells. **C.** Multinucleated giant cells generally line the alveoli, although some are found lying free within alveolar spaces. **D.** High-power of multinucleated giant cells showing numerous eosinophilic cytoplasmic inclusions. The inclusions may be large in size and have a characteristic "melted tallow" appearance. Intranuclear inclusions are also seen, but are ill-defined, eosinophilic, and lack clear circumscription. **E.** Viral antigens in cytoplasm of giant cells as seen by immunohistochemical staining. The multinucleated giant cells can be seen to originate by fusion of infected alveolar lining epithelial cells. **F.** Numerous measles giant cells are seen in lung by colorimetric in-situ hybridization using digoxigenin-

labeled probes. **G.** Multinucleated epithelial and endothelial giant cells in adrenal gland of a fatal case of measles. **H.** Measles antigens in the same giant cells as seen in **G.** **I,J.** Measles antigen in nuclei of a giant cell (**I**) detected by immunohistochemistry. Intranuclear measles virus nucleocapsids as seen by electron microscopy (**J**) in the neuron of a patient who died from subacute sclerosing panencephalitis (SSPE) associated with measles. (**J**: courtesy of Sylvia Whitfield, Centers for Disease Control and Prevention, Atlanta, GA.) **A-D,G,** H&E; **E,H,I,** immunoalkaline phosphatase staining, naphthol fast-red, and hematoxylin counterstain; **F,** digoxigenin-labeled probes followed by immunoalkaline phosphatase staining, naphthol fast-red, and hematoxylin counterstain; **J,** uranyl acetate and lead citrate stain.



diagnosis. Other viral and rickettsial agents may also cause a similar interstitial pneumonitis, but without the typical giant cells, and should be differentiated.²²⁹ As previously noted, the histopathologic features in measles pneumonia can be somewhat variable,²²⁶ and secondary bacterial and viral infections may modify the histology, further complicating the pathologic diagnosis (Fig. 11.5D).^{207,229} Other viral pathogens, such as respiratory syncytial virus,²³⁸ parainfluenza,^{239,240} VZV,²⁴¹ and a recently discovered Hendra virus,²⁴² as well as granulomatous diseases of the lung, may give rise to pneumonia with giant cells and should also be considered in the differential diagnosis. However, these clinical entities can be distinguished by history, histopathologic features, and laboratory tests. Immunohistochemistry^{237,243,244} or ISH^{243,244} tests demonstrate viral antigens or nucleic acids in the majority of cases.

Laboratory confirmation is useful to avoid possible confusion with other rash-causing illnesses. Diagnostic laboratory procedures consist of direct detection of either the virus or the viral antigens, usually by indirect immunofluorescence or by serologic methods using hemagglutination inhibition, neutralization, or enzyme immunoassay. Specimens for serologic testing consist of acute- and convalescent-phase serum pairs. Antibody appears within 1 to 2 days after onset of rash, and titers peak approximately 2 weeks later. Alternatively, the presence of specific immunoglobulin M (IgM) antibody can be used to diagnose recent infection.²⁴⁵

Human Parainfluenza Viruses

Human parainfluenza viruses (HPIVs) are second only to RSV as a cause of lower respiratory tract disease in young children. Human parainfluenza viruses are negative-sense, nonsegmented, single-stranded, enveloped RNA viruses that possess fusion and hemagglutinin-neuraminidase glycoprotein “spikes” on their surface (Fig. 11.1G). The four serotypes of HPIV belong in the family Paramyxoviridae, subfamily Paramyxovirinae, and genera *Respirovirus* (HPIV-1 and -3) and *Rubulavirus* (HPIV-2 and -4). The virions are variable in shape and size, ranging from 150 to 300 nm.²⁴⁶

Human parainfluenza viruses are spread from respiratory secretions through close contact with infected persons or contact with contaminated surfaces or objects. Infection can occur when infectious material contacts mucous membranes of the eyes, mouth, or nose, and possibly through the inhalation of droplets generated by a sneeze or cough. Human parainfluenza viruses are unstable in the environment (surviving a few hours on environmental surfaces), and are readily inactivated with soap and water. They are ubiquitous, and infect most

people during childhood. The highest rates of serious HPIV illnesses occur among young children. Serologic surveys have shown that 90% to 100% of children aged 5 years and older have antibodies to HPIV-3, and about 75% have antibodies to HPIV-1 and -2. The different HPIV serotypes differ in their seasonality, with HPIV-1 causing biennial outbreaks of croup in the fall and HPIV-2 causing annual or biennial fall outbreaks. Human parainfluenza virus-3 peak activity occurs during the spring and early summer months each year, but the virus can be isolated throughout the year.

Similar to RSV, HPIVs can cause repeated infections throughout life, usually manifested by an upper respiratory tract illness (e.g., cold and sore throat). Human parainfluenza viruses can also cause serious lower respiratory tract disease with repeat infection (e.g., pneumonia, bronchitis, and bronchiolitis), especially among the elderly, and among patients with compromised immune systems. Each of the four HPIVs has different clinical and epidemiologic features. The most distinctive clinical feature of HPIV-1 and HPIV-2 is croup (i.e., laryngotracheobronchitis); HPIV-1 is the leading cause of croup in children, whereas HPIV-2 is less frequently detected. Both HPIV-1 and -2 can cause other upper and lower respiratory tract illnesses. Human parainfluenza virus-3 is more often associated with bronchiolitis and pneumonia. Human parainfluenza virus-4 is infrequently detected, possibly because it is less likely to cause severe disease. The incubation period for HPIVs is generally from 1 to 7 days.²⁴⁷

Most HPIV infections cause a mild, self-limited illness; however, HPIV-3 infections are an important cause of bronchiolitis, croup, and pneumonia that may be life-threatening in infants and newborns.²⁴⁷ Human parainfluenza virus infections are also increasingly being recognized as an important cause of severe morbidity and mortality in immunocompromised patients.^{20,248–252} The mortality of bone marrow transplant patients with HPIV-3 infection has been reported to be as high as 60%.^{249,253,254} In patients with severe HPIV infection, multinucleated giant cells derived from the respiratory epithelium may be seen in association with an interstitial pneumonitis and organizing changes (Fig. 11.12A,B).^{239,240,249,255–260} These giant cells, which may contain intracytoplasmic eosinophilic inclusions (Fig. 11.12C), have also been reported in extrapulmonary tissues such as kidney, bladder, and pancreas.²⁵⁸ Other viral causes of giant cell pneumonia, including measles, RSV, VZV, and HSV, should be considered in the histopathologic differential and laboratory testing, including IHC, can be useful in making this differentiation possible (Fig. 11.12D). Diagnosis of infection with HPIVs can also be made by virus isolation, direct detection of viral antigens by enzyme-linked immunoassay (EIA) or immunofluorescent assay (IFA) in clinical specimens, detection of viral RNA by RT-PCR, demonstration of a rise in

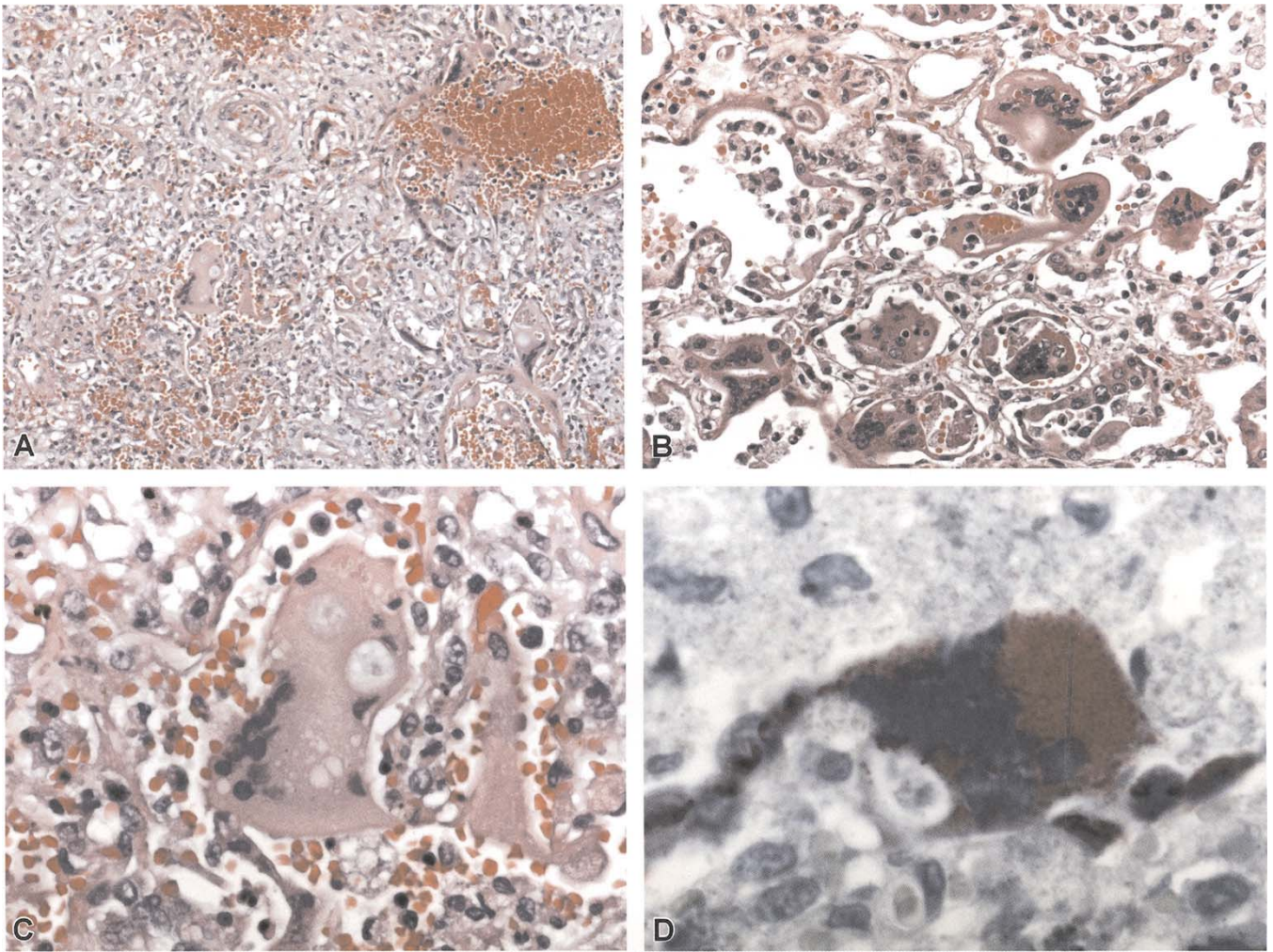


FIGURE 11.12. Parainfluenza pneumonia. **A.** Giant cell pneumonia associated with parainfluenza virus infection with numerous giant cells, interstitial pneumonitis and hemorrhage. **B.** Multinucleated giant cells that originate from respiratory alveolar epithelium. **C.** High-power magnification of a giant cell contain-

ing poorly defined cytoplasmic eosinophilic inclusions. **D.** Parainfluenza virus antigens in giant cells localized by using immunohistochemistry. **A–C,** H&E; **D,** immunoalkaline phosphatase staining, naphthol fast-red, and hematoxylin counterstain.

specific serum antibodies, or a combination of these approaches.^{261–264}

Respiratory Syncytial Virus

Respiratory syncytial virus (RSV) is the most common cause of bronchiolitis and pneumonia among infants and children under 1 year of age. The causative agent is a negative-sense, nonsegmented, single-stranded, enveloped RNA virus. The virion is variable in shape and size and ranges from 120 to 300 nm. Respiratory syncytial virus is a member of the family Paramyxoviridae, subfamily Pneumovirinae, in the genus *Pneumovirus*, and can be

further distinguished genetically and antigenically into two subgroups, A and B. The subgroup A strains are usually associated with more severe infections. Two surface glycoproteins, G and F, are present in the envelope and mediate attachment and fusion with respiratory epithelium. The F protein also mediates coalescence of neighboring cells to form the characteristic multinucleated syncytial giant cells for which the virus name is derived.²⁶⁵

Respiratory syncytial virus is spread from respiratory secretions through close contact with infected persons or contact with contaminated surfaces or objects.²⁶⁶ Infection can occur when infectious material contacts mucous membranes of the eyes, mouth, or nose, and possibly

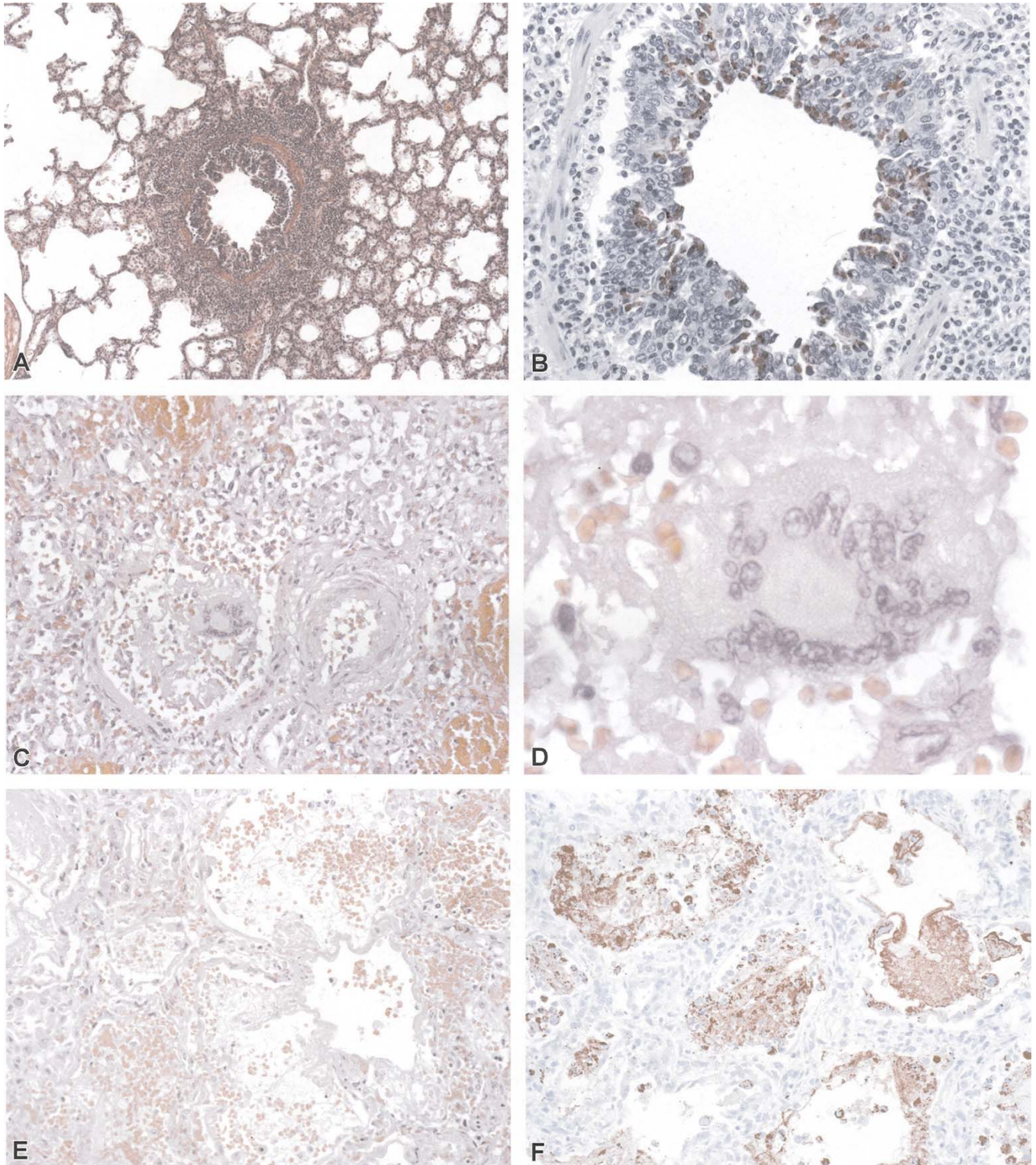


FIGURE 11.13. Respiratory syncytial virus (RSV) pneumonia. **A.** Bronchiolar and peribronchiolar inflammation in RSV infection. **B.** Respiratory syncytial virus antigens are seen in lining epithelial cells of same bronchiole by using immunohistochemistry. **C.** Diffuse interstitial pneumonitis, hemorrhage, and giant cells in RSV pneumonia. **D.** Higher-power magnification showing giant cells lacking unequivocal viral inclusions.

E. Diffuse alveolar damage with septal thickening and hyaline membranes in RSV pneumonia. No giant cells can be seen. **F.** Respiratory syncytial virus antigens associated with hyaline membranes and necrotic debris within alveolar spaces. **A,C-E,** H&E; **B,F,** immunoalkaline phosphatase staining, naphthol fast-red, and hematoxylin counterstain.

through the inhalation of droplets generated by a sneeze or cough. Respiratory syncytial virus is unstable in the environment, surviving a few hours on environmental surfaces, and is readily inactivated with soap and water. In temperate climates, RSV infections usually occur during annual community outbreaks, often lasting several months, during the late fall, winter, or early spring months. The timing and severity of outbreaks in a community vary from year to year. Respiratory syncytial virus spreads efficiently among children during the annual outbreaks, and most children will have serologic evidence of RSV infection by 2 years of age.

Illness begins most frequently with fever, runny nose, cough, and sometimes wheezing. During their first RSV infection, between 25% and 40% of infants and young children have signs or symptoms of bronchiolitis or pneumonia, and 0.5% to 2% require hospitalization. Most children recover from illness in 8 to 15 days. The majority of children hospitalized for RSV infection are under 6 months of age. Respiratory syncytial virus also causes repeated infections throughout life, usually associated with moderate-to-severe cold-like symptoms; however, severe lower respiratory tract disease may occur at any age, especially among the elderly or among those with compromised cardiac, pulmonary, or immune systems.

The major histopathologic changes described in fatal RSV infections include necrotizing bronchiolitis and interstitial pneumonia (Fig. 11.13A,B).^{238,267-272} Bronchial lumina and airways are usually filled with necrotic debris and inflammatory cells. These findings may be accompanied by various degrees of diffuse alveolar damage (Fig. 11.13E), organizational changes, and secondary bacterial superinfection. Giant cell pneumonia is a feature seen in some cases (Fig. 11.13C,D). The multinucleated giant cells contain irregular, intracytoplasmic, eosinophilic inclusions surrounded by a clear halo. These inclusions are extremely difficult to identify with any degree of certainty and are only seen in about half the cases (Fig. 11.13D). Other viral causes of giant cell pneumonia should be considered in the histopathologic differential and laboratory testing, including IHC,^{271,273,274} can be useful in making this differentiation possible (Fig. 11.13B,F). Diagnosis of RSV infection can also be made by virus isolation, direct detection of viral antigens in clinical specimens by EIA or IFA, detection of viral RNA by RT-PCR, demonstration of a rise in RSV-specific serum antibodies, or a combination of these approaches (see also Fig. 7.43, Chapter 7).^{264,275-281}

Human Metapneumovirus

In 2001, van den Hoogen et al.²⁸² described the identification of this new viral agent from clinical specimens obtained from patients with respiratory illness, which

they designated human metapneumovirus (HMPV). It is a negative-sense, nonsegmented, single-stranded, enveloped RNA virus. The virion is variable in shape and size, ranging from 150 to 300 nm (Fig. 11.1F). It has been categorized in the family Paramyxoviridae, subfamily Pneumovirinae, genus *Metapneumovirus*, based on genomic sequence and gene constellation. Human metapneumovirus can be further distinguished genetically and antigenically into two subgroups, A and B.

Similar to RSV, HMPV infection is ubiquitous and occurs during infancy and early childhood, with annual epidemic peaks occurring in the winter and spring months in temperate regions. Seroprevalence studies reveal that 25% of all children aged 6 to 12 months have antibodies to HMPV; by age 5 years, 100% of patients have evidence of past infection.

Like RSV, HMPV has been associated with a wide spectrum of respiratory illnesses.²⁸³⁻²⁸⁷ The patient may be asymptomatic, or symptoms may range from mild upper respiratory tract illness to severe bronchiolitis and pneumonia. Although RSV, HPIV-1, and HPIV-3 have been definitively linked to cases of lower respiratory tract disease in infants and young children, the relative contribution of HMPV remains undetermined. Like RSV and the HPIVs, studies suggest that HMPV may also contribute to respiratory disease in elderly adults and the immunocompromised.²⁸⁸⁻²⁹⁰

Histopathologic descriptions of features of HMPV infections are few and have not been well described.²⁹¹⁻²⁹⁴ This is partly related to interpreting the clinical significance of virus detection in context with the ubiquitous nature of the virus. Virus detection in such cases is usually made by culture isolation of the virus from upper airways or by PCR assays performed on nasopharyngeal aspirates or BAL washings. In nonhuman primates viral antigens are observed in ciliated epithelial cells, type 1 pneumocytes, and alveolar macrophages. This distribution is associated with mild, multifocal, erosive, and inflammatory changes in airways, and an increased number of foamy macrophages in alveoli.²⁹¹ The BAL specimens collected from patients within a few days of a positive HMPV assay show degenerative changes and cytoplasmic inclusions within epithelial cells, multinucleated giant cells, and histiocytes. The intracytoplasmic inclusions are ill-defined, eosinophilic structures that measure 3 to 4 μm .²⁹³ Lung biopsy or autopsy tissue obtained and examined later in the disease show chronic airway inflammation, intraalveolar foamy and hemosiderin-laden macrophages, and acute and organizing lung injury including areas of diffuse alveolar damage with hyaline membrane formation and foci of a bronchiolitis obliterans/organizing pneumonia like reaction (Fig. 11.14). In such cases, typical multinucleated giant cells or viral inclusion cannot be identified.²⁹²⁻²⁹⁴ In-situ hybridization studies on limited number of human cases

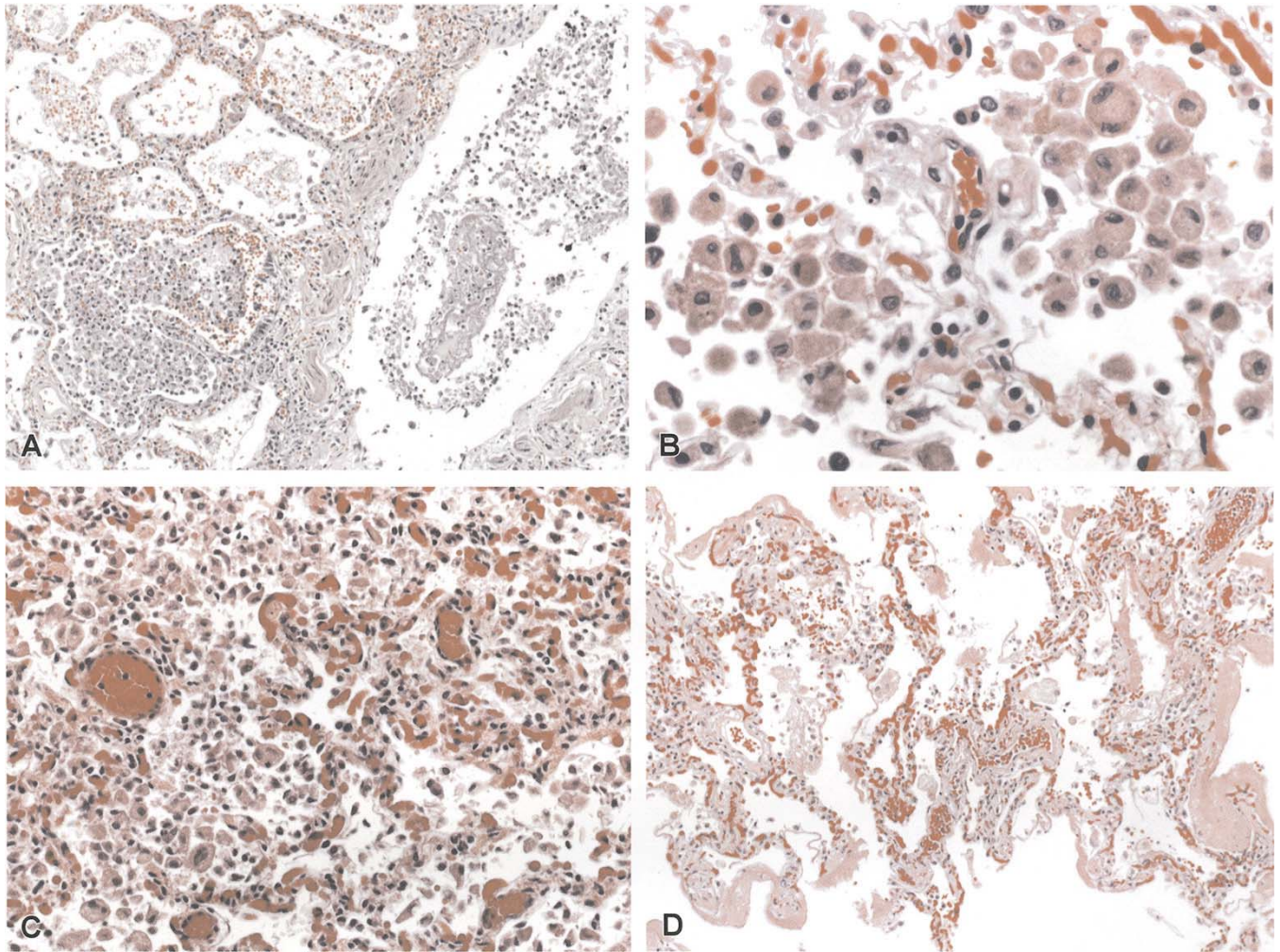


FIGURE 11.14. Human metapneumovirus (HMPV) infection. **A.** Marked bronchiolitis, intraalveolar macrophages, and hemorrhages are seen in this photomicrograph. The bronchiolar epithelium is focally ulcerated. **B.** Higher-power magnification showing accumulation of intraalveolar foamy macrophages. (Patient bronchoalveolar lavage [BAL] specimen positive for

HMPV by polymerase chain reaction [PCR].) **C.** Pulmonary congestion, edema, and mild interstitial lymphocytic inflammation. (Patient lung positive for HMPV by PCR.) **D.** Organizing pneumonia with marked interstitial thickening and hyaline membrane formation. HMPV was detected. (Patient BAL positive for HMPV by PCR.) **A–D,** H&E.

suggest infection of alveolar and bronchial epithelial cells.²⁹²

Human metapneumovirus is difficult to identify with commonly used viral diagnostic procedures. The virus replicates slowly in primary and tertiary monkey kidney cell lines, and the cytopathic effect can be difficult to discern. Commercial monoclonal antibody reagents to HMPV are not widely available. Most HMPV studies have been conducted using RT-PCR assays or by demonstration of a rise in HMPV-specific serum antibodies.

Henipah Viruses

Two novel paramyxoviruses, Hendra and Nipah, have been recently identified in Australia and Malaysia; these viruses have been associated with acute febrile encephalitis and respiratory tract disease. Both infections are zoonotic. Hendra was first identified in 1994 when patients who came in close contact with sick horses developed an influenza-like illness. Two patients died with pneumonitis and multiorgan failure.³⁰ The closely related Nipah virus was identified during an outbreak in

Malaysia and Singapore during 1998–1999 that included more than 250 patients. Patients presented with a severe acute encephalitic syndrome, but some also had significant pulmonary manifestations.^{22,295–302} Most of the patients had a history of contact with pigs, most of them being pig farmers. In Bangladesh in 2001 and 2003, outbreaks of Nipah encephalitis occurred.^{303,304} Similar to the Malaysian outbreak, the most prominent symptoms were fever, headache, vomiting, and an altered level of consciousness. Respiratory illness was much more common in the Bangladesh cases, however, with 64% having cough and dyspnea. The reason for increased involvement of the respiratory tract in this outbreak is not known. Epidemiologic and laboratory investigations identified fruit bats of the *Pteropus* genus as asymptomatic carriers of Hendra and Nipah viruses and possible animal reservoirs.^{305–309}

Hendra and Nipah viruses belong to the recently designated genus *Henipavirus* within the family Paramyxoviridae, subfamily Paramyxovirinae. Both viruses are nonsegmented, negative-stranded RNA viruses composed of helical nucleocapsids enclosed within an envelope to form roughly spherical, pleomorphic virus particles.^{310–312} The structure of their genome is consistent with the other members of the subfamily.³⁰

Histopathologic findings in fatal cases of Hendra and Nipah infections are similar with varying degrees of CNS and respiratory tract involvement.^{104,313–315} Findings include a systemic vasculitis with extensive thrombosis, endothelial cell damage, necrosis, and syncytial giant cell formation in affected vessels (Fig. 11.15A,B,F). Plaques with various degrees of necrosis, in association with inclusion-bearing neurons, can be found in both the gray and white matter of the CNS (Fig. 11.15E). Multinucleated giant cells with intranuclear inclusions can occasionally be seen in lung, spleen, lymph nodes, and kidneys (Fig. 11.15C,G). In the lung, vasculitis and fibrinoid necrosis can be seen in majority of cases. Fibrinoid necrosis often involves several adjacent alveoli and is frequently associated with small vessel vasculitis. The multinucleated giant cells with intranuclear inclusions are usually noted in alveolar spaces adjacent to necrotic areas. Histopathologic changes of bronchiolar epithelium are uncommon; rarely, the large bronchi may show transmural inflammation and ulceration. Widespread presence of Nipah virus antigens can be seen by IHC in endothelial and smooth muscle cells of blood vessels as well as in various parenchymal cells (Fig. 11.15D).

The diagnosis of Nipah virus infection, suspected by patient history and clinical manifestations, can be supported by characteristic histopathologic findings. From a diagnostic standpoint, perhaps the most unique histopathologic finding is the presence of syncytial and parenchymal multinucleated endothelial cells. This feature

occurs in only approximately one fourth of the cases and cannot be used as a sensitive criterion for the diagnosis of Henipah virus infections; furthermore, these cells can also be seen in measles virus, RSV, HPIV, herpesviruses, and other infections. Unequivocal diagnosis can be made only by laboratory tests such as IHC, cell culture isolation, PCR, or serology.^{104,304,316–319}

Other Unusual Infections

Parvoviruses

The parvoviruses are small (18 to 26 nm) naked viruses that possess a single-stranded DNA genome and require actively dividing cells to complete the viral replication cycle. In 2005, Allander et al.³²⁰ identified a new parvovirus (genus *Bocavirus*) associated with lower respiratory tract infections in children; however, there is no information as yet that describes specific pulmonary pathology attributed to this newly identified agent. On the other hand, human parvovirus B19, a member of the genus *Erythrovirus*, has long been known to cause human disease and has been well studied.^{321,322}

The most commonly recognized manifestation of B19 infections is erythema infectiosum, and approximately one third of the cases of maternal parvovirus infections result in intrauterine parvovirus B19 infections. This places the fetus at increased risk for severe anemia, hydrops, and death. Hydrops fetalis is the most commonly recognized complication of intrauterine parvovirus infection, accounting for 4% to 18% of all cases of nonimmune hydrops. Cases tend to be clustered during community outbreaks of erythema infectiosum.^{321,322} Pathophysiologic effects and histopathologic findings are a result of the tropism of B19 parvovirus for erythroid precursor cells. Villi from placentas from patients with B19-associated nonimmune hydrops are edematous, and fetal capillaries show numerous nucleated erythroid precursors, some containing parvovirus inclusions. The infected cells with eosinophilic “ground glass” intranuclear inclusions and ring-like margination of nuclear chromatin are easily recognized and in the context of a hydropic fetus are pathognomonic of B19 infection. The liver is the major site of blood production in the fetus and the principal organ affected by intrauterine B19 infection. Inclusion-bearing nucleated erythrocytes can also be frequently identified in the lung, making histopathologic examination of this organ a worthwhile endeavor for confirming the diagnosis of intrauterine B19 infection (Fig. 11.16A,B).^{323–332} However, these cells may be infrequent and irregularly distributed, requiring examination of multiple sections and use of IHC to confirm the diagnosis (Fig. 11.16C,D).

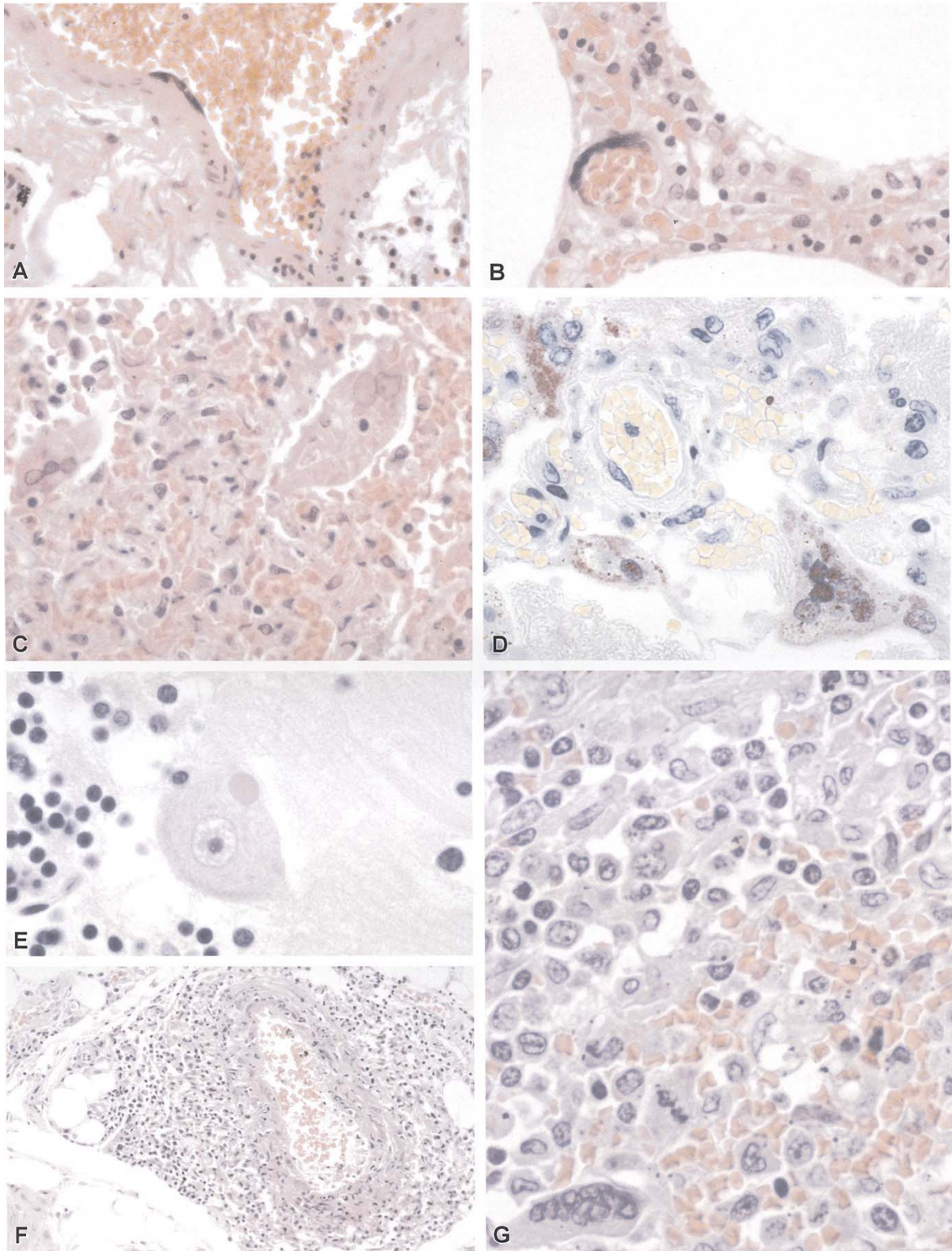


FIGURE 11.15. Nipah virus. **A.** Pulmonary vessels showing a mild vasculitis and a multinucleated endothelial syncytium. **B.** Interstitial pneumonitis. Note small vessel lined by a multinucleated endothelial cell. **C.** Interstitial pneumonitis with intraalveolar multinucleated giant cells with nuclear inclusions. **D.** Viral nature of giant cells, in **C**, as evidenced by immunostaining for Nipah viral antigens. **E.** Typical eosinophilic viral inclusion

("Negri-like") in cytoplasm of a neuron. **F.** Moderate vasculitis in soft tissue in a fatal case of Nipah virus infection. **G.** Multinucleated giant cell as seen in the splenic parenchyma. Besides in lung, giant cells can also be seen in other organs such as kidney and lymphoid organs. **A–C, E–G,** H&E; **D,** immunoalkaline phosphatase staining, naphthol fast-red, and hematoxylin counterstain.

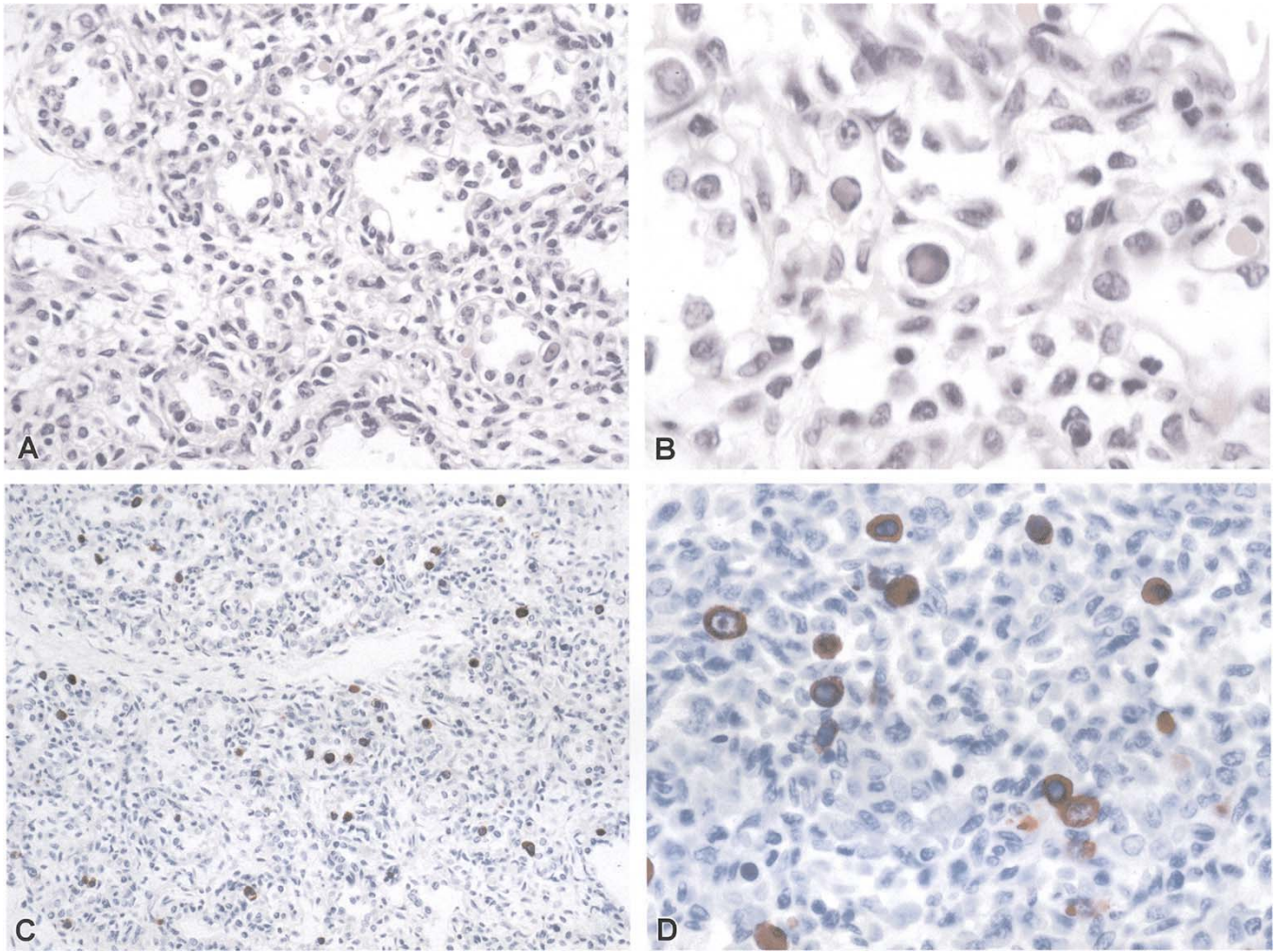


FIGURE 11.16. Parvovirus. **A,B**. Histopathologic findings in the lung of a B19-infected hydropic fetus. Several erythroid precursors contain ground-glass inclusions typical of parvovirus B19. Inclusions-bearing erythrocytes can frequently be identified in the vascular spaces. **C,D**. Localization of parvovirus antigens

in the nucleus and cytoplasm of erythroid precursors by using immunohistochemistry (IHC) (same patient as in **A,B**). **A,B**, H&E; **C,D**, immunoalkaline phosphatase staining, naphthol fast-red, and hematoxylin counterstain.

Hemorrhagic Fever Viruses

The combination of fever and hemorrhage can be caused by different viruses, rickettsiae, bacteria, protozoa, and fungi. However, the term *viral hemorrhagic fever* (VHF) is usually reserved for systemic infections characterized by fever and hemorrhage caused by a special group of viruses transmitted to humans by arthropods and rodents. The VHFs are febrile illnesses characterized by abnormal vascular regulation and vascular damage and are caused by small, lipid-enveloped RNA viruses. This syndrome can be caused by viruses belonging to four different families that differ in their genomic structure, replication strategy, and morphologic features (Table 11.4). Arenaviruses, bunyaviruses, and filoviruses are negative-stranded,

whereas flaviviruses are positive-stranded RNA viruses. Hemorrhagic fever viruses are distributed worldwide, and the diseases they cause are traditionally named according to the location where they were first described. The oldest and best known is yellow fever virus; others include Lassa fever, lymphocytic choriomeningitis, Ebola, and Dengue viruses.

Viral hemorrhagic fevers share many common pathologic features, although the overall changes vary among the different diseases. The similar pathologic and immunopathologic findings in cases of VHF suggest that microvascular involvement and instability is an important common pathogenic pathway leading to shock and bleeding in many instances. Infection of the mononuclear phagocytic system and endothelium are thought to play

TABLE 11.4. Viruses associated with the hemorrhagic fever syndromes

Arenaviridae	Bunyviridae	Flaviviridae	Filoviridae
Junin	<i>Nairovirus</i>	Mosquito-borne	Marburg
Machupo	Crimean-Congo	Yellow fever	Ebola (four subtypes)
Guanarito	Hemorrhagic fever	Dengue viruses 1–4	
Sabia	<i>Phlebovirus</i>	Tick-borne	
Lassa	Rift Valley fever	Kyasanur Forest disease	
	<i>Hantavirus</i>	Omsk hemorrhagic fever	
	Hantaan, Puumala, Seoul, Sin Nombre, Black Creek Canal, Bayou, others		

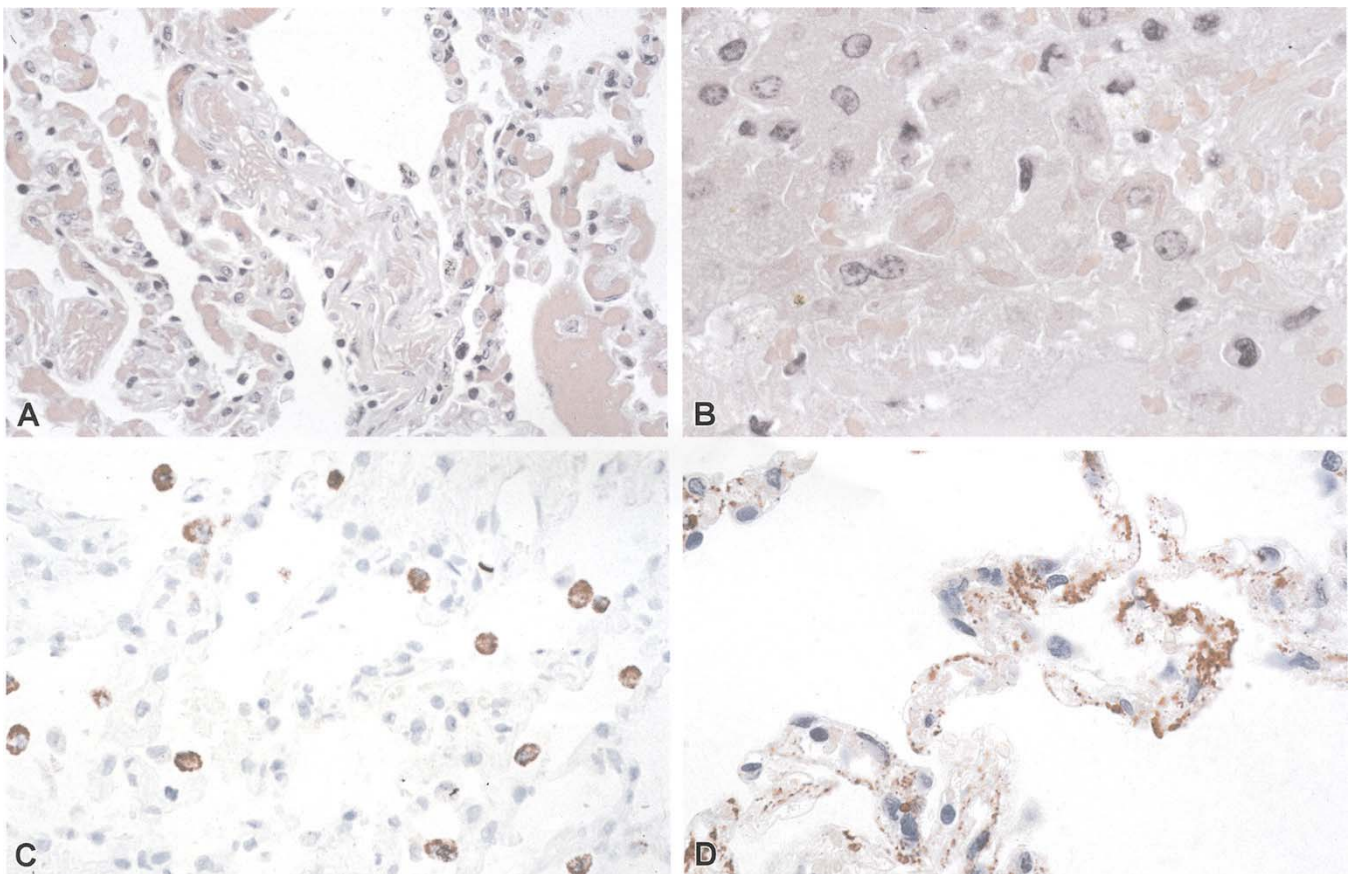


FIGURE 11.17. Ebola virus hemorrhagic fever. **A.** Pulmonary congestion and lack of inflammation. **B.** Numerous filamentous Ebola virus inclusions are seen within hepatocytes in association with hepatocellular necrosis. **C.** Ebola virus-infected intraalveolar macrophages as seen by colorimetric in-situ hybridization using digoxigenin-labeled probes. **D.** Viral anti-

gens are seen in endothelial cells and other interstitial cells in this lung section. **A,B,** H&E; **C,** digoxigenin-labeled probes followed by immunoalkaline phosphatase staining, naphthol fast-red, and hematoxylin counterstain; **D,** immunoalkaline phosphatase staining, naphthol fast-red, and hematoxylin counterstain.

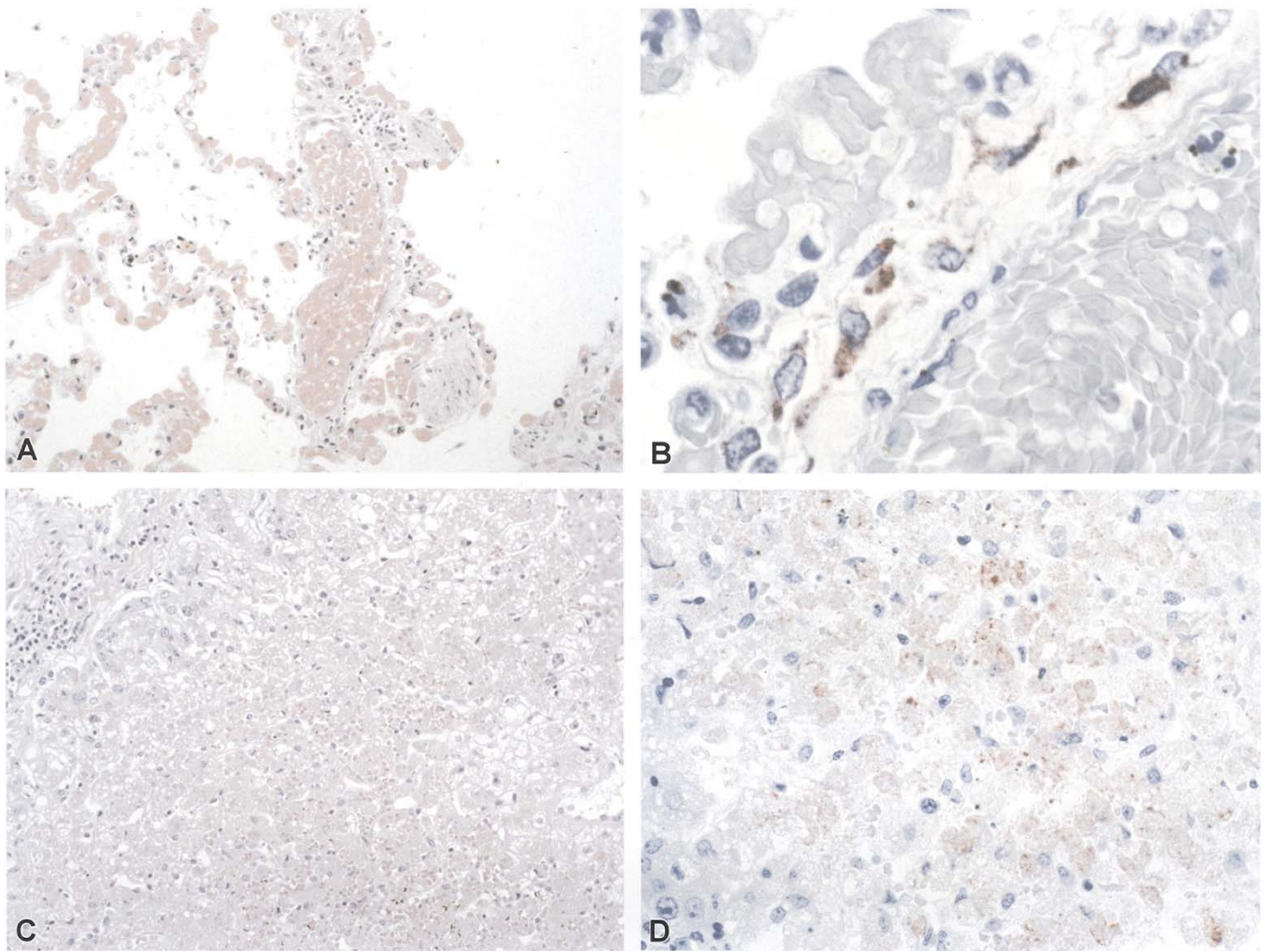


FIGURE 11.18. Yellow fever. **A.** Pulmonary congestion in fatal case of yellow fever associated with vaccination. **B.** Yellow fever antigens in the pulmonary interstitium of the same patient. In natural infections, yellow fever antigens are usually not seen outside the liver in fatal cases. In contrast, in vaccine-associated cases viral antigens can be found in a variety of extrapulmonary

organs, including heart, lung, and spleen. **C.** Extensive midzonal hepatic necrosis characteristic of yellow fever. **D.** Abundant antigens of yellow fever virus are observed in midzonal area of hepatic lobule in this immunohistochemical preparation. **A,C,** H&E; **B,D,** immunoalkaline phosphatase staining, naphthol fast-red, and hematoxylin counterstain.

a critical role in the pathogenesis of VHFs through the secretion of physiologically active substances, including cytokines and other inflammatory mediators (Figs. 11.17C,D, 11.18B, 11.19B,C, and 11.20B). At autopsy common findings include widespread petechial hemorrhages and ecchymoses involving skin, mucous membranes, and internal organs. However, in many HF patients manifestations of bleeding may be minimal or absent. Effusions, occasionally hemorrhagic, are also frequently seen. Widespread, focal, and sometimes massive necrosis can be commonly observed in all organ systems and is often ischemic in nature. Necrosis is usually most prominent in the liver and lymphoid tissues. The most con-

sistent microscopic feature is found in the liver and consists of multifocal hepatocellular necrosis with cytoplasmic eosinophilia, Councilman bodies, nuclear pyknosis, and cytolysis (Figs. 11.17B and 11.18C). Inflammatory cell infiltrates and necrotic areas are usually mild and, when present, consist of neutrophils and mononuclear cells. Commonly observed histopathologic changes in the lung include various degrees of hemorrhage, intraalveolar edema, interstitial pneumonitis, and diffuse alveolar damage (Figs. 11.17A, 11.18A, 11.19A, 11.20A, and 11.21A). Several references containing detailed pathologic descriptions in human cases are recommended.^{29,72,333-350}

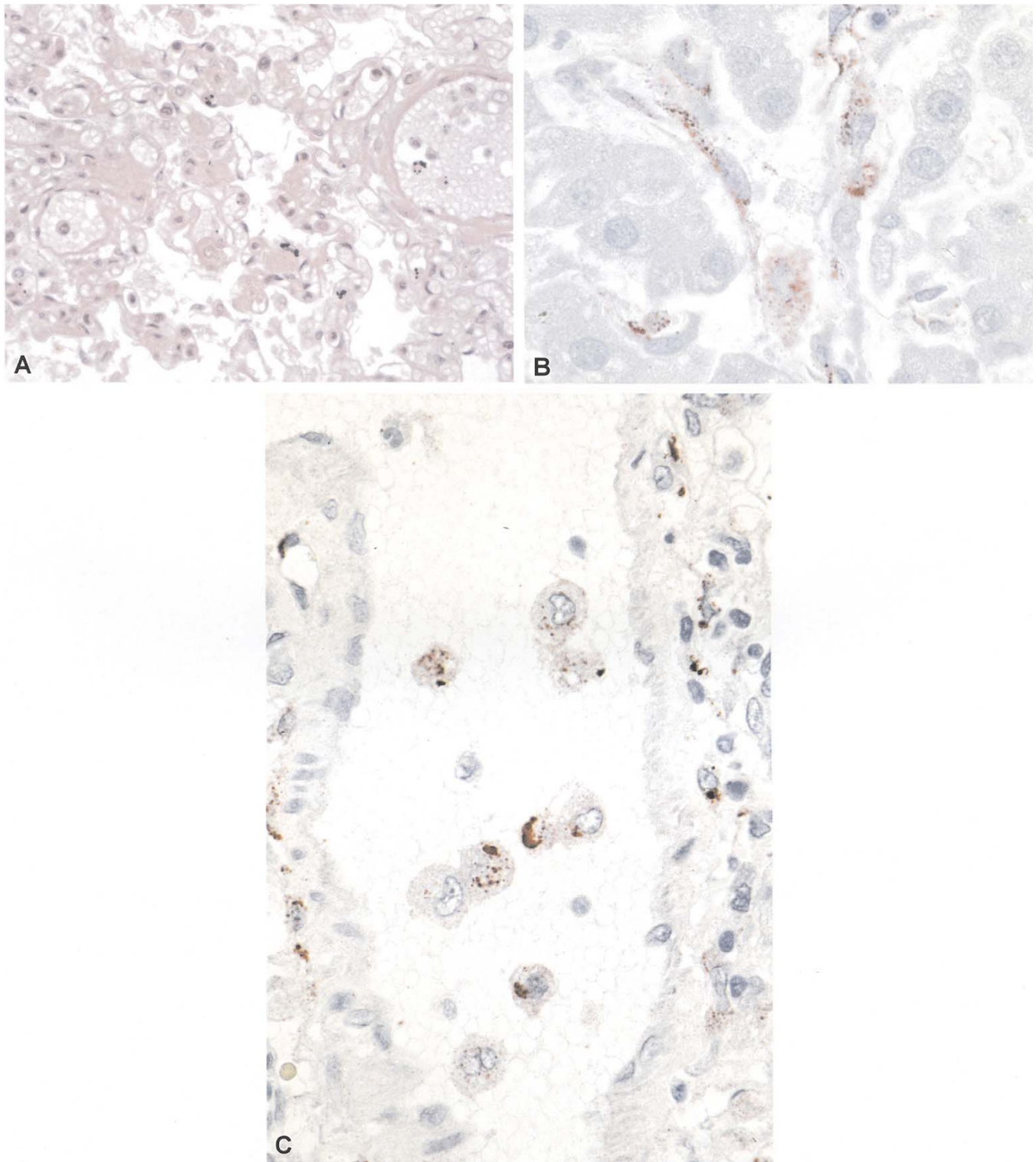


FIGURE 11.19. Dengue hemorrhagic fever. **A.** Lung showing severe congestion and a mild mononuclear interstitial pneumonitis. **B.** Immunostaining of liver showing viral antigens predominantly within sinusoidal Kupffer cells. Note absence of

staining of hepatocytes. **C.** Numerous viral antigen-containing circulating mononuclear cells in a pulmonary vessel. **A,** H&E; **B,C,** immunoalkaline phosphatase staining, naphthol fast-red, and hematoxylin counterstain.

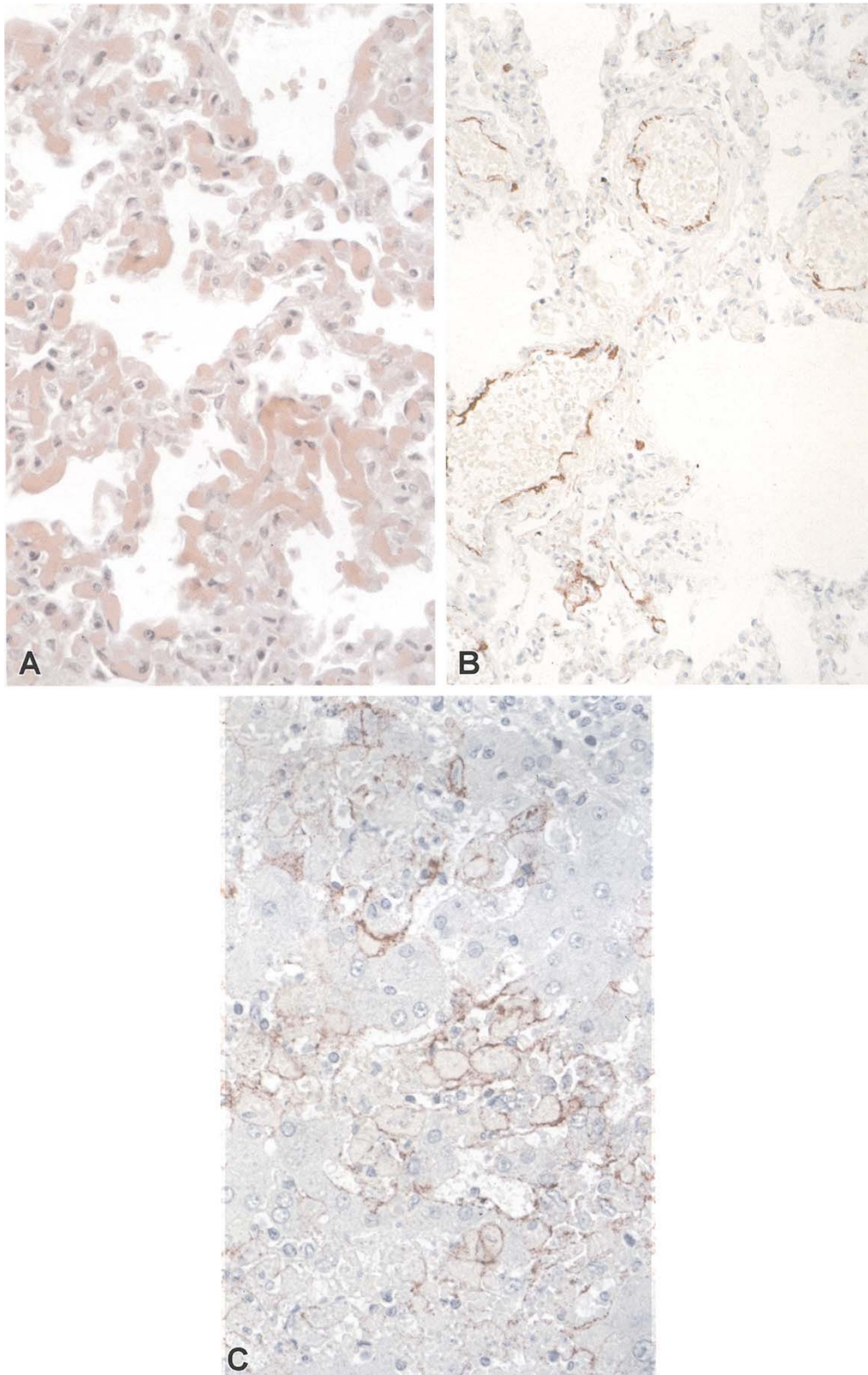


FIGURE 11.20. Lassa fever. **A.** Pulmonary congestion and an absence of significant inflammatory response. **B.** Lassa viral antigens are seen in endothelial cells lining medium-sized vessels in this section of the lung. **C.** Using immunohistochemistry, abundant Lassa virus antigens are seen within cytoplasm

of hepatocytes and sinusoidal lining cells in association with areas of hepatocellular necrosis. **A,** H&E; **B,C,** immunoalkaline phosphatase staining, naphthol fast-red, and hematoxylin counterstain.

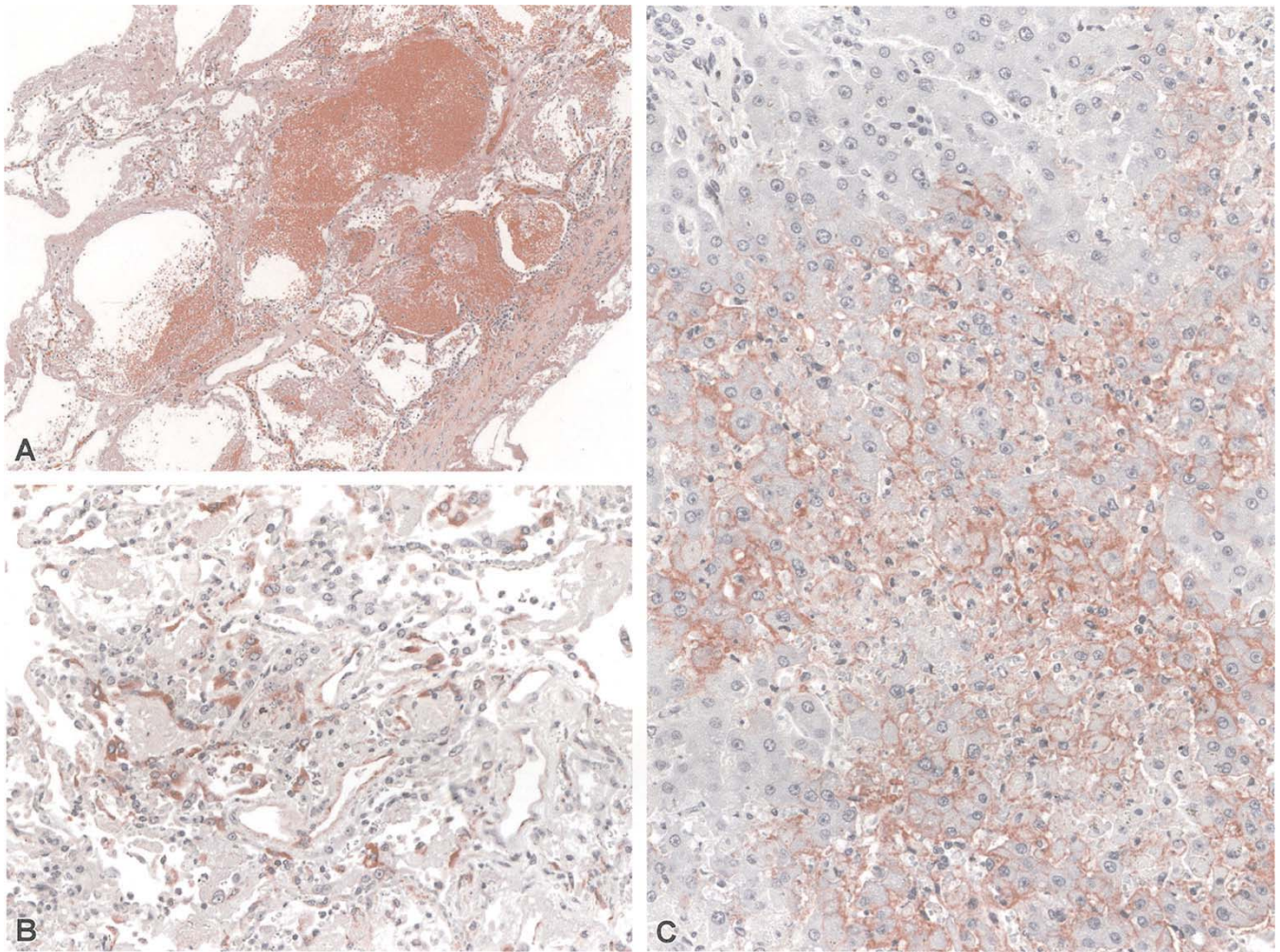


FIGURE 11.21. Lymphocytic choriomeningitis virus (LCMV). **A.** Pulmonary hemorrhage and diffuse alveolar damage in a patient who was infected through organ transplantation. Note that, unlike this case, which occurred due to immunosuppression, LCMV infections are rarely fatal and usually resolve with no specific treatment. **B.** Abundant LCMV antigens in areas of

lung showing diffuse alveolar damage. **C.** Using immunohistochemistry, abundant LCMV antigens are seen within cytoplasm of hepatocytes and sinusoidal lining cells in association with areas of hepatocellular necrosis. **A,** H&E; **B,C,** immunoalkaline phosphatase staining, naphthol fast-red, and hematoxylin counterstain.

The diagnosis of VHF should be suspected in patients with appropriate clinical manifestations returning from an endemic area, particularly if there is travel to rural areas during seasonal or epidemic disease activity. The diagnosis suspected by history and clinical manifestations can also be supported histopathologically, and the overall pattern of histopathologic lesions may suggest a specific diagnosis. However, because of similar pathologic features seen in VHF and a variety of other viral, rickettsial, and bacterial infections, unequivocal diagnosis can only be made by

laboratory tests such as cell culture isolation, serology, PCR, and IHC (Figs. 11.18D, 11.20C, and 11.21B,C).

Acknowledgments. The authors gratefully acknowledge the invaluable assistance of Gillian Genrich, of the CDC, for her comments and help with organization of the references, Cynthia Goldsmith for her comments, and Mitesh Patel, of the CDC, for his help with preparation and assembly of the images.

References

1. Osler W. The principles and practice of medicine. 4th ed. New York: D. Appleton, 1901.
2. Perkins BA, Flood JM, Danila R, et al. Unexplained deaths due to possibly infectious causes in the United States: defining the problem and designing surveillance and laboratory approaches. The Unexplained Deaths Working Group. *Emerg Infect Dis* 1996;2(1):47–53.
3. Hoyert DL, Kung HC, Smith BL. Deaths: preliminary data for 2003. *Natl Vital Stat Rep* 2005;53(15):1–48.
4. Reid AH, Taubenberger JK. The origin of the 1918 pandemic influenza virus: a continuing enigma. *J Gen Virol* 2003;84(pt 9):2285–2292.
5. Update: Outbreak of severe acute respiratory syndrome—worldwide, 2003. *MMWR Morb Mortal Wkly Rep* 2003; 52(12):241–246, 248.
6. Greenberg SB. Viral pneumonia. *Infect Dis Clin North Am* 1991;5(3):603–621.
7. Ortqvist A, Hedlund J, Grillner L, et al. Aetiology, outcome and prognostic factors in community-acquired pneumonia requiring hospitalization. *Eur Respir J* 1990;3(10):1105–1113.
8. Macfarlane JT, Finch RG, Ward MJ, Macrae AD. Hospital study of adult community-acquired pneumonia. *Lancet* 1982;2(8292):255–258.
9. Sullivan RJ Jr, Dowdle WR, Marine WM, Hierholzer JC. Adult pneumonia in a general hospital. Etiology and host risk factors. *Arch Intern Med* 1972;129(6):935–942.
10. Woodhead MA, Macfarlane JT, McCracken JS, Rose DH, Finch RG. Prospective study of the aetiology and outcome of pneumonia in the community. *Lancet* 1987;1(8534):671–674.
11. Fekety FR Jr, Caldwell J, Gump D, et al. Bacteria, viruses, and mycoplasmas in acute pneumonia in adults. *Am Rev Respir Dis* 1971;104(4):499–507.
12. de Roux A, Marcos MA, Garcia E, et al. Viral community-acquired pneumonia in nonimmunocompromised adults. *Chest* 2004;125(4):1343–1351.
13. Ksiazek TG, Erdman D, Goldsmith CS, et al. A novel coronavirus associated with severe acute respiratory syndrome. *N Engl J Med* 2003;348(20):1953–1966.
14. Bartlett J. Approach to the patient with pneumonia. In: Gorbach SL, Bartlett JG, Blacklow NR, ed. *Infectious disease*. 3rd ed. Philadelphia: Lippincott Williams & Wilkins, 2004:470–479.
15. Beadling C, Slifka MK. How do viral infections predispose patients to bacterial infections? *Curr Opin Infect Dis* 2004; 17(3):185–191.
16. Takala AK, Meurman O, Kleemola M, et al. Preceding respiratory infection predisposing for primary and secondary invasive *Haemophilus influenzae* type b disease. *Pediatr Infect Dis J* 1993;12(3):189–195.
17. Babiuk LA, Lawman MJ, Ohmann HB. Viral-bacterial synergistic interaction in respiratory disease. *Adv Virus Res* 1988;35:219–249.
18. Jakab GJ. Immune impairment of alveolar macrophage phagocytosis during influenza virus pneumonia. *Am Rev Respir Dis* 1982;126(5):778–782.
19. Jakab GJ. Mechanisms of bacterial superinfections in viral pneumonias. *Schweiz Med Wochenschr* 1985;115(3): 75–86.
20. Glezen WP, Greenberg SB, Atmar RL, Piedra PA, Couch RB. Impact of respiratory virus infections on persons with chronic underlying conditions. *JAMA* 2000;283(4): 499–505.
21. Ksiazek TG, Peters CJ, Rollin PE, et al. Identification of a new North American hantavirus that causes acute pulmonary insufficiency. *Am J Trop Med Hyg* 1995;52(2): 117–123.
22. Chua KB, Bellini WJ, Rota PA, et al. Nipah virus: a recently emergent deadly paramyxovirus. *Science* 2000;288(5470): 1432–1435.
23. Nichol ST, Spiropoulou CF, Morzunov S, et al. Genetic identification of a hantavirus associated with an outbreak of acute respiratory illness. *Science* 1993;262(5135):914–917.
24. McCoy L, Sorvillo F, Simon P. Varicella-related mortality in California, 1988–2000. *Pediatr Infect Dis J* 2004;23(6): 498–503.
25. Nguyen HQ, Jumaan AO, Seward JF. Decline in mortality due to varicella after implementation of varicella vaccination in the United States. *N Engl J Med* 2005;352(5): 450–458.
26. Taplitz RA, Jordan MC. Pneumonia caused by herpesviruses in recipients of hematopoietic cell transplants. *Semin Respir Infect* 2002;17(2):121–129.
27. Taubenberger JK, Reid AH, Krafft AE, Bijwaard KE, Fanning TG. Initial genetic characterization of the 1918 “Spanish” influenza virus. *Science* 1997;275(5307): 1793–1796.
28. Tumpey TM, Basler CF, Aguilar PV, et al. Characterization of the reconstructed 1918 Spanish influenza pandemic virus. *Science* 2005;310(5745):77–80.
29. Fischer SA, Graham MB, Kuehnert MJ, et al. Transmission of lymphocytic choriomeningitis virus by organ transplantation. *N Engl J Med* 2006;354(21):2235–2249.
30. Murray K, Selleck P, Hooper P, et al. A morbillivirus that caused fatal disease in horses and humans. *Science* 1995; 268(5207):94–97.
31. Cushing MM, Brat DJ, Mosunjac MI, et al. Fatal West Nile virus encephalitis in a renal transplant recipient. *Am J Clin Pathol* 2004;121(1):26–31.
32. Iwamoto M, Jernigan DB, Guasch A, et al. Transmission of West Nile virus from an organ donor to four transplant recipients. *N Engl J Med* 2003;348(22):2196–2203.
33. Srinivasan A, Burton EC, Kuehnert MJ, et al. Transmission of rabies virus from an organ donor to four transplant recipients. *N Engl J Med* 2005;352(11):1103–1111.
34. Rowe WP, Huebner RJ, Gilmore LK, Parrott RH, Ward TG. Isolation of a cytopathogenic agent from human adenoids undergoing spontaneous degeneration in tissue culture. *Proc Soc Exp Biol Med* 1953;84(3):570–573.
35. Hilleman MR, Werner JH. Recovery of new agent from patients with acute respiratory illness. *Proc Soc Exp Biol Med* 1954;85(1):183–188.

36. Enders JF, Bell JA, Dingle JH, et al. Adenoviruses: group name proposed for new respiratory-tract viruses. *Science* 1956;124(3212):119–120.
37. Hierholzer JC. Adenoviruses in the immunocompromised host. *Clin Microbiol Rev* 1992;5(3):262–274.
38. Pham TT, Burchette JL Jr, Hale LP. Fatal disseminated adenovirus infections in immunocompromised patients. *Am J Clin Pathol* 2003;120(4):575–583.
39. Buescher EL. Respiratory disease and the adenoviruses. *Med Clin North Am* 1967;51(3):769–779.
40. De Jong JC, Wermenbol AG, Verweij-Uijterwaal MW, et al. Adenoviruses from human immunodeficiency virus-infected individuals, including two strains that represent new candidate serotypes Ad50 and Ad51 of species B1 and D, respectively. *J Clin Microbiol* 1999;37(12):3940–3945.
41. Brandt CD, Kim HW, Vargosko AJ, et al. Infections in 18,000 infants and children in a controlled study of respiratory tract disease. I. Adenovirus pathogenicity in relation to serologic type and illness syndrome. *Am J Epidemiol* 1969;90(6):484–500.
42. Ruuskanen O, Meurman O, Sarkkinen H. Adenoviral diseases in children: a study of 105 hospital cases. *Pediatrics* 1985;76(1):79–83.
43. Carballal G, Videla C, Misirlian A, Requeijo PV, Aguilar Mdel C. Adenovirus type 7 associated with severe and fatal acute lower respiratory infections in Argentine children. *BMC Pediatr* 2002;2:6.
44. Simila S, Ylikorkala O, Wasz-Hockert O. Type 7 adenovirus pneumonia. *J Pediatr* 1971;79(4):605–611.
45. Lang WR, Howden CW, Laws J, Burton JF. Bronchopneumonia with serious sequelae in children with evidence of adenovirus type 21 infection. *Br Med J* 1969;1(636):73–79.
46. Munoz FM, Piedra PA, Demmler GJ. Disseminated adenovirus disease in immunocompromised and immunocompetent children. *Clin Infect Dis* 1998;27(5):1194–1200.
47. Zahradnik JM. Adenovirus pneumonia. *Semin Respir Infect* 1987;2(2):104–111.
48. Dudding BA, Wagner SC, Zeller JA, Gmelich JT, French GR, Top FH Jr. Fatal pneumonia associated with adenovirus type 7 in three military trainees. *N Engl J Med* 1972;286(24):1289–1292.
49. Two fatal cases of adenovirus-related illness in previously healthy young adults—Illinois, 2000. *MMWR Morb Mortal Wkly Rep* 2001;50(26):553–555.
50. Becroft DM. Histopathology of fatal adenovirus infection of the respiratory tract in young children. *J Clin Pathol* 1967;20(4):561–569.
51. Ohori NP, Michaels MG, Jaffe R, Williams P, Yousem SA. Adenovirus pneumonia in lung transplant recipients. *Hum Pathol* 1995;26(10):1073–1079.
52. Bayon MN, Drut R. Cytologic diagnosis of adenovirus bronchopneumonia. *Acta Cytol* 1991;35(2):181–182.
53. Rocholl C, Gerber K, Daly J, Pavia AT, Byington CL. Adenoviral infections in children: the impact of rapid diagnosis. *Pediatrics* 2004;113(1 pt 1):e51–56.
54. Pinto A, Beck R, Jadavji T. Fatal neonatal pneumonia caused by adenovirus type 35. Report of one case and review of the literature. *Arch Pathol Lab Med* 1992;116(1):95–99.
55. Garcia AG, Fonseca ME, de Bonis M, Ramos HI, Ferro ZP, Nascimento JP. Morphological and virological studies in six autopsies of children with adenovirus pneumonia. *Mem Inst Oswaldo Cruz* 1993;88(1):141–147.
56. Hierholzer JC, Stone YO, Broderson JR. Antigenic relationships among the 47 human adenoviruses determined in reference horse antisera. *Arch Virol* 1991;121(1–4):179–197.
57. Turner PC, Bailey AS, Cooper RJ, Morris DJ. The polymerase chain reaction for detecting adenovirus DNA in formalin-fixed, paraffin-embedded tissue obtained post mortem. *J Infect* 1993;27(1):43–46.
58. Tran PL, Weinbach J, Opolon P, et al. Prevention of bleomycin-induced pulmonary fibrosis after adenovirus-mediated transfer of the bacterial bleomycin resistance gene. *J Clin Invest* 1997;99(4):608–617.
59. Demmler GJ. Adenoviruses. In: Balows A, ed. *Manual of clinical microbiology*. Washington, DC: American Society for Microbiology, 1994:947–955.
60. Schmaljohn CS. Nucleotide sequence of the L genome segment of Hantaan virus. *Nucleic Acids Res* 1990;18(22):6728.
61. Schmaljohn CS, Dalrymple JM. Analysis of Hantaan virus RNA: evidence for a new genus of bunyaviridae. *Virology* 1983;131(2):482–491.
62. Xiao SY, Leduc JW, Chu YK, Schmaljohn CS. Phylogenetic analyses of virus isolates in the genus Hantavirus, family Bunyaviridae. *Virology* 1994;198(1):205–217.
63. Hung T, Chou ZY, Zhao TX, Gan S, Yanagihara R. Morphology and morphogenesis of viruses of hemorrhagic fever with renal syndrome: inclusion bodies-ultrastructure marker of hantavirus-infected cells. *Intervirology* 1987;27:45–52.
64. Goldsmith CS, Elliott LH, Peters CJ, Zaki SR. Ultrastructural characteristics of Sin Nombre virus, causative agent of hantavirus pulmonary syndrome. *Arch Virol* 1995;140(12):2107–2122.
65. Martin ML, Lindsey-Regnery H, Sasso DR, McCormick JB, Palmer E. Distinction between Bunyaviridae genera by surface structure and comparison with Hantaan virus using negative stain electron microscopy. *Arch Virol* 1985;86(1–2):17–28.
66. Elliott LH, Ksiazek TG, Rollin PE, et al. Isolation of the causative agent of hantavirus pulmonary syndrome. *Am J Trop Med Hyg* 1994;51(1):102–108.
67. Update: hantavirus pulmonary syndrome—United States, 1993. Centers for Disease Control and Prevention, 1993.
68. Lee HW. World Health Organization (WHO) collaborating center for virus reference and research. In: Lee HW, Dalrymple JM, ed. *Manual of hemorrhagic fever with renal syndrome*. Seoul: Korea University, 1989:11–18.
69. Duchin JS, Koster FT, Peters CJ, et al. Hantavirus pulmonary syndrome: a clinical description of 17 patients with a newly recognized disease. The Hantavirus Study Group. *N Engl J Med* 1994;330(14):949–955.
70. Lee HW, Lee PW, Johnson KM. Isolation of the etiologic agent of Korean Hemorrhagic fever. *J Infect Dis* 1978;137(3):298–308.

71. Centers for Disease Control and Prevention. Outbreak of acute illness-southwestern United States, 1993. *MMWR* 1993;42:421-424.
72. Zaki SR, Greer PW, Coffield LM, et al. Hantavirus pulmonary syndrome. Pathogenesis of an emerging infectious disease. *Am J Pathol* 1995;146(3):552-579.
73. Zaki SR. Hantavirus-associated diseases. In: Connor DH, Chandler FW, Schwartz DA, Manz HJ, Lack EE, ed. *Diagnostic pathology of infectious diseases*. Stamford: Appleton and Lange, 1997:125-136.
74. Nolte KB, Feddersen RM, Foucar K, et al. Hantavirus pulmonary syndrome in the United States: a pathological description of a disease caused by a new agent. *Hum Pathol* 1995;26(1):110-120.
75. Lukes RJ. The pathology of thirty-nine fatal cases of epidemic hemorrhagic fever. *Am J Med* 1954;16(5):639-650.
76. Hullinghorst RL, Steer A. Pathology of epidemic hemorrhagic fever. *Ann Intern Med* 1953;38(1):77-101.
77. Kessler WH. Gross anatomic features found in 27 autopsies of epidemic hemorrhagic fever. *Ann Intern Med* 1953;38(1):73-76.
78. Steer A. Pathology of hemorrhagic fever: a comparison of the findings, 1951 and 1952. *Am J Pathol* 1955;31(2):201-221.
79. Hung T, Zhou JY, Tang YM, Zhao TX, Baek LJ, Lee HW. Identification of Hantaan virus-related structures in kidneys of cadavers with haemorrhagic fever with renal syndrome. *Arch Virol* 1992;122:187-199.
80. Kikuchi K, Imamura M, Ueno H, et al. An autopsy case of epidemic hemorrhagic fever (Korean hemorrhagic fever). *Sapporo Medical Journal* 1982;51:K17-K31.
81. Schmaljohn CS, Sugiyama K, Schmaljohn AL, Bishop DH. Baculovirus expression of the small genome segment of Hantaan virus and potential use of the expressed nucleocapsid protein as a diagnostic antigen. *J Gen Virol* 1988;69(pt 4):777-786.
82. Feldmann H, Sanchez A, Morzunov S, et al. Utilization of autopsy RNA for the synthesis of the nucleocapsid antigen of a newly recognized virus associated with hantavirus pulmonary syndrome. *Virus Res* 1993;30(3):351-367.
83. Schwarz TF, Zaki SR, Morzunov S, Peters CJ, Nichol ST. Detection and sequence confirmation of Sin Nombre virus RNA in paraffin-embedded human tissues using one-step RT-PCR. *J Virol Methods* 1995;51(2-3):349-356.
84. Zaki SR, Khan AS, Goodman RA, et al. Retrospective diagnosis of hantavirus pulmonary syndrome, 1978-1993: implications for emerging infectious diseases. *Arch Pathol Lab Med* 1996;120(2):134-139.
85. Zaki SR, Albers RC, Greer PW, et al. Retrospective diagnosis of a 1983 case of fatal hantavirus pulmonary syndrome. *Lancet* 1994;343(8904):1037-1038.
86. Goldsmith CS, Tatti KM, Ksiazek TG, et al. Ultrastructural characterization of SARS coronavirus. *Emerg Infect Dis* 2004;10(2):320-326.
87. Ng ML, Tan SH, See EE, Ooi EE, Ling AE. Proliferative growth of SARS coronavirus in Vero E6 cells. *J Gen Virol* 2003;84(pt 12):3291-3303.
88. Becker WB, McIntosh K, Dees JH, Chanock RM. Morphogenesis of avian infectious bronchitis virus and a related human virus (strain 229E). *J Virol* 1967;1(5):1019-1027.
89. Dubois-Dalcq M, Holmes KV, Rentier B. *Assembly of enveloped RNA viruses*. New York: Springer-Verlag, 1984:100-119.
90. Oshiro LS, Schieble JH, Lennette EH. Electron microscopic studies of coronavirus. *J Gen Virol* 1971;12:161-168.
91. Peiris JS, Lai ST, Poon LL, et al. Coronavirus as a possible cause of severe acute respiratory syndrome. *Lancet* 2003;361(9366):1319-1325.
92. Chong PY, Chui P, Ling AE, et al. Analysis of deaths during the severe acute respiratory syndrome (SARS) epidemic in Singapore: challenges in determining a SARS diagnosis. *Arch Pathol Lab Med* 2004;128(2):195-204.
93. Ding Y, Wang H, Shen H, et al. The clinical pathology of severe acute respiratory syndrome (SARS): a report from China. *J Pathol* 2003;200(3):282-289.
94. Franks TJ, Chong PY, Chui P, et al. Lung pathology of severe acute respiratory syndrome (SARS): a study of 8 autopsy cases from Singapore. *Hum Pathol* 2003;34(8):743-748.
95. Lang ZW, Zhang LJ, Zhang SJ, et al. A clinicopathological study on 3 cases of severe acute respiratory syndrome. *Zhonghua Bing Li Xue Za Zhi* 2003;32(3):201-204.
96. Leung WK, To KF, Chan PK, et al. Enteric involvement of severe acute respiratory syndrome-associated coronavirus infection. *Gastroenterology* 2003;125(4):1011-1017.
97. Nicholls JM, Poon LL, Lee KC, et al. Lung pathology of fatal severe acute respiratory syndrome. *Lancet* 2003;361(9371):1773-1778.
98. Hwang DM, Chamberlain DW, Poutanen SM, Low DE, Asa SL, Butany J. Pulmonary pathology of severe acute respiratory syndrome in Toronto. *Mod Pathol* 2005;18(1):1-10.
99. Nakajima N, Asahi-Ozaki Y, Nagata N, et al. SARS coronavirus-infected cells in lung detected by new in situ hybridization technique. *Jpn J Infect Dis* 2003;56(3):139-141.
100. Shieh WJ, Hsiao CH, Paddock CD, et al. Immunohistochemical, in situ hybridization, and ultrastructural localization of SARS-associated coronavirus in lung of a fatal case of severe acute respiratory syndrome in Taiwan. *Hum Pathol* 2005;36(3):303-309.
101. To KF, Tong JH, Chan PK, et al. Tissue and cellular tropism of the coronavirus associated with severe acute respiratory syndrome: an in-situ hybridization study of fatal cases. *J Pathol* 2004;202(2):157-163.
102. Katzenstein AL. Acute lung injury patterns: diffuse alveolar damage and bronchiolitis obliterans-organizing pneumonia. In: Katzenstein AL, ed. *Katzenstein and Askin's surgical pathology of non-neoplastic lung diseases*. Philadelphia: Saunders, 1997:14-47.
103. Zaki SR. Measles. In: Connor DH, Chandler FW, Schwartz DA, Manz HJ, Lack EE, eds. *Pathology of infectious diseases*. Stamford, CT: Appleton and Lange, 1997:233-244.

104. Wong KT, Shieh WJ, Kumar S, et al. Nipah virus infection: pathology and pathogenesis of an emerging paramyxoviral zoonosis. *Am J Pathol* 2002;161(6):2153–2167.
105. Guarner J, Shieh WJ, Dawson J, et al. Immunohistochemical and in situ hybridization studies of influenza A virus infection in human lungs. *Am J Clin Pathol* 2000;114(2):227–233.
106. Kuiken T, Fouchier RA, Schutten M, et al. Newly discovered coronavirus as the primary cause of severe acute respiratory syndrome. *Lancet* 2003;362(9380):263–270.
107. Haagmans BL, Kuiken T, Martina BE, et al. Pegylated interferon-alpha protects type 1 pneumocytes against SARS coronavirus infection in macaques. *Nat Med* 2004;10(3):290–293.
108. McAuliffe J, Vogel L, Roberts A, et al. Replication of SARS coronavirus administered into the respiratory tract of African Green, rhesus and cynomolgus monkeys. *Virology* 2004;330(1):8–15.
109. Subbarao K, McAuliffe J, Vogel L, et al. Prior infection and passive transfer of neutralizing antibody prevent replication of severe acute respiratory syndrome coronavirus in the respiratory tract of mice. *J Virol* 2004;78(7):3572–3577.
110. Roberts A, Vogel L, Guarner J, et al. Severe acute respiratory syndrome coronavirus infection of golden Syrian hamsters. *J Virol* 2005;79(1):503–511.
111. Ribbert D. Uber protozoenartige Zellen in der Niere eines syphilitischen Neugoborenen und in der Parotis von Kindern. *Zentralbl Allg Pathol* 1904;15:945–948.
112. Goodpasture EW, Talbot FB. Concerning the nature of “protozoan-like” cells in certain lesions of infancy. *Am J Dis Child* 1921;21:415–425.
113. Farber S, Wolback SB. Intranuclear and cytoplasmic inclusions (“protozoan-like bodies”) in the salivary glands and other organs of infants. *Am J Pathol* 1932;8:123–135.
114. Weller TH, Hanshaw JB, Scott DE. Serologic differentiation of viruses responsible for cytomegalic inclusion disease. *Virology* 1960;12:130–132.
115. Perot K, Walker CM, Spaete RR. Primary chimpanzee skin fibroblast cells are fully permissive for human cytomegalovirus replication. *J Gen Virol* 1992;73(pt 12):3281–3284.
116. Riegler S, Hebart H, Einsele H, Brossart P, Jahn G, Sinzger C. Monocyte-derived dendritic cells are permissive to the complete replicative cycle of human cytomegalovirus. *J Gen Virol* 2000;81(pt 2):393–399.
117. Mocarski ES. Cytomegaloviruses and their replication. In: Fields BN, Knipe DM, Howley PM, eds. *Fields virology*. 3rd ed. Philadelphia: Lippincott-Raven, 1996:2447–2492.
118. Wright HT Jr, Goodheart CR, Lielausis A. Human cytomegalovirus. Morphology by negative staining. *Virology* 1964;23:419–424.
119. Klemola E, Von Essen R, Henle G, Henle W. Infectious-mononucleosis-like disease with negative heterophil agglutination test. Clinical features in relation to Epstein-Barr virus and cytomegalovirus antibodies. *J Infect Dis* 1970;121(6):608–614.
120. Cohen JI, Corey GR. Cytomegalovirus infection in the normal host. *Medicine (Baltimore)* 1985;64(2):100–114.
121. Medearis DN Jr. Cytomegalic inclusion disease; an analysis of the clinical features based on the literature and six additional cases. *Pediatrics* 1957;19(3):467–480.
122. Ison MG, Fishman JA. Cytomegalovirus pneumonia in transplant recipients. *Clin Chest Med* 2005;26(4):691–705, viii.
123. Meyers JD, Flournoy N, Thomas ED. Nonbacterial pneumonia after allogeneic marrow transplantation: a review of ten years’ experience. *Rev Infect Dis* 1982;4(6):1119–1132.
124. Kotloff RM, Ahya VN, Crawford SW. Pulmonary complications of solid organ and hematopoietic stem cell transplantation. *Am J Respir Crit Care Med* 2004;170(1):22–48.
125. Balthesen M, Messerle M, Reddehase MJ. Lungs are a major organ site of cytomegalovirus latency and recurrence. *J Virol* 1993;67(9):5360–5366.
126. Stover DE, White DA, Romano PA, Gellene RA, Robeson WA. Spectrum of pulmonary diseases associated with the acquired immune deficiency syndrome. *Am J Med* 1985;78(3):429–437.
127. Herry I, Cadranet J, Antoine M, et al. Cytomegalovirus-induced alveolar hemorrhage in patients with AIDS: a new clinical entity? *Clin Infect Dis* 1996;22(4):616–620.
128. Myerson D, Hackman RC, Nelson JA, Ward DC, McDougall JK. Widespread presence of histologically occult cytomegalovirus. *Hum Pathol* 1984;15(5):430–439.
129. Beschorner WE, Hutchins GM, Burns WH, Saral R, Tutschka PJ, Santos GW. Cytomegalovirus pneumonia in bone marrow transplant recipients: miliary and diffuse patterns. *Am Rev Respir Dis* 1980;122(1):107–114.
130. Wallace JM, Hannah J. Cytomegalovirus pneumonitis in patients with AIDS. Findings in an autopsy series. *Chest* 1987;92(2):198–203.
131. Strano AJ. Light microscopy of selected viral diseases (morphology of viral inclusion bodies). *Pathol Annu* 1976;11:53–75.
132. Kanich RE, Craighead JE. Human cytomegalovirus infection of cultured fibroblasts. II. Viral replicative sequence of a wild and an adapted strain. *Lab Invest* 1972;27(3):273–282.
133. Gorelkin L, Chandler FW, Ewing EP Jr. Staining qualities of cytomegalovirus inclusions in the lungs of patients with the acquired immunodeficiency syndrome: a potential source of diagnostic misinterpretation. *Hum Pathol* 1986;17(9):926–929.
134. Ljungman P, Griffiths P, Paya C. Definitions of cytomegalovirus infection and disease in transplant recipients. *Clin Infect Dis* 2002;34(8):1094–1097.
135. Gleaves CA, Myerson D, Bowden RA, Hackman RC, Meyers JD. Direct detection of cytomegalovirus from bronchoalveolar lavage samples by using a rapid in situ DNA hybridization assay. *J Clin Microbiol* 1989;27(11):2429–2432.
136. Singer DB. Pathology of neonatal Herpes simplex virus infection. *Perspect Pediatr Pathol* 1981;6:243–278.
137. Feldman S, Stokes DC. Varicella zoster and herpes simplex virus pneumonias. *Semin Respir Infect* 1987;2(2):84–94.

138. Whitley RJ. Herpes simplex viruses. In: Fields BN, Knipe DM, Howley PM, eds. *Fields virology*. 3rd ed. Philadelphia: Lippincott-Raven, 1996:2297–2342.
139. Baringer JR. Recovery of herpes simplex virus from human sacral ganglions. *N Engl J Med* 1974;291(16):828–830.
140. Bastain FO, Rabson AS, Yee CL. Herpesvirus hominis: isolation from human trigeminal ganglion. *Science* 1972;178:306–307.
141. Corey L, Spear PG. Infections with herpes simplex viruses (1). *N Engl J Med* 1986;314(11):686–691.
142. Corey L, Spear PG. Infections with herpes simplex viruses (2). *N Engl J Med* 1986;314(12):749–757.
143. Nash G, Foley FD. Herpetic infection of the middle and lower respiratory tract. *Am J Clin Pathol* 1970;54(6):857–863.
144. Ramsey PG, Fife KH, Hackman RC, Meyers JD, Corey L. Herpes simplex virus pneumonia: clinical, virologic, and pathologic features in 20 patients. *Ann Intern Med* 1982;97(6):813–820.
145. Cherr GS, Meredith JW, Chang M. Herpes simplex virus pneumonia in trauma patients. *J Trauma* 2000;49(3):547–549.
146. Ferrari A, Luppi M, Potenza L, et al. Herpes simplex virus pneumonia during standard induction chemotherapy for acute leukemia: case report and review of literature. *Leukemia* 2005;19(11):2019–2021.
147. Hass GM. Hepato-adrenal necrosis with intranuclear inclusion bodies. *Am J Pathol* 1935;11:127–147.
148. Raga J, Chrystal V, Coovadia HM. Usefulness of clinical features and liver biopsy in diagnosis of disseminated herpes simplex infection. *Arch Dis Child* 1984;59(9):820–824.
149. Kimberlin DW. Neonatal herpes simplex infection. *Clin Microbiol Rev* 2004;17(1):1–13.
150. Lissauer TJ, Shaw PJ, Underhill G. Neonatal herpes simplex pneumonia. *Arch Dis Child* 1984;59(7):668–670.
151. Morrison SC, Comisky E, Fletcher BD. Calcification in the adrenal glands associated with disseminated herpes simplex infection. *Pediatr Radiol* 1988;18(3):240–241.
152. Nash G. Necrotizing tracheobronchitis and bronchopneumonia consistent with herpetic infection. *Hum Pathol* 1972;3(2):283–291.
153. Sherry MK, Klainer AS, Wolff M, Gerhard H. Herpetic tracheobronchitis. *Ann Intern Med* 1988;109(3):229–233.
154. Graham BS, Snell JD Jr. Herpes simplex virus infection of the adult lower respiratory tract. *Medicine (Baltimore)* 1983;62(6):384–393.
155. Morgan HR, Finland M. Isolation of herpes virus from a case of atypical pneumonia and erythema multiforme exudativum. *Am J Med Sci* 1949;217:92–95.
156. Prellner T, Flamholz L, Haidl S, Lindholm K, Widell A. Herpes simplex virus—the most frequently isolated pathogen in the lungs of patients with severe respiratory distress. *Scand J Infect Dis* 1992;24(3):283–292.
157. Tuxen DV, Cade JF, McDonald MI, Buchanan MR, Clark RJ, Pain MC. Herpes simplex virus from the lower respiratory tract in adult respiratory distress syndrome. *Am Rev Respir Dis* 1982;126(3):416–419.
158. Cowdry EV. The problem of intranuclear inclusions in virus diseases. *Arch Pathol* 1934;18:527–540.
159. Strickler JG, Manivel JC, Copenhaver CM, Kubic VL. Comparison of in situ hybridization and immunohistochemistry for detection of cytomegalovirus and herpes simplex virus. *Hum Pathol* 1990;21(4):443–448.
160. Arvin A. Varicella-zoster virus. In: Fields BN, Knipe DM, Howley PM, eds. *Fields virology*. 3rd ed. Philadelphia: Lippincott-Raven, 1996.
161. Silverstein S, Straus SE. Varicella-zoster virus: pathogenesis of latency and reactivation. In: Arvin AM, Gershon AA, eds. *Varicella-zoster virus: virology and clinical practice*. Cambridge, UK: Cambridge University Press, 2000:123–141.
162. Varicella-related deaths among adults—United States, 1997. *MMWR Morb Mortal Wkly Rep* 1997;46(19):409–412.
163. Kaneko T, Ishigatsubo Y. Varicella pneumonia in adults. *Intern Med* 2004;43(12):1105–1106.
164. Waring JJ, Neuburger K, Geever EF. Severe forms of chickenpox in adults. *Arch Intern Med* 1942:384–408.
165. Choo PW, Donahue JG, Manson JE, Platt R. The epidemiology of varicella and its complications. *J Infect Dis* 1995;172(3):706–712.
166. Weber DM, Pellicchia JA. Varicella pneumonia: study of prevalence in adult men. *JAMA* 1965;192:572–573.
167. Triebwasser JH, Harris RE, Bryant RE, Rhoades ER. Varicella pneumonia in adults. Report of seven cases and a review of literature. *Medicine (Baltimore)* 1967;46(5):409–423.
168. Mermelstein RH, Freireich AW. Varicella pneumonia. *Ann Intern Med* 1961;55:456–463.
169. Feldman S. Varicella-zoster virus pneumonitis. *Chest* 1994;106(1 suppl):22S–27S.
170. Fehr T, Bossart W, Wahl C, Binswanger U. Disseminated varicella infection in adult renal allograft recipients: four cases and a review of the literature. *Transplantation* 2002;73(4):608–611.
171. Harger JH, Ernest JM, Thurnau GR, et al. Risk factors and outcome of varicella-zoster virus pneumonia in pregnant women. *J Infect Dis* 2002;185(4):422–427.
172. Miliauskas JR, Webber BL. Disseminated varicella at autopsy in children with cancer. *Cancer* 1984;53(7):1518–1525.
173. Sargent EN, Carson MJ, Reilly ED. Roentgenographic manifestations of varicella pneumonia with postmortem correlation. *Am J Roentgenol Radium Ther Nucl Med* 1966;98(2):305–317.
174. Johnson HN. Visceral lesions associated with varicella. *Arch Pathol* 1940;30:292–307.
175. Raider L. Calcification in chickenpox pneumonia. *Chest* 1971;60(5):504–507.
176. Brunton FJ, Moore ME. A survey of pulmonary calcification following adult chicken-pox. *Br J Radiol* 1969;42(496):256–259.
177. Grant RM, Weitzman SS, Sherman CG, Sirkin WL, Petric M, Tellier R. Fulminant disseminated varicella zoster virus infection without skin involvement. *J Clin Virol* 2002;24(1–2):7–12.

178. Grose C, Perrotta DM, Brunell PA, Smith GC. Cell-free varicella-zoster virus in cultured human melanoma cells. *J Gen Virol* 1979;43(1):15–27.
179. Wright PF, Webster RG. Orthomyxoviruses. In: Knipe DM, Howley PM, eds. *Fields virology*. 4th ed. Philadelphia: Lippincott Williams & Wilkins, 2001:1533–1579.
180. Cox NJ, Kawaoka Y. Orthomyxoviruses: Influenza. In: Mahy BWJ, Collier L, eds. *Topley and Wilson's microbiology and microbial infections*. London: Arnold, 1998: 385–433.
181. Hers JFP. Changes in the respiratory mucosa resulting from infection with influenza virus. *Br J Pathol Bacteriol* 1957;73:565–568.
182. Hers JF, Masurel N, Mulder J. Bacteriology and histopathology of the respiratory tract and lungs in fatal Asian influenza. *Lancet* 1958;2(7057):1141–1143.
183. Martin CM, Kunin CM, Gottlieb LS, Barnes MW, Liu C, Finland M. Asian influenza A in Boston, 1957–1958. I. Observations in thirty-two influenza-associated fatal cases. *AMA Arch Intern Med* 1959;103(4):515–531.
184. Martin CM, Kunin CM, Gottlieb LS, Finland M. Asian influenza A in Boston, 1957–1958. II. Severe staphylococcal pneumonia complicating influenza. *AMA Arch Intern Med* 1959;103(4):532–542.
185. Noble RL, Lillington GA, Kempson RL. Fatal diffuse influenzal pneumonia: premortem diagnosis by lung biopsy. *Chest* 1973;63(4):644–646.
186. Oseasohn R, Adelson L, Kaji M. Clinicopathologic study of thirty-three fatal cases of Asian influenza. *N Engl J Med* 1959;260(11):509–518.
187. Yeldandi AV, Colby TV. Pathologic features of lung biopsy specimens from influenza pneumonia cases. *Hum Pathol* 1994;25(1):47–53.
188. Walsh JJ, Dietlein LF, Low FN, Burch GE, Mogabgab WJ. Bronchotracheal response in human influenza. Type A, Asian strain, as studied by light and electron microscopic examination of bronchoscopic biopsies. *Arch Intern Med* 1961;108:376–388.
189. Nolte KB, Alakija P, Oty G, et al. Influenza A virus infection complicated by fatal myocarditis. *Am J Forensic Med Pathol* 2000;21(4):375–379.
190. Guarner J, Paddock CD, Shieh WJ, et al. Histopathologic and immunohistochemical features of fatal influenza virus infections in children during the 2003–2004 season. *Clin Infect Dis* 2006;43:132–140.
191. Ungchusak K, Auewarakul P, Dowell SF, et al. Probable person-to-person transmission of avian influenza A (H5N1). *N Engl J Med* 2005;352(4):333–340.
192. Mulder J, Hers JFPh. *Influenza*. Groningen: Wolters-Noordhoff, 1972.
193. Bhat N, Wright JG, Broder KR, et al. Influenza-associated deaths among children in the United States, 2003–2004. *N Engl J Med* 2005;353(24):2559–2567.
194. van Riel D, Munster VJ, de Wit E, et al. H5N1 virus attachment to lower respiratory tract. *Science* 2006;312(5772): 399.
195. Shinya K, Ebina M, Yamada S, Ono M, Kasai N, Kawaoka Y. Avian flu: influenza virus receptors in the human airway. *Nature* 2006;440(7083):435–436.
196. Uyeki TM. Influenza diagnosis and treatment in children: a review of studies on clinically useful tests and antiviral treatment for influenza. *Pediatr Infect Dis J* 2003;22(2): 164–177.
197. Ruest A, Michaud S, Deslandes S, Frost EH. Comparison of the Directigen flu A+B test, the Quick Vue influenza test, and clinical case definition to viral culture and reverse transcription-PCR for rapid diagnosis of influenza virus infection. *J Clin Microbiol* 2003;41(8):3487–3493.
198. Kingsbury DW. Paromyxoviridae and their replication. In: Fields BN, Knipe DM, eds. *Fields virology*. 2nd ed. New York: Raven Press, 1990:945–962.
199. Kingsbury DW, Bratt MA, Choppin PW, et al. Paramyxoviridae. *Intervirology* 1978;10:137–152.
200. Palmer EL, Martin ML. *Electron microscopy in viral diagnosis*. Boca Raton, FL: CRC Press, 1988.
201. Centers for Disease Control and Prevention. Measles surveillance—United States. *MMWR* 1991;41(SS-6):1–7.
202. Babbott FL Jr, Gordon JE. Modern measles. *Am J Med Sci* 1954;228(3):334–361.
203. Goldberger J, Anderson JF. An experimental demonstration of the presence of the virus of measles in the mixed buccal and nasal secretions. *JAMA* 1911;57:476–478.
204. Norrby E, Oxman MN. Measles virus. In: Fields BN, Knipe DM, Chanock RM, Hirsch MS, Melnick JL, Monath TP, Roizman B, eds. *Virology*. 2nd ed. New York: Raven, 1990:1013–1044.
205. Centers for Disease Control and Prevention. Measles—Duval County, Florida, 1991–1992. *MMWR* 1993;42:81–83.
206. Gremillion DH, Crawford GE. Measles pneumonia in young adults. An analysis of 106 cases. *Am J Med* 1981; 71(4):539–542.
207. Kipps A, Kaschula RO. Virus pneumonia following measles: a virological and histological study of autopsy material. *S Afr Med J* 1976;50(28):1083–1088.
208. Archibald RW, Weller RO, Meadow SR. Measles pneumonia and the nature of the inclusion-bearing giant cells: a light- and electron-microscope study. *J Pathol* 1971;103(1): 27–34.
209. Breitfeld V, Hashida Y, Sherman FE, Odagiri K, Yunis EJ. Fatal measles infection in children with leukemia. *Lab Invest* 1973;28(3):279–291.
210. Monafo WJ, Haslam DB, Roberts RL, Zaki SR, Bellini WJ, Coffin CM. Disseminated measles infection after vaccination in a child with a congenital immunodeficiency. *J Pediatr* 1994;124(2):273–276.
211. Akhtar M, Young I. Measles giant cell pneumonia in an adult following long-term chemotherapy. *Arch Pathol* 1973;96(3):145–148.
212. Christensen PE, Schmidt H, Bang HO, Andersen V, Jordal B, Jensen O. An epidemic of measles in southern Greenland, 1951; measles in virgin soil. II. The epidemic proper. *Acta Med Scand* 1953;144(6):408–429.
213. Nanche D, Varior-Krishnan G, Cervoni F, et al. Human membrane cofactor protein (CD46) acts as a cellular receptor for measles virus. *J Virol* 1993;67(10): 6025–6032.

214. Wild TF, Malvoisin E, Buckland R. Measles virus: both the haemagglutinin and fusion glycoproteins are required for fusion. *J Gen Virol* 1991;72(pt 2):439–442.
215. Robbins FC. Measles: clinical features, pathogenesis, pathology and complications. *Am J Dis Child* 1962;103:266–273.
216. Sherman FE, Ruckle G. In vivo and in vitro cellular changes specific for measles. *AMA Arch Pathol* 1958;65(6):587–599.
217. Lewis MJ, Cameron AH, Shah KJ, Purdham DR, Mann JR. Giant-cell pneumonia caused by measles and methotrexate in childhood leukaemia in remission. *Br Med J* 1978;1(6109):330–331.
218. Joliat G, Abetel G, Schindler AM, Kapanci Y. Measles giant cell pneumonia without rash in a case of lymphocytic lymphosarcoma. An electron microscopic study. *Virchows Arch A Pathol Pathol Anat* 1973;358(3):215–224.
219. Merz DC, Scheid A, Choppin PW. Importance of antibodies to the fusion glycoprotein of paramyxoviruses in the prevention of spread of infection. *J Exp Med* 1980;151(2):275–288.
220. Rauh LW, Schmidt R. Measles immunization with killed virus vaccine. Serum antibody titers and experience with exposure to measles epidemic. *Am J Dis Child* 1965;109:232–237.
221. Fulginiti VA, Eller JJ, Downie AW, Kempe CH. Altered reactivity to measles virus. Atypical measles in children previously immunized with inactivated measles virus vaccines. *JAMA* 1967;202(12):1075–1080.
222. Laptook A, Wind E, Nussbaum M, Shenker IR. Pulmonary lesions in atypical measles. *Pediatrics* 1978;62(1):42–46.
223. Norrby E, Enders-Ruckle G, ter Meulen V. Difference in the appearance of antibodies to structural components of measles virus after immunization with inactivated and live virus. *J Infect Dis* 1975;132:262–269.
224. Mallory FB, Medlar EM. The skin lesion in measles. *J Med Res* 1920;41:327–348.
225. Enders JF, McCarthy K, Mitus A, Cheatham WJ. Isolation of measles virus at autopsy in cases of giant-cell pneumonia without rash. *N Engl J Med* 1959;261:875–881.
226. Radoycich GE, Zuppan CW, Weeks DA, Krous HF, Langston C. Patterns of measles pneumonitis. *Pediatr Pathol* 1992;12(6):773–786.
227. Sobonya RE, Hiller FC, Pingleton W, Watanabe I. Fatal measles (rubeola) pneumonia in adults. *Arch Pathol Lab Med* 1978;102(7):366–371.
228. Suringa DW, Bank LJ, Ackerman AB. Role of measles virus in skin lesions and Koplik's spots. *N Engl J Med* 1970;283(21):1139–1142.
229. Strano AJ. Viral pneumonias (viral interstitial pneumonitis). In: Binford DH, Connor DH, eds. *Pathology of tropical and extraordinary diseases*. Washington, DC: Armed Forces Institute of Pathology, 1976:57–64.
230. Becroft DM, Osborne DR. The lungs in fatal measles infection in childhood: pathological, radiological and immunological correlations. *Histopathology* 1980;4(4):401–412.
231. Kimura A, Tosaka K, Nakao T. Measles rash. Light and electron microscopic study of skin eruptions. *Arch Virol* 1975;47:295–307.
232. Allen MS, Talbot WH, McDonald RM. Atypical lymph-node hyperplasia after administration of attenuated, live measles vaccine. *N Engl J Med* 1966;274:667–678.
233. Dorfman RF, Warnke R. Lymphadenopathy simulating the malignant lymphomas. *Hum Pathol* 1974;5(5):519–550.
234. Stejskal J. Measles lymphadenopathy. *Ultrastruct Pathol* 1980;1(2):243–247.
235. Koffler D. Giant cell pneumonia; fluorescent antibody and histochemical studies on alveolar giant cells. *Arch Pathol* 1964;78:267–273.
236. McQuillin J, Bell TM, Gardner PS, Downham PS. Application of immunofluorescence to a study of measles. *Arch Dis Child* 1976;51(6):411–419.
237. Sata T, Kurata T, Aoyama Y, Sakaguchi M, Yamanouchi K, Takeda K. Analysis of viral antigens in giant cells of measles pneumonia by immunoperoxidase method. *Virchows Arch A Pathol Pathol Anat Histopathol* 1986;410(2):133–138.
238. Delage G, Brochu P, Robillard L, Jasmin G, Joncas JH, Lapointe N. Giant cell pneumonia due to respiratory syncytial virus. Occurrence in severe combined immunodeficiency syndrome. *Arch Pathol Lab Med* 1984;108(8):623–625.
239. Little BW, Tihen WS, Dickerman JD, Craighead JE. Giant cell pneumonia associated with parainfluenza virus type 3 infection. *Hum Pathol* 1981;12(5):478–481.
240. Weintrub PS, Sullender WM, Lombard C, Link MP, Arvin A. Giant cell pneumonia caused by parainfluenza type 3 in a patient with acute myelomonocytic leukemia. *Arch Pathol Lab Med* 1987;111(6):569–570.
241. Saito F, Yutani C, Imakita M, Ishibashi-Ueda H, Kanzaki T, Chiba Y. Giant cell pneumonia caused by varicella zoster virus in a neonate. *Arch Pathol Lab Med* 1989;113(2):201–203.
242. Murray K, Rogers R, Selvey L, et al. A novel morbillivirus pneumonia of horses and its transmission to humans. *Emerg Infect Dis* 1995;1(1):31–33.
243. McQuaid S, Isserte S, Allan GM, Taylor MJ, Allen IV, Cosby SL. Use of immunocytochemistry and biotinylated in situ hybridization for detecting measles virus in central nervous system tissue. *J Clin Pathol* 1990;43(4):329–333.
244. Kim TM, Brown HR, Lee SH, et al. Delayed acute measles inclusion body encephalitis in a 9-year-old girl: ultrastructural, immunohistochemical, and in situ hybridization studies. *Mod Pathol* 1992;5(3):348–352.
245. Hummel KB, Erdman DD, Heath J, Bellini WJ. Baculovirus expression of the nucleoprotein gene of measles virus and utility of the recombinant protein in diagnostic enzyme immunoassays. *J Clin Microbiol* 1992;30(11):2874–2880.
246. Collins PL, Chanock RM, McIntosh K. Parainfluenza viruses. In: Fields BN, Knipe DM, Howley PM, eds. *Fields virology*. 3rd ed. Philadelphia: Lippincott-Raven, 1996:1205–1241.

247. Glezen WP, Denny FW. Parainfluenza viruses. In: Evans A, Kaslow R, eds. *Viral infections in humans: epidemiology and control*. 4th ed. New York: Plenum, 1997: 551–567.
248. Wendt CH, Weisdorf DJ, Jordan MC, Balfour HH Jr, Hertz MI. Parainfluenza virus respiratory infection after bone marrow transplantation. *N Engl J Med* 1992;326(14): 921–926.
249. Lewis VA, Champlin R, Englund J, et al. Respiratory disease due to parainfluenza virus in adult bone marrow transplant recipients. *Clin Infect Dis* 1996;23(5):1033–1037.
250. Ljungman P. Respiratory virus infections in bone marrow transplant recipients: the European perspective. *Am J Med* 1997;102(3A):44–47.
251. Matar LD, McAdams HP, Palmer SM, et al. Respiratory viral infections in lung transplant recipients: radiologic findings with clinical correlation. *Radiology* 1999;213(3): 735–742.
252. Cortez KJ, Erdman DD, Peret TC, et al. Outbreak of human parainfluenza virus 3 infections in a hematopoietic stem cell transplant population. *J Infect Dis* 2001;184(9): 1093–1097.
253. Elizaga J, Olavarria E, Apperley J, Goldman J, Ward K. Parainfluenza virus 3 infection after stem cell transplant: relevance to outcome of rapid diagnosis and ribavirin treatment. *Clin Infect Dis* 2001;32(3):413–418.
254. Chakrabarti S, Collingham KE, Holder K, Fegan CD, Osman H, Milligan DW. Pre-emptive oral ribavirin therapy of paramyxovirus infections after haematopoietic stem cell transplantation: a pilot study. *Bone Marrow Transplant* 2001;28(8):759–763.
255. Akizuki S, Nasu N, Setoguchi M, Yoshida S, Higuchi Y, Yamamoto S. Parainfluenza virus pneumonitis in an adult. *Arch Pathol Lab Med* 1991;115(8):824–826.
256. Apalsch AM, Green M, Ledesma-Medina J, Nour B, Wald ER. Parainfluenza and influenza virus infections in pediatric organ transplant recipients. *Clin Infect Dis* 1995;20(2): 394–399.
257. Butnor KJ, Sporn TA. Human parainfluenza virus giant cell pneumonia following cord blood transplant associated with pulmonary alveolar proteinosis. *Arch Pathol Lab Med* 2003;127(2):235–238.
258. Madden JF, Burchette JL Jr, Hale LP. Pathology of parainfluenza virus infection in patients with congenital immunodeficiency syndromes. *Hum Pathol* 2004;35(5): 594–603.
259. Jarvis WR, Middleton PJ, Gelfand EW. Parainfluenza pneumonia in severe combined immunodeficiency disease. *J Pediatr* 1979;94(3):423–425.
260. Frank JA Jr, Warren RW, Tucker JA, Zeller J, Wilfert CM. Disseminated parainfluenza infection in a child with severe combined immunodeficiency. *Am J Dis Child* 1983;137(12): 1172–1174.
261. Gardner PS, McQuillin J, McGuckin R, Ditchburn RK. Observations on clinical and immunofluorescent diagnosis of parainfluenza virus infections. *Br Med J* 1971;2(752): 7–12.
262. Welliver RC, Wong DT, Sun M, McCarthy N. Parainfluenza virus bronchiolitis. *Epidemiology and pathogenesis*. *Am J Dis Child* 1986;140(1):34–40.
263. Waner JL, Whitehurst NJ, Downs T, Graves DG. Production of monoclonal antibodies against parainfluenza 3 virus and their use in diagnosis by immunofluorescence. *J Clin Microbiol* 1985;22(4):535–538.
264. Minnich L, Ray CG. Comparison of direct immunofluorescent staining of clinical specimens for respiratory virus antigens with conventional isolation techniques. *J Clin Microbiol* 1980;12(3):391–394.
265. Collins PL, McIntosh K, Chanock RM. Respiratory syncytial virus. In: Fields BN, Knipe DM, Howley PM, eds. *Fields virology*. 3rd ed. Philadelphia: Lippincott-Raven, 1996: 1313–1351.
266. McIntosh K. Respiratory syncytial virus. In: Evans A, Kaslow R, eds. *Viral infections in humans: epidemiology and control*. 4th ed. New York: Plenum, 1997:691–705.
267. Adams JM. Primary virus infection with cytoplasmic inclusion bodies. Study of an epidemic involving thirty-two infants with nine deaths. *JAMA* 1947;116:1037–1039.
268. Aherne W, Bird T, Court SD, Gardner PS, McQuillin J. Pathological changes in virus infections of the lower respiratory tract in children. *J Clin Pathol* 1970;23(1):7–18.
269. Englund JA, Sullivan CJ, Jordan MC, Dehner LP, Vercellotti GM, Balfour HH Jr. Respiratory syncytial virus infection in immunocompromised adults. *Ann Intern Med* 1988;109(3):203–208.
270. Hall CB, Kopelman AE, Douglas RG Jr, Geiman JM, Meagher MP. Neonatal respiratory syncytial virus infection. *N Engl J Med* 1979;300(8):393–396.
271. Kurlandsky LE, French G, Webb PM, Porter DD. Fatal respiratory syncytial virus pneumonitis in a previously healthy child. *Am Rev Respir Dis* 1988;138(2): 468–472.
272. Levenson RM, Kantor OS. Fatal pneumonia in an adult due to respiratory syncytial virus. *Arch Intern Med* 1987;147(4):791–792.
273. Neilson KA, Yunis EJ. Demonstration of respiratory syncytial virus in an autopsy series. *Pediatr Pathol* 1990; 10(4):491–502.
274. Zaki SR, Bellini WJ. Measles. In: Connor DH, Chandler FW, Schwartz DA, Manz HJ, Lack EE, eds. *Pathology of infectious diseases*. Stamford, CT: Appleton and Lange, 1997:233–244.
275. Ahluwalia GS, Hammond GW. Comparison of cell culture and three enzyme-linked immunosorbent assays for the rapid diagnosis of respiratory syncytial virus from nasopharyngeal aspirate and tracheal secretion specimens. *Diagn Microbiol Infect Dis* 1988;9(3):187–192.
276. Bustamante-Calvillo ME, Velazquez FR, Cabrera-Munoz L, et al. Molecular detection of respiratory syncytial virus in postmortem lung tissue samples from Mexican children deceased with pneumonia. *Pediatr Infect Dis J* 2001; 20(5):495–501.
277. Hall CB, Douglas RG Jr. Clinically useful method for the isolation of respiratory syncytial virus. *J Infect Dis* 1975; 131(1):1–5.
278. Hall CB, Douglas RG Jr, Geiman JM. Respiratory syncytial virus infections in infants: quantitation and duration of shedding. *J Pediatr* 1976;89(1):11–15.

279. Kao CL, McIntosh K, Fernie B, Talis A, Pierik L, Anderson L. Monoclonal antibodies for the rapid diagnosis of respiratory syncytial virus infection by immunofluorescence. *Diagn Microbiol Infect Dis* 1984;2(3):199–206.
280. Kim HW, Wyatt RG, Fernie BF, et al. Respiratory syncytial virus detection by immunofluorescence in nasal secretions with monoclonal antibodies against selected surface and internal proteins. *J Clin Microbiol* 1983;18(6):1399–1404.
281. King JC Jr, Burke AR, Clemens JD, et al. Respiratory syncytial virus illnesses in human immunodeficiency virus- and noninfected children. *Pediatr Infect Dis J* 1993;12(9):733–739.
282. van den Hoogen BG, de Jong JC, Groen J, et al. A newly discovered human pneumovirus isolated from young children with respiratory tract disease. *Nat Med* 2001;7(6):719–724.
283. van den Hoogen BG, van Doornum GJ, Fockens JC, et al. Prevalence and clinical symptoms of human metapneumovirus infection in hospitalized patients. *J Infect Dis* 2003;188(10):1571–1577.
284. Boivin G, Abed Y, Pelletier G, et al. Virological features and clinical manifestations associated with human metapneumovirus: a new paramyxovirus responsible for acute respiratory-tract infections in all age groups. *J Infect Dis* 2002;186(9):1330–1334.
285. Esper F, Boucher D, Weibel C, Martinello RA, Kahn JS. Human metapneumovirus infection in the United States: clinical manifestations associated with a newly emerging respiratory infection in children. *Pediatrics* 2003;111(6 pt 1):1407–1410.
286. Peiris JS, Tang WH, Chan KH, et al. Children with respiratory disease associated with metapneumovirus in Hong Kong. *Emerg Infect Dis* 2003;9(6):628–633.
287. Williams JV, Harris PA, Tollefson SJ, et al. Human metapneumovirus and lower respiratory tract disease in otherwise healthy infants and children. *N Engl J Med* 2004;350(5):443–450.
288. Williams JV, Martino R, Rabella N, et al. A prospective study comparing human metapneumovirus with other respiratory viruses in adults with hematologic malignancies and respiratory tract infections. *J Infect Dis* 2005;192(6):1061–1065.
289. Cane PA, van den Hoogen BG, Chakrabarti S, Fegan CD, Osterhaus AD. Human metapneumovirus in a haematopoietic stem cell transplant recipient with fatal lower respiratory tract disease. *Bone Marrow Transplant* 2003;31(4):309–310.
290. Pelletier G, Dery P, Abed Y, Boivin G. Respiratory tract reinfections by the new human Metapneumovirus in an immunocompromised child. *Emerg Infect Dis* 2002;8(9):976–978.
291. Kuiken T, van den Hoogen BG, van Riel DA, et al. Experimental human metapneumovirus infection of cynomolgus macaques (*Macaca fascicularis*) results in virus replication in ciliated epithelial cells and pneumocytes with associated lesions throughout the respiratory tract. *Am J Pathol* 2004;164(6):1893–1900.
292. Sumino KC, Agapov E, Pierce RA, et al. Detection of severe human metapneumovirus infection by real-time polymerase chain reaction and histopathological assessment. *J Infect Dis* 2005;192(6):1052–1060.
293. Vargas SO, Kozakewich HP, Perez-Atayde AR, McAdam AJ. Pathology of human metapneumovirus infection: insights into the pathogenesis of a newly identified respiratory virus. *Pediatr Dev Pathol* 2004;7(5):478–486; discussion 421.
294. Chan PK, To KF, Wu A, et al. Human metapneumovirus-associated atypical pneumonia and SARS. *Emerg Infect Dis* 2004;10(3):497–500.
295. From the Centers for Disease Control and Prevention. Outbreak of Hendra-like virus—Malaysia and Singapore, 1998–1999. *JAMA* 1999;281(19):1787–1788.
296. Chua KB, Goh KJ, Wong KT, et al. Fatal encephalitis due to Nipah virus among pig-farmers in Malaysia. *Lancet* 1999;354(9186):1257–1259.
297. Paton NI, Leo YS, Zaki SR, et al. Outbreak of Nipah-virus infection among abattoir workers in Singapore. *Lancet* 1999;354(9186):1253–1256.
298. Tambyah PA, Tan JH, Ong BK, Ho KH, Chan KP. First case of Nipah virus encephalitis in Singapore. *Intern Med J* 2001;31(2):132–133.
299. Parashar UD, Sunn LM, Ong F, et al. Case-control study of risk factors for human infection with a new zoonotic paramyxovirus, Nipah virus, during a 1998–1999 outbreak of severe encephalitis in Malaysia. *J Infect Dis* 2000;181(5):1755–1759.
300. Goh KJ, Tan CT, Chew NK, et al. Clinical features of Nipah virus encephalitis among pig farmers in Malaysia. *N Engl J Med* 2000;342(17):1229–1235.
301. Lee KE, Umapathi T, Tan CB, et al. The neurological manifestations of Nipah virus encephalitis, a novel paramyxovirus. *Ann Neurol* 1999;46(3):428–432.
302. Harcourt BH, Tamin A, Ksiazek TG, et al. Molecular characterization of Nipah virus, a newly emergent paramyxovirus. *Virology* 2000;271(2):334–349.
303. Hsu VP, Hossain MJ, Parashar UD, et al. Nipah virus encephalitis reemergence, Bangladesh. *Emerg Infect Dis* 2004;10(12):2082–2087.
304. Chadha MS, Comer JA, Lowe L, et al. Nipah virus-associated encephalitis outbreak, Siliguri, India. *Emerg Infect Dis* 2006;12(2):235–240.
305. Yob JM, Field H, Rashdi AM, et al. Nipah virus infection in bats (order Chiroptera) in peninsular Malaysia. *Emerg Infect Dis* 2001;7(3):439–441.
306. Halpin K, Young PL, Field HE, Mackenzie JS. Isolation of Hendra virus from pteropid bats: a natural reservoir of Hendra virus. *J Gen Virol* 2000;81(pt 8):1927–1932.
307. Olson JG, Rupprecht C, Rollin PE, et al. Antibodies to Nipah-like virus in bats (*Pteropus lylei*), Cambodia. *Emerg Infect Dis* 2002;8(9):987–988.
308. Reynes JM, Counor D, Ong S, et al. Nipah virus in Lyle's flying foxes, Cambodia. *Emerg Infect Dis* 2005;11(7):1042–1047.
309. Field H, Young P, Yob JM, Mills J, Hall L, Mackenzie J. The natural history of Hendra and Nipah viruses. *Microbes Infect* 2001;3(4):307–314.
310. Lamb RA, Kolakofsky D. Paramyxoviridae. In: Knipe DM, Howley PM, eds. *Fields virology*. 4th ed. Philadelphia: Lippincott Williams & Wilkins, 2001:1305–1340.

311. Goldsmith CS, Whistler T, Rollin PE, et al. Elucidation of Nipah virus morphogenesis and replication using ultrastructural and molecular approaches. *Virus Res* 2003;92(1): 89–98.
312. Hyatt AD, Zaki SR, Goldsmith CS, Wise TG, Hengstberger SG. Ultrastructure of Hendra virus and Nipah virus within cultured cells and host animals. *Microbes Infect* 2001;3(4): 297–306.
313. Selvey LA, Wells RM, McCormack JG, et al. Infection of humans and horses by a newly described morbillivirus. *Med J Aust* 1995;162(12):642–645.
314. O'Sullivan JD, Allworth AM, Paterson DL, et al. Fatal encephalitis due to novel paramyxovirus transmitted from horses. *Lancet* 1997;349(9045):93–95.
315. Hooper P, Zaki S, Daniels P, Middleton D. Comparative pathology of the diseases caused by Hendra and Nipah viruses. *Microbes Infect* 2001;3(4):315–322.
316. Tanimura N, Imada T, Kashiwazaki Y, et al. Reactivity of anti-Nipah virus monoclonal antibodies to formalin-fixed, paraffin-embedded lung tissues from experimental Nipah and Hendra virus infections. *J Vet Med Sci* 2004;66(10): 1263–1266.
317. Harcourt BH, Lowe L, Tamin A, et al. Genetic characterization of Nipah virus, Bangladesh, 2004. *Emerg Infect Dis* 2005;11(10):1594–1597.
318. Smith IL, Halpin K, Warrilow D, Smith GA. Development of a fluorogenic RT-PCR assay (TaqMan) for the detection of Hendra virus. *J Virol Methods* 2001;98(1): 33–40.
319. Guillaume V, Lefeuvre A, Faure C, et al. Specific detection of Nipah virus using real-time RT-PCR (TaqMan). *J Virol Methods* 2004;120(2):229–237.
320. Allander T, Tammi MT, Eriksson M, Bjerkner A, Tiveljung-Lindell A, Andersson B. Cloning of a human parvovirus by molecular screening of respiratory tract samples. *Proc Natl Acad Sci USA* 2005;102(36):12891–12896.
321. Heegaard ED, Brown KE. Human parvovirus B19. *Clin Microbiol Rev* 2002;15(3):485–505.
322. Anderson L, Zaki SR, Török TJ. Parvovirus infections (*Erythema infectiosum*). In: Wilfert CM, ed. *Pediatric Infectious Diseases*. Philadelphia: Current Medicine, 1999: 3.1–3.20.
323. Schwarz TF, Nerlich A, Hottentrager B, et al. Parvovirus B19 infection of the fetus. *Histology and in situ hybridization*. *Am J Clin Pathol* 1991;96(1):121–126.
324. Anand A, Gray ES, Brown T, Clewley JP, Cohen BJ. Human parvovirus infection in pregnancy and hydrops fetalis. *N Engl J Med* 1987;316(4):183–186.
325. Caul EO, Usher MJ, Burton PA. Intrauterine infection with human parvovirus B19: a light and electron microscopy study. *J Med Virol* 1988;24(1):55–66.
326. Krause JR, Penchansky L, Knisely AS. Morphological diagnosis of parvovirus B19 infection. A cytopathic effect easily recognized in air-dried, formalin-fixed bone marrow smears stained with hematoxylin-eosin or Wright-Giemsa. *Arch Pathol Lab Med* 1992;116(2):178–180.
327. Morey AL, Keeling JW, Porter HJ, Fleming KA. Clinical and histopathological features of parvovirus B19 infection in the human fetus. *Br J Obstet Gynaecol* 1992;99(7): 566–574.
328. Salimans MM, van de Rijke FM, Raap AK, van Elsacker-Niele AM. Detection of parvovirus B19 DNA in fetal tissues by in situ hybridisation and polymerase chain reaction. *J Clin Pathol* 1989;42(5):525–530.
329. Morey AL, O'Neill HJ, Coyle PV, Fleming KA. Immunohistological detection of human parvovirus B19 in formalin-fixed, paraffin-embedded tissues. *J Pathol* 1992; 166(2):105–108.
330. Morey AL, Ferguson DJ, Fleming KA. Combined immunocytochemistry and non-isotopic in situ hybridization for the ultrastructural investigation of human parvovirus B19 infection. *Histochem J* 1995;27(1):46–53.
331. Morey AL, Ferguson DJ, Leslie KO, Taatjes DJ, Fleming KA. Intracellular localization of parvovirus B19 nucleic acid at the ultrastructural level by in situ hybridization with digoxigenin-labelled probes. *Histochem J* 1993;25(6): 421–429.
332. Musiani M, Roda A, Zerbini M, et al. Detection of parvovirus B19 DNA in bone marrow cells by chemiluminescence in situ hybridization. *J Clin Microbiol* 1996;34(5): 1313–1316.
333. Zaki SR, Peters CJ. Viral hemorrhagic fevers. In: Connor DH, Chandler FW, Schwartz DA, Manz HJ, Lack EE, eds. *Pathology of infectious diseases*. Stamford, CT: Appleton and Lange, 1997:347–364.
334. Edington GM, White HA. The pathology of Lassa fever. *Trans R Soc Trop Med Hyg* 1972;66(3):381–389.
335. McCormick JB, Walker DH, King IJ, et al. Lassa virus hepatitis: a study of fatal Lassa fever in humans. *Am J Trop Med Hyg* 1986;35(2):401–407.
336. Walker DH, McCormick JB, Johnson KM, et al. Pathologic and virologic study of fatal Lassa fever in man. *Am J Pathol* 1982;107(3):349–356.
337. Elsner B, Schwarz E, Mando OG, Maiztegui J, Vilches A. Pathology of 12 fatal cases of Argentine hemorrhagic fever. *Am J Trop Med Hyg* 1973;22(2):229–236.
338. Child PL, MacKenzie RB, Valverde LR, Johnson KM. Bolivian hemorrhagic fever. A pathologic description. *Arch Pathol* 1967;83(5):434–445.
339. Baskerville A, Satti A, Murphy FA, Simpson DI. Congo-Crimean haemorrhagic fever in Dubai: histopathological studies. *J Clin Pathol* 1981;34(8):871–874.
340. Joubert JR, King JB, Rossouw DJ, Cooper R. A nosocomial outbreak of Crimean-Congo haemorrhagic fever at Tygerberg Hospital. Part III. Clinical pathology and pathogenesis. *S Afr Med J* 1985;68(10):722–728.
341. Abdel-Wahab KS, El Baz LM, El-Tayeb EM, Omar H, Ossman MA, Yasin W. Rift Valley Fever virus infections in Egypt: pathological and virological findings in man. *Trans R Soc Trop Med Hyg* 1978;72(4):392–396.
342. Burt FJ, Swanepoel R, Shieh WJ, et al. Immunohistochemical and in situ localization of Crimean-Congo hemorrhagic fever (CCHF) virus in human tissues and implications for CCHF pathogenesis. *Arch Pathol Lab Med* 1997;121(8): 839–846.
343. Strano AJ. Yellow fever. In: Binford CH, Connor DH, eds. *Pathology of tropical and extraordinary diseases*. Washington, DC: Armed Forces Institute of Pathology, 1976:1–4.

344. Burke T. Dengue haemorrhagic fever: a pathological study. *Trans R Soc Trop Med Hyg* 1968;62(5):682–692.
345. Maiztegui JI, Laguens RP, Cossio PM, et al. Ultrastructural and immunohistochemical studies in five cases of Argentine hemorrhagic fever. *J Infect Dis* 1975;132(1): 35–53.
346. Salas R, de Manzione N, Tesh RB, et al. Venezuelan haemorrhagic fever. *Lancet* 1991;338(8774):1033–1036.
347. van Velden DJ, Meyer JD, Olivier J, Gear JH, McIntosh B. Rift Valley fever affecting humans in South Africa: a clinicopathological study. *S Afr Med J* 1977;51(24):867–871.
348. Bhamarapavati N, Tuchinda P, Boonyapaknavik V. Pathology of Thailand haemorrhagic fever: a study of 100 autopsy cases. *Ann Trop Med Parasitol* 1967;61(4):500–510.
349. Gubler DJ, Zaki SR. Dengue and other viral hemorrhagic fevers. In: Horsburgh CR, Nelson AM, eds. *Pathology of emerging infections*. Washington, DC: American Society for Microbiology, 1998:43–72.
350. Paddock CD, Nicholson WL, Bhatnagar J, et al. Fatal hemorrhagic fever caused by West Nile virus in the United States. *Clin Infect Dis* 2006;42(11):1527–1535.